

**Investigating the Application of N, N'-Disubstituted-1,8-Diamidonaphthalene as a Ligand in Transition Metal and Main Group Chemistry**

**Nawal Almalki**

Thesis submitted to the  
Faculty of Graduate and Postdoctoral Studies  
in partial fulfillment of the requirements for the degree of

**Master of Science  
in  
Chemistry**

University of Ottawa

**Candidate**

Nawal Almalki

**Supervisor**

Darrin S. Richeson

© Nawal Almalki, Ottawa, Canada, 2018

## **Acknowledgments**

I would like to thank first and foremost the important person in my studies in Canada Dr. Darrin Richeson. He was more than my supervisor for me he is my inspiration and motivation of my work, like what he did in the lab to enthuse me for scientific research. From him, I have learned not only a large cross-section of chemistry but also a way to think, teach and inspire. I have truly loved every minute that I spent it in the lab. I will not forget all the moments we shared that talking about different topics such as science, politics, and religions. He always considers us as a family and understood the struggle that we, international students, have to deal with being away from home in a completely different environment and culture. Without his support and guidance over the last two years, this work would not be what it is

Second, I would like a special thank you to the great group for their help and support as well as all the great moments we shared together. I would like to thank Dr.Gambarotta for allowing me to use the dry solvent system.

To my family, my mother, father, daughters, and siblings, I say thank you for always standing up beside me. I would like to especially thank my husband Atiah for taking care of my daughters Elaf and Sulaf during my long nights in the lab.

And last, but not least warm thanks to The Ministry of Education in Saudi Arabia and Saudi cultural bureau in Canada for the financial support during my journey in Canada.

## Abstract

This thesis focuses on the design and development of novel versatile diamido ligands for transition metal and main group element chemistry. The central concept of this work deal relied on the design of N, N'-disubstituted-1,8-diaminonaphthalene ( $H_2RR'$ -DAN) as proligands to dianionic diamido ligand scaffolds. These ligands would then be employed for stabilization of main group element (e.g. Li, B, Al) and transition metal (e.g. Ti, Zn) compounds.

**Chapter I** presents the basic concepts in terms of the coordination compounds and ligand designs. Furthermore, the rationale for the choice of the N, N'-disubstituted-1,8-diaminonaphthalene as the framework will be presented.

**Chapter II** presents the synthesis and characterization of different proligands constructed with the 1,8-diaminonaphthalene core. Due to the nature of this scaffold different synthetic methods were required; reductive amination, acylation with halide followed by reduction, and copper catalyzed C-N coupling reactions. Three potential ligands were successfully prepared and characterized.

**Chapter III** describes efforts to use N, N'-disubstituted-1,8-diaminonaphthalene species prepared in Chapter II with tetravalent titanium and zirconium. Several routes were explored, and one required the preparation and characterization of the dilithium salts of

the dianions of the diaminonaphthalene species (e.g., RR'-DAN<sup>2-</sup>). This chapter will also present attempts to prepare some Zn(II) complexes of the RR'-DAN<sup>2-</sup> ligands.

**Chapter IV** presents the application of the dianion, N, N'-disubstituted-1,8-diamidonaphthalene (R, R'-DAN<sup>2-</sup>) as a supporting framework for group 13 compounds. The emphasis was on boron and aluminum species. The synthetic routes to these species relied on the use of either dilithium diamido reaction with group 13 halides or reaction of the proligand with trimethylaluminum via a proton transfer reaction.

## **Table of Contents**

Acknowledgements.....	II
Abstract.....	III
Table of Contents.....	V
List of Figure.....	VI
List of Table.....	X
List of Abbreviations.....	XI

### **Chapter I Introduction**

1.1 General Introduction.....	1
1.2 Ligand Design.....	6
1.3 1,8-disubstituted-diamidonaphthalene ligand.....	9
1.4 References.....	21

### **Chapter II Ligand Synthesis**

2.1 Introduction.....	27
2.2 Results and discussion.....	30
2.3 Conclusion.....	37
2.4 Experimental section.....	37
2.5 References.....	48

### **Chapter III Efforts Toward Synthesis of Transition Metal Complexes Supported by N,N' Diamidonaphthalene Framework Ligands**

3.1	Introduction .....	50
3.2	Results and discussion .....	53
3.3	Conclusion.....	65
3.4	Experimental section.....	65
3.5	References.....	74

## **Chapter IV N, N' Diamidonaphthalene as a Versatile Ligand to Stabilize Complexes of Group 13**

4.1	Introduction .....	76
4.2	Results and discussion .....	79
4.3	Conclusion .....	88
4.4	Experimental section.....	89
4.5	References.....	100

### **List of Figures**

<b>Figure 1.1:</b>	$\sigma$ and $\pi$ orbitals in amido, $R_2N^{-2}$ , ligand .....	7
<b>Figure 1.2:</b>	$\beta$ -diketimine (“NacNac”) and 1,8-disubstituted-diaminonaphthalene proligand ( $H_2R,R'$ -DAN) .....	10
<b>Figure 1.3:</b>	Different 1,8diaminonaphthalene (1,8-DAN) frameworks .....	10
<b>Figure 1.4:</b>	N,N,N'N'-tetramethyl-1,8-DAN.....	11
<b>Figure 1.5:</b>	Frontier orbitals of $R,R'$ -DAN <sup>2-</sup> and $\beta$ -diketimate .....	13
<b>Figure 1.6:</b>	N,N'-disilylated 1,8-diaminonaphthalene proligands .....	14
<b>Figure 1.7:</b>	Different routes of synthesis $Sn[1,8-(iPrN)_2C_{10}H_6]$ .....	15

<b>Figure 1.8:</b> Different routes to obtain Ge[1,8-(iPrN) <sub>2</sub> C <sub>10</sub> H <sub>6</sub> ]	15
<b>Figure 1.9:</b> Molecular structure showing one of the two symmetry unique molecules of Ni{Ge[( <sup>i</sup> PrN) <sub>2</sub> C <sub>10</sub> H <sub>6</sub> ]} <sub>2</sub>	16
<b>Figure 1.10:</b> The isolation of metalaaziridine complex [η <sup>3</sup> (Me <sub>2</sub> CN)(Me <sub>2</sub> CHN)C <sub>10</sub> H <sub>6</sub> ]TaC <sub>12</sub> ] by β-H activation	18
<b>Figure 1.11:</b> Synthesis of bis(imido)W(VI) complexes	19
<b>Figure 1.12:</b> The reactivity of bis(imido)W(VI) complexes	19
<b>Figure 1.13:</b> Synthetic approaches to group 15	20
<b>Figure 2.1:</b> Deprotonating 1,8-disubstituted-diaminonaphthalene	28
<b>Figure 2.2:</b> Generic scheme for the preparation of amine by using acyl halide	28
<b>Figure 2.3:</b> Generic scheme of the reductive amination reaction	29
<b>Figure 2.4:</b> Generic scheme for the Cu-catalyzed cross-coupling of amine	29
<b>Figure 2.5:</b> Preparation of (NpNH) <sub>2</sub> C <sub>10</sub> H <sub>6</sub> group	31
<b>Figure 2.6:</b> Initial attempts for the alkylation of 1,8-DAN	32
<b>Figure 2.7:</b> Preparation of ( <sup>i</sup> PrNH)(NpNH)C <sub>10</sub> H <sub>6</sub> group	33
<b>Figure 2.8:</b> Preparation of ( <sup>i</sup> PrNH) <sub>2</sub> C <sub>10</sub> H <sub>6</sub> ligand	34
<b>Figure 2.9:</b> Proposed mechanism of reduction reactions	35
<b>Figure 2.10:</b> Preparation of 1H, 3H-perimidin-2-one	36
<b>Figure 2.11:</b> A copper catalyzed reaction to prepare (PhNH) <sub>2</sub> C <sub>10</sub> H <sub>6</sub>	36
<b>Figure 2.12:</b> Structural representation of <b>2.4</b> (Hydrogen atoms bonded to carbon have been omitted for clarity)	45
<b>Figure 2.13:</b> Structural representation of <b>2.7</b> (Hydrogen atoms bonded to carbon have been omitted for clarity)	45

<b>Figure 2.14:</b> NMR Spectroscopy for N, N'-diisopropyl-1, 8-diaminonaphthalene, ( <sup>i</sup> PrNH) <sub>2</sub> C <sub>10</sub> H <sub>6</sub> .....	46
<b>Figure 2.15:</b> NMR Spectroscopy for N,N'-dineopentyl-1,8-diaminonaphthalene, (NpCH <sub>2</sub> NH) <sub>2</sub> C <sub>10</sub> H <sub>6</sub> .....	46
<b>Figure 2.16:</b> NMR Spectroscopy for N-(isopropyl)-N'-(neopentyl)-1,8- diaminonaphthalene (NpN)( <sup>i</sup> PrN)C <sub>10</sub> H <sub>6</sub> .....	47
<b>Figure 3.1:</b> Examples of ligands that their complexes have been used as catalysts in polymerization reactions.....	51
<b>Figure 3.2</b> Different amido ligand frameworks that have been used in group 4 complexes. ....	52
<b>Figure 3.3:</b> Synthesis of dilithium salts of different R, R'-DAN ligands .....	55
<b>Figure 3.4:</b> Molecular structure for <b>3.3</b> (hydrogen atoms have been omitted for clarity) .....	55
<b>Figure 3.5:</b> Molecular structure for <b>3.4</b> (hydrogen atoms have been omitted for clarity)	56
<b>Figure 3.6:</b> Synthetic approaches to group 4.....	57
<b>Figure 3.7:</b> Molecular structure for <b>3.5</b> (hydrogen atoms have been omitted for clarity)	58
<b>Figure 3.8:</b> Reaction of ZrCl <sub>4</sub> .THF with H <sub>2</sub> O.....	58
<b>Figure 3.9:</b> Molecular structure for ( <sup>i</sup> PrNH) <sub>2</sub> C <sub>10</sub> H <sub>6</sub> salt.....	59
<b>Figure 3.10:</b> Synthesis route of Ti(CH <sub>2</sub> Ph) <sub>4</sub> .....	60
<b>Figure 3.11:</b> Molecular structure of compound <b>3.6</b> (hydrogen atoms have been omitted for clarity) .....	60
<b>Figure 3.12:</b> Proposed reaction of TiBn <sub>4</sub> complex by alkane elimination.....	61
<b>Figure 3.13:</b> Preparation of Zn complex by alkane elimination route .....	62
<b>Figure 3.14:</b> Preparation of Zr complex by amine elimination.....	62

<b>Figure 3.15</b> X-ray crystal structure of the Zr complex.....	63
<b>Figure 3.16</b> Bonding Orbitals for the optimized Zr complex.....	64
<b>Figure 4.1:</b> Some applications of diamidonaphthalene-based ligands in group 13 ..... chemistry	77
<b>Figure 4.2:</b> Preparation of different diamidonaphthalene proligands ( $H_2 R, R^1$ -DAN) ...	78
<b>Figure 4.3:</b> Synthesis of boron complexes by a hydrogen elimination route .....	80
<b>Figure 4.4:</b> Synthesis of boron complex by an alkanle elimination.....	81
<b>Figure 4.5:</b> Structural representation of $HB[1,8-(iPrN)_2C_{10}H_6]$ ( <b>4.4</b> ). Carbon-bound hydrogen atoms have been omitted for clarity.....	83
<b>Figure 4.6:</b> Structural representation of $HB[1,8-(PhN)_2C_{10}H_6]$ ( <b>4.5</b> ).Carbon-bound hydrogen atoms have been omitted for clarity.....	83
<b>Figure 4.7:</b> Structural representation of $BF[ iPrNH)(NpNH)C_{10}H_6]$ ( <b>4.7</b> ).Carbon bound hydrogen atoms have been omitted for clarity.....	83
<b>Figure 4.8:</b> The frontier orbitals (HOMO-2 to LUMO) representing the $\pi$ -bonding in 3 obtained from DFT (B3LYP, 6-311+G(d,p)) on compound <b>4.4</b> .....	84
<b>Figure 4.9:</b> Synthesis Al complexes by methane elimination.....	85
<b>Figure 4.10:</b> The molecular structure for $(AlMe_2)_2[1,8-(iPrN)_2C_{10}H_6]$ ( <b>4.8</b> ). Hydrogen atoms have been omitted for clarity.....	86
<b>Figure 4.11:</b> The molecular structure for $(AlMe_2)_2[1,8-(PhN)_2C_{10}H_6]$ ( <b>4.9</b> ). Hydrogen atoms have been omitted for clarity.....	87
<b>Figure 4.12:</b> The molecular structure for $(AlMe_2)_2[1,8-(iPrN)(NpN)C_{10}H_6]$ ( <b>4.10</b> ) Hydrogen atoms have been omitted for clarity.....	87
<b>Figure 4.13:</b> Captured intermediate in reaction of $AlMe_3$ with proligand <b>4.11</b> .....	88

## **List of Tables**

<b>Table 3.1:</b> Crystal data and structure refinement for <b>3.3</b> and <b>3.4</b> .....	70
<b>Table 3.2:</b> Selected Bond Lengths [Å] and Angles [°] for <b>3.3</b> and <b>3.4</b> .....	70
<b>Table 3.3:</b> Crystal data and structure refinement for <b>3.6</b> .....	71
<b>Table 3.4:</b> Selected Bond Lengths [Å] and Angles [°] for <b>3.6</b> .....	72
<b>Table 4.1.</b> Selected bond lengths [Å] and angles [°] for HB[( <i>i</i> PrN) <sub>2</sub> C <sub>10</sub> H <sub>6</sub> ] ( <b>4.4</b> ), HB[(PhN) <sub>2</sub> C <sub>10</sub> H <sub>6</sub> ] ( <b>4.5</b> ) and HB [1,8 ( <i>i</i> PrNH)(NpNH)C <sub>10</sub> H <sub>6</sub> ] ( <b>4.7</b> ) .....	95
<b>Table 4.2.</b> Selected Bond lengths [Å] and angles [°] for [Al(CH <sub>3</sub> ) <sub>2</sub> ] <sub>2</sub> [( <i>i</i> PrN) <sub>2</sub> C <sub>10</sub> H <sub>6</sub> ] ( <b>4.8</b> ) .....	96
<b>Table 4.3</b> Selected Bond lengths [Å] and angles [°] for) [Al(CH <sub>3</sub> ) <sub>2</sub> ] <sub>2</sub> [(PhN) <sub>2</sub> C <sub>10</sub> H <sub>6</sub> ] ( <b>4.9</b> ) .....	96
<b>Table 4.4</b> Selected Bond lengths [Å] and angles [°] for [Al(CH <sub>3</sub> ) <sub>2</sub> ] <sub>2</sub> [( <i>i</i> PrN)(NpN)C <sub>10</sub> H <sub>6</sub> ] ( <b>4.10</b> ) .....	97
<b>Table 4.5</b> Crystal data and structure refinement for <b>4.11</b> .....	98

## List of Abbreviations

### 1. Chemicals and Ligands

Ar	Aromatic group
Bu	Butyl ( <i>t</i> Bu, <i>tertiary</i> -butyl)
Bn	Benzyl
Cp	Cyclopentadienyl, C <sub>5</sub> H <sub>5</sub>
1, 8-DAN	1,8-diaminonaphthalene, 1, 8-(NH <sub>2</sub> ) <sub>2</sub> C <sub>10</sub> H <sub>6</sub>
H <sub>2</sub> R, R'-DAN	1,8-disubstituted-diaminonaphthalene
R, R'-DAN <sup>-2</sup>	Dianionic disubstituted-diaminonaphthalene
Et	Ethyl
<i>i</i> Pr	Iso-propyl
Np	Neopetyl
NacNac	β-diketimate
Acac	Acetylacetonate
L	Ligand
M	Central atom (usually a metal) in a compound
Me	Methyl
<i>t</i> Bu	t-butyl
Ph	Phenyl, C <sub>6</sub> H <sub>5</sub>
BuLi	Butyl lithium
R	Alkyl or Aryl group

THF                    Tetrahydrofuran

X                      Halogen

## 2. Miscellaneous

Å                      Angstrom unit  $10^{-10}\text{m}$

°                      Degree

Hz                     Hertz

NMR                  Nuclear magnetic resonance

PPM                  Part per million

# Chapter I

## Introduction to ligand design concepts

### 1.1 General introduction

This thesis is built around the concept of exploring the fundamental chemistry of the main group and transition metals through their coordination by a unique chelating  $\pi$ -conjugated diamido ligand, N, N'-dialkyl-1,8-diamidonaphthalene. Before presenting the specific background and hypotheses of this work, it is important to provide some outline of the broader background of coordination chemistry, the general application of amido ligands, and some history of one of the key inspirations for this project, the  $\beta$ -diketiminato ligands.

The periodic table is dominated by metal and metalloid elements. Of the 118 elements in the modern periodic table, 93 are classified as metals with 7 as metalloids (i.e. B, Si, Ge, As, Sb, Te, At). Only 18 elements fall into the non-metal group. These 100 metal elements are broadly classified as the alkali and alkaline earth metals, the transition metals, the post-transition metals and metalloids, and the lanthanide and actinide metals. In addition, the alkali, alkaline earth and post-transition elements are often referred to as the main group elements. The elements can also be classified by the identity of the orbitals that are used for the outermost electrons on the element. The alkali and

alkaline earth metals are thus called the s-block elements, the post-transition elements are members of the p-block elements, the d-block elements correspond to the transition metals, and the lanthanide and actinide elements belong to the f-block<sup>1,2</sup>.

Although metal coordination compounds have a long history, the birth of modern coordination chemistry is attributed to the seminal work of Alfred Werner. In 1893, at the age of 27, Werner was the first chemist to propose the correct structures for coordination compounds containing species in which a central transition metal atom is surrounded by neutral or anionic ligands. Werner established the formulas, structures and isomers of a number of coordination compounds.<sup>3</sup> For example, he showed that many Co(III) and Cr(III) compounds displayed six coordinated ligands that are in an octahedral geometry. His work differentiated coordinated anions from counterions, and his rationalization clarified the formation of isomers observed for these species. For these contributions, Werner was awarded the Nobel Prize in Chemistry in 1913, which was, in fact, the first prize given to the field of inorganic chemistry. Due to the impact of these contributions, the field of coordination chemistry has historically been dominated by transition metal complexes. However, main group metals and metalloids also appear in complexes that would fall under the definitions of coordination compounds.<sup>2</sup>

Coordination compounds, also known as coordination complexes or metal complexes consist of a central metal atom or ion known as the coordination center and a number of surrounding molecules or ions, known as complexing agents or ligands. A simple view is that the coordination center functions as a Lewis acid and the ligands are

Lewis bases. The metal-ligand interactions have been classified as coordinate covalent bonds. Some examples of ligands are neutral molecules like ammonia, water, ethers, and anions such as halides, alkoxides, and carboxylate. Coordination complexes are common among biological systems as indicated by the presence of metal ions in about 30% of proteins. The metals in these systems serve both structural and catalytic functions. Examples include the cobalt in vitamin B<sub>12</sub>, iron in the heme group of hemoglobin and the cytochromes and magnesium in chlorophyll<sup>4</sup>.

The concepts originally developed by Werner for transition metal are transportable to main group metal coordination chemistry and organometallic chemistry. As a result, unlike the situation with Werner, there is no single chemist who is attributed to originating main group coordination chemistry or organometallic chemistry. However, one early and notable example of complexes that fit both the main group and the organometallic classification are Grignard reagents. These organometallic Mg complexes are named in honour of Victor Grignard, and the significance of this contribution is reflected by the fact that he was awarded a Nobel Prize in Chemistry in 1912<sup>5,6</sup>.

When a metal or metalloid element forms a molecular species that consists of a central element being surrounded by an array of bonded molecules or ions, the resulting species is called a coordination complex. In such a complex, the central metal (atom or ion) is the coordination center and the surrounding bonded species are termed ligands. This definition of coordination complexes provides for a very broad, prevalent class of compounds with a huge variety of structures and reactions. The atom within a ligand that

is bonded to the central metal atom or ion is called the donor atom. In a typical complex, a metal is bonded to several donor atoms, which can be the same or different. The original term coordination referred to the "coordinate covalent bonds" between the ligands and the central atom, and the term complex implied a reversible association of the ligands<sup>1</sup>. This meaning has evolved, and many metal complexes are formed in which the metal-ligand bonds are quite strong.

Certainly, any discussion of modern coordination chemistry will rely on a common description of metal-ligand bonding. As previously stated, the simplest model of metal-ligand bonding has ligands viewed as electron donors and the metals as electron acceptors. With the advent of quantum mechanics and atomic and molecular orbital approaches to bonding, metal-ligand bonding models also evolved. These ideas lead to a more modern view of metal-ligand interactions. The bonding between ligands and the central metal involve the donation of one or more of the electron pairs of the ligand to empty orbitals of the metal. Using molecular orbital terminology, this implies that the highest occupied molecular orbital (HOMO) is localized on the ligands while the lowest unoccupied molecular orbital (LUMO) is localized on the metal. Using the concepts of molecular orbital theory, this view indicates that the HOMO of the ligand houses the donor electron and should have energy and symmetry appropriate for overlaps with the LUMO of the metal. The result of ligand-metal bonding leads to a new HOMO and LUMO for the complex with these resulting orbitals leading to the properties and reactivity of the resulting complex<sup>7</sup>. These metal-ligand bonds can range from covalent to ionic.

Interesting and important effects in metal-ligand interactions can be observed when the ligand possesses a low energy unoccupied orbital (LUMO) that can accept electron density from a metal center<sup>6</sup>. This process, known as back-bonding or back-donation, involves the donation of electron density from a metal back to the ligand-centered orbitals and can further stabilize a metal complex. Of course, this type of interaction requires orbitals of appropriate symmetry (e.g.,  $\pi$ -type bonding symmetry) and energy for significant bonding. The most well-known example of this type of interaction is observed for the carbon monoxide (CO) ligand, which is known to engage in strong metal bonding via back-donation.<sup>7,8</sup> Similarly, phosphine ( $\text{PR}_3$ ) and olefins ligands can demonstrate  $\pi$ -interactions as well<sup>9,2</sup>.

From the perspective of the ligand, complexes that display bonds to any carbon atom, including non-organic ones, are generally classified to be organometallic complexes, given the number of metal complexes that possess organic ligands but that lack metal-carbon bonds, the term “metalorganic compound” is often used to distinguish these complexes from organometallic species. Examples of metalorganic complexes include complexes that bear alkoxide ( $\text{RO}^-$ ), amido ( $\text{R}_2\text{N}^-$ ), phosphine ( $\text{PR}_3$ ) ligands as well as complexes of a ligand like  $\beta$ -diketonate<sup>10</sup>. Organometallic and metalorganic compounds continue to be widely explored in inorganic chemistry and are used in chemical reactions as stoichiometric reagents and homogenous catalysts. Finally, it is important to realize that ligand donation can essentially come from any pair of electrons. As a result, unsaturated organic species, such as alkenes, alkynes, and arenes, can

coordinate to metals through their  $\pi$  electrons. In these organic species, the  $\pi$ -electrons are in the HOMO, and like all other ligands, these can be donated to a metal LUMO<sup>1</sup>.

## 1.2. Ligand design

Based on the discussion above, it should be obvious that ligand design and development are key components of coordination chemistry. Ligand selection is a critical consideration in many aspects of this chemistry such as homogenous catalysis, environmental chemistry, and bioinorganic chemistry. The ligands in a complex are key to dictate the reactivity of the central atom and of the complex overall. Ligands are designed so that when they bind to metals, they influence the reactivity of interest and achieve a pre-defined goal. Generally the greater the need for controlling the reactivity, the more specific the metal-ligand interaction<sup>2</sup>. It should be obvious that there will be no all-purpose ligand; each reaction has an ideal ligand of unique composition and structure. In general, a suitable ligand should form strong bonds with the metal to form stable complexes and should not react with reagents during catalysis. The motivation of the design of different ligands is to control the structure, stability, and reactivity of the complex. These characteristics can be influenced through modification of the ligand framework and by changing the ligand substituents. The properties and reactions of metal complexes are highly dependent on the choice of supporting ligand, and this choice is one of the keys to successful coordination chemistry. Of course, this is a vast and daunting task, and covering the range of potential features used in ligand design is beyond the

scope of this particular thesis. Therefore, the remainder of this thesis will focus on nitrogen-based ligands and more specifically on amido anion ligands.

### 1.2.1 Amido ligands

An amido ligand refers to a deprotonated primary or secondary amine:  $R(H)N^-$  or  $RR'N^-$  ( $R, R' = \text{alkyl, aryl or silyl groups}$ ). This definition deliberately excludes deprotonated organic amides,  $N(R)COR'$ .<sup>11</sup>

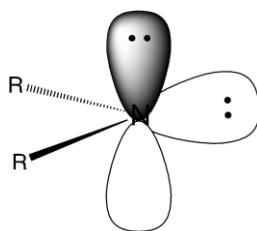


**Figure 1.1:**  $\sigma$  and  $\pi$  orbitals in amido,  $R_2N^-$ , ligand.

The frontier orbital array for an amido ligand is shown in Figure 1.1. The nitrogen-centered anion possesses two lone electron pairs. One in a formally  $sp^2$  orbital and the second in a p-orbital. These two orbitals are orthogonal to each other and have particular dispositions relative to the  $NR_2$  unit as shown. The  $sp^2$  orbital would be the primary ligand donor orbital and interaction with an appropriate metal/metalloid orbital results in formation of a  $\sigma$  bond and an unoccupied  $\sigma^*$  molecular orbital. The electron pair that is localized in the p-orbital is of correct symmetry to overlap with a metal/metalloid orbital in a  $\pi$ -fashion<sup>2</sup>. Of course, this relies on an empty orbital on the central elements. In the presence of such an interaction, the coordinated metal/metalloid, N, and the two R groups should be coplanar. This orientation is required for effective  $\pi$  overlap and results

in formally four electron donations from the ligand and observation of this structural features is the first indication that both  $\sigma$  and  $\pi$  donation is occurring.

This bonding model suggests the common strategy for modification of the steric and or electronic features of the amido ligand by control of the R groups bonded to nitrogen. For example, steric properties can be changed by using R groups of different size such as methyl versus tertiary-butyl. The electronic properties can be controlled by using electron donating groups such as  $\text{CH}_3(\text{R})$  or electron-withdrawing alkyls like  $\text{CF}_3$  or a potentially  $\pi$  binding group such as an aromatic ring<sup>12</sup>.

Another more extensive modification for this type of framework would be to link more than one donor amido center together to yield a polydentate scaffold. In the case of a bidentate diamido ligand, the proligand would be a diamine species. One of the most obvious features of such a species is that the linker or spacer between the donor sites plays an important role by controlling the size of the ligand bite or chelate ring size<sup>13</sup>. In principle, the structure of the bridging unit can be varied to give rigid or flexible ligands, depending on what is desired. The nitrogen substituents can give steric protection and can also influence the electronic properties of the ligand. A less obvious feature of the spacer in a bidentate diamido ligand would be the role of electronic overlap between the donor centers. For example, linking two amido bonding sites through a  $\pi$ -conjugated linker could play a critical role in the ligand electronic characteristics<sup>14</sup>. Of course, since amido ligands are strong  $\sigma$  and  $\pi$  electron donors, this bidentate coordination will lead to strong bonds to the metal.<sup>15</sup>

### 1.3 The $\beta$ -diketimate ligand and 1,8-disubstituted-diamidonaphthalene ligand

This thesis is focused on the chemistry of a  $\pi$ -conjugated diamido ligand constructed from the 1,8-diaminonaphthalene core. The most important inspiration in the design of this central player in this thesis came from the broad success of the  $\beta$ -diketimate ligand family. A general  $\beta$ -diketimate ligand is depicted in Figure 1.2, and this ligand family has shown increasing popularity as a supporting ligand for transition and main group metals since their introduction in 1968<sup>16</sup>. Ligands with this architecture are commonly referred to as “NacNac” because of the replacement of the oxygen centers of the well-known acetylacetonate (acac) ligand with nitrogen centers for metal bonding. The  $\beta$ -diketimate ligand scaffold offers steric protection at the metal center through the variation of N-substituents<sup>17</sup>. In addition to the variation of the N-R substituents, the R' and R'' positions are also points of variation<sup>12</sup>. A vast number of ligand modifications and different coordination modes have been reported, and chemists have only scratched the surface for the large number of possible ligands in the  $\beta$ -diketimate family<sup>10</sup>. The most popular versions of this ligand family are the N-aryl  $\beta$ -diketimate ligands, and they have been most widely used to support a variety of main group metal and transition metals in many oxidation states<sup>18,19,20,21</sup>

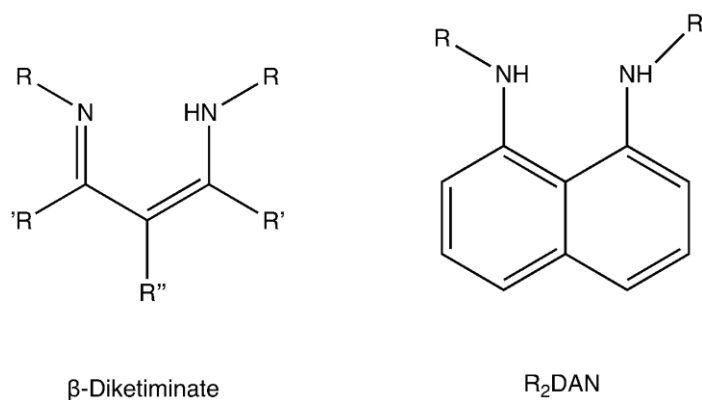


**Figure 1.2:**  $\beta$ -diketimine (“NacNac”) and 1,8-disubstituted-diaminonaphthalene proligand ( $H_2R,R'$ -DAN)

The success achieved with  $\beta$ -diketiminate ligands motivated our interest in the design of ligands constructed around the 1,8-diaminonaphthalene scaffold. 1, 8-Diaminonaphthalene frameworks can be formed as unsubstituted, monosubstituted, and disubstituted species (Figure 1.3). There are a number of examples for unsubstituted diamine 1,8- $NH_2(C_{10}H_6)$  (A) as a ligand. This includes the formation of diamidonaphthalene bridged diiridium complexes<sup>22,23</sup> a bridged trimetallic magnesium cage<sup>24</sup>, chelated ruthenium, and platinum complexes<sup>25</sup>, bridged dinuclear rhodium complexes,<sup>26</sup> ligated osmium carbonyl clusters<sup>27</sup>, and some chelated boron complexes<sup>28,29</sup>.

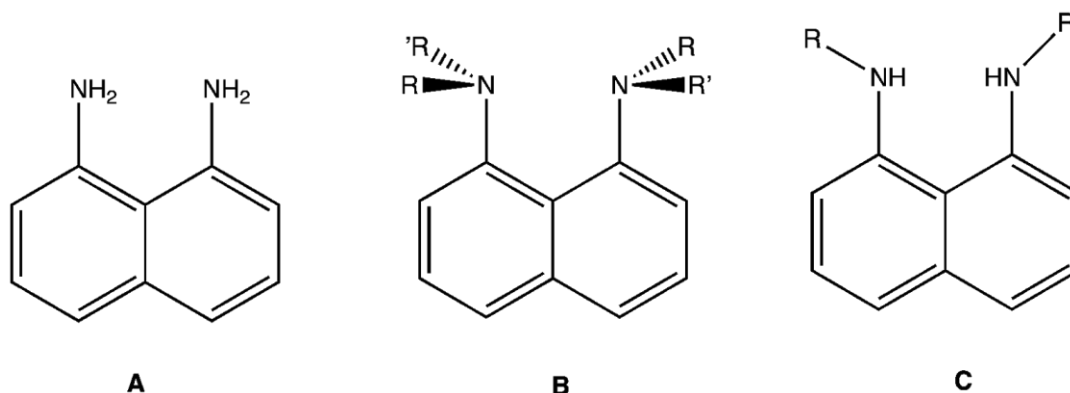


**Figure 1.3:** Different 1,8-diaminonaphthalene (1,8-DAN) frameworks

In addition, unsubstituted diamine **A** ligand have used as supporting ligand for boron complexes as example seemingly exist as three coordinate B species. However, none of the compounds have been structurally characterized, and they still possess reactive N-H groups three coordinated boron complex<sup>30</sup>. Unfortunately, unsubstituted 1,8-DAN ligand suffers from absences of steric and electronic properties due to the lack of nitrogen substituents.

1,8-DAN can also be present as fully tetrasubstituted derivatives. An example is 1,8-bis(dimethylamino)naphthalene (Figure 1.3, **B**) also called "proton sponge." This compound demonstrates unusually strong basicity for diamines and results in its unique ability to accept protons. N,N,N',N'-tetramethyl-1,8-DAN have also been employed as neutral chelating diamines for transition metals<sup>13,31</sup>. N,N,N',N'-tetramethyl-1,8-DAN has been used as a neutral chelating ligand for boron, usually generating cationic salts by displacement of one anionic ligand (hydride or halide)<sup>32,33</sup>. However, the lack of anionic charge for these species has limited their applications (Figure 1.4).

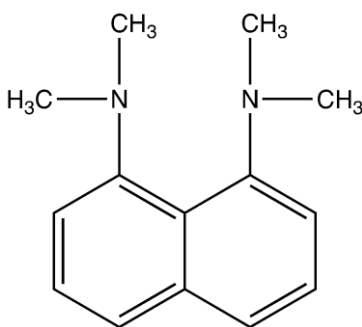


**Figure 1.4:** N,N,N',N'-tetramethyl-1,8-DAN

As consequence of the limitations of unsubstituted (**A**) and tetrasubstituted (**B**) 1,8-diaminonaphthalene, we chose to focus on the design and development of new ligand systems based on the N, N'-disubstituted-1,8-diaminonaphthalene scaffold (Figure 1.3). The importance of having a robust ligand structure was one of the reasons we targeted alkyl and aryl groups with a sturdy C-N linkage preventing unfavorable rearrangements. To our knowledge, prior to 1999,<sup>34</sup> there was no reported use of bis(alkyl) or bis(aryl) 1,8-diaminonaphthalene as a dianionic ligand for main-group or transition metals. Considering the anticipated potential of this architecture as a versatile ligand platform, we set forth the goal of developing the coordination chemistry of diamide ligands derived from 1,8-diaminonaphthalene, with a particular focus on using derivatives possessing robust N-substituent groups.

The larger charge for the R, R'-DAN<sup>2-</sup> ligands will make them a stronger donor and hence a better stabilizer of high oxidation state complexes. A comparison of the topology/shape and relative energies of the ligand orbitals for disubstituted R,R'-DAN<sup>2-</sup> and a  $\beta$ -diketiminato anion is presented in Figure 1.5. The frontier molecular orbitals are very similar. The major difference between these ligands is the occupancy of the orbitals. The diamidonaphthalene ligand is a dianionic ligand which means that an additional MO is filled and the HOMO of the R, R'-DAN<sup>2-</sup> system correlates with the LUMO of the  $\beta$ -diketiminato ligand. In the NacNac ligand we can see that the LUMO and the HOMO are  $\pi$ -type orbitals this is also true for the HOMO and HOMO-1 for the R,R'-DAN<sup>2-</sup>ligand. The HOMO-1 and HOMO-2 for the NacNac ligand and the HOMO-2 and HOMO-3 for

the R,R'-DAN<sup>2-</sup> ligand represent  $\sigma$  orbitals. The similarity of these orbitals suggests that R,R'-DAN<sup>2-</sup> and NacNac ligands may demonstrate some parallel features in their metal interactions.

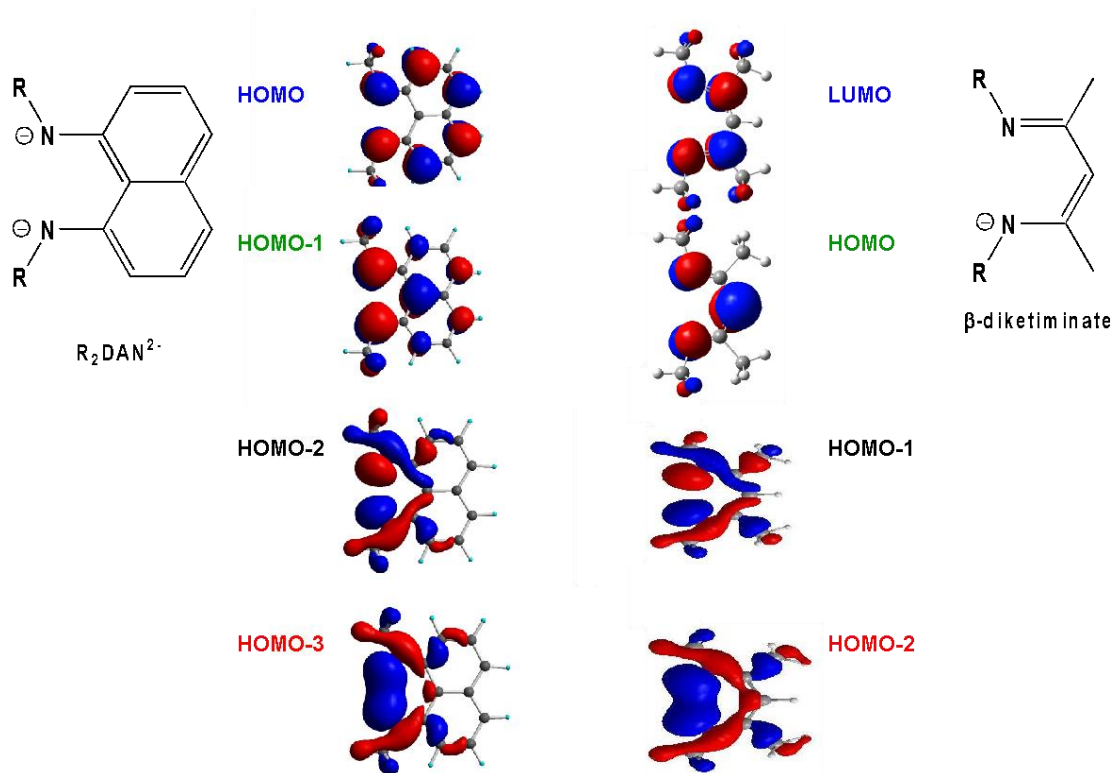


**Figure 1.5.** Frontier orbitals of R,R'-DAN<sup>2-</sup> and  $\beta$ -diketiminate done with Gaussian program with B3LYP functional and a basis set 6-311+g(d,p)

As mentioned, the significant differences between the two ligands are the dianionic charge and the naphthalene backbone of R, R'-DAN<sup>2-</sup>. The 1,8-disubstituted diamidonaphthalene H<sub>2</sub>R, R'-DAN ligand possesses a fused aromatic backbone that provides both rigidity and a  $\pi$ -system capable of charge delocalization. The orientation of the N-substituents is favorable for steric protection of a chelated metal center, and the size and shape of the substituents can be varied providing an opportunity for optimization. Upon chelation, the N lone-pairs would be aligned for  $\pi$ -donation to the

metal/element center and allow for flexibility in electronic interaction. We also realized that since the resulting compound is a six-membered heterocycle, the steric impact of the substituents on the nitrogen centers is greater than that for the related five-membered metalloheterocycles<sup>35</sup>.

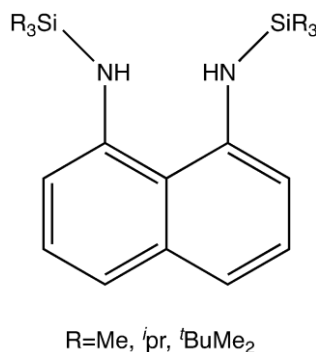


**Figure 1.6:** N,N'-disilylated 1,8-diaminonaphthalene proligands

The bis(trimethylsilyl) derivative (R, R' = SiMe<sub>3</sub>), Figure 1.6 was first reported as a ligand for an Sn(II) compound in the mid-seventies<sup>36</sup>. The ancillary dianionic ligands began to receive attention only very recently. This ligand resembles 1,8-disubstituted diaminonaphthalene (H<sub>2</sub>R,R'-DAN) but is slightly less versatile. It possesses the same rigid backbone and is dianionic like R,R'-DAN<sup>2-</sup>. The nitrogen substituents are alkylsilyl groups consequently the electronics and sterics cannot be tuned as with the aryl and alkyl group in the H<sub>2</sub>R,R'-DAN ligands. The limitation with the nitrogen substituents means that the structural features of this ligand in metal complexes might not be the same as in R,R'-DAN complexes.

The disubstituted 1,8-diaminonaphthalene proligands have also shown some flexibility of complexes synthesized in our lab. For example, divalent group 14 element

Sn(II) and Ge(II) complexes have been prepared. The synthesis of Sn(II) complex was achieved using two routes as seen in Figure 1.7. First, Sn(NSiMe<sub>3</sub>)<sub>2</sub> was used as a reagent as well as a base to deprotonate both N-H groups. In the second approach, the dilithium salt of H<sub>2</sub>R,R'-DAN ligand reacted with SnCl<sub>2</sub>. The X-ray structure of the complex showed a bent geometry of the Sn center<sup>36,37</sup>.

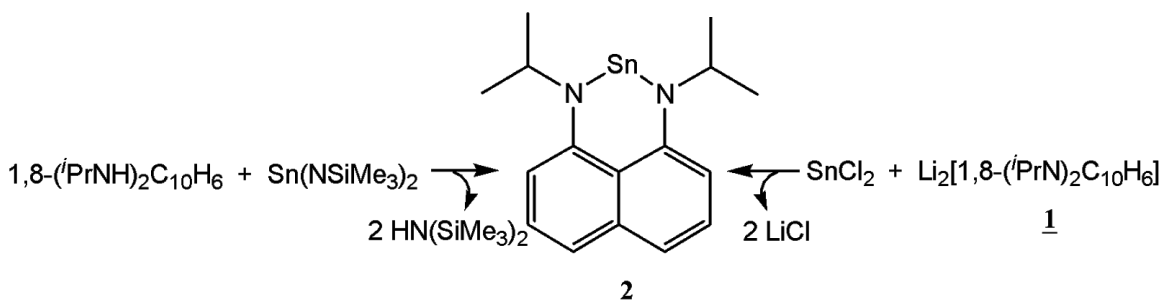


**Figure 1.7:** Different routes of synthesis Sn[1,8-(iPrN)<sub>2</sub>C<sub>10</sub>H<sub>6</sub>].

The Ge(II) complex was also isolated by two routes as shown in Figure 1.8. In both cases, the desired product was obtained and revealed a six-membered heterocyclic ring of Ge complex<sup>35</sup>.

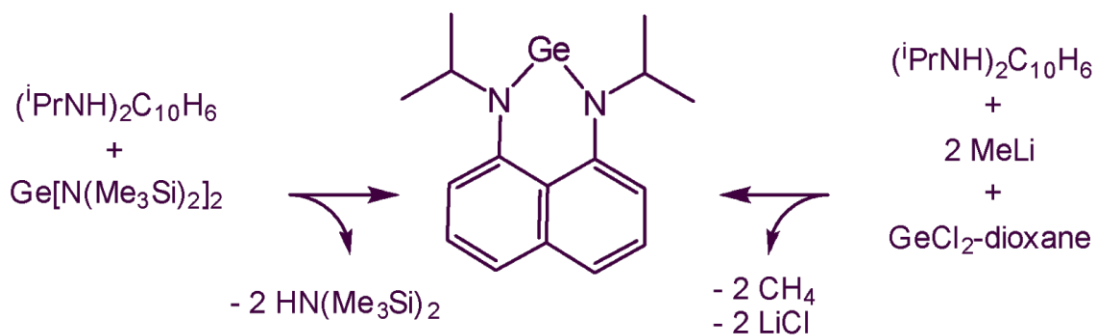


**Figure 1.8:** Different routes to obtain Ge[1,8-(iPrN)<sub>2</sub>C<sub>10</sub>H<sub>6</sub>].

Additionally, a lone pair of electrons on the Ge(II) center allows this species to function as a novel ligand for the preparation of the unique tetrakis-(germylene) complex  $\text{Ni}\{\text{Ge}[1,8\text{-}(\text{iPrN})_2\text{C}_{10}\text{H}_6]\}_4$ . The structural features of this later complex were determined by X-ray showing that the Ge(II) center is coordinated to the Ni(0) and the ligand displayed a twisted heterometallocycle, with a cone angle  $145^\circ$  (Figure 1.9)<sup>35</sup>.

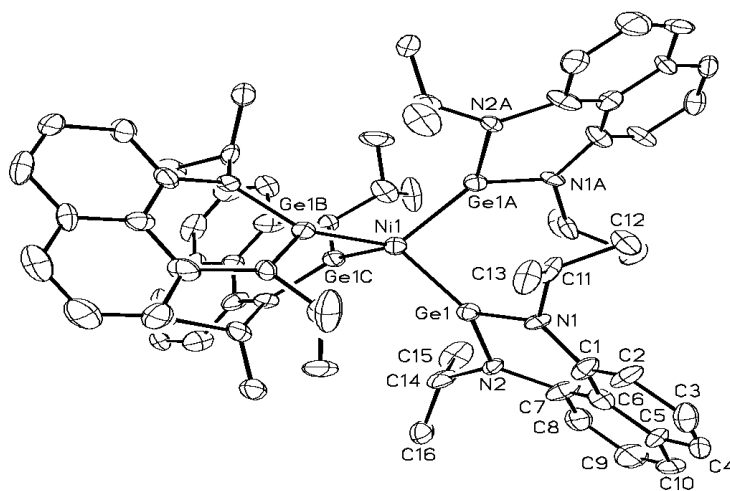


**Figure 1.9:** Molecular structure showing one of the two symmetry unique molecules of  $\text{Ni}\{\text{Ge}[(\text{iPrN})_2\text{C}_{10}\text{H}_6]\}_2$

Another set of compounds showing the application of 1,8-disubstituted diamidonaphthalene with transition metals is provided by the Ta(V) complexes with aryl and alkyl substituted ligands  $\{(3,5\text{-}(\text{Me})_2\text{-C}_6\text{H}_3)_2\text{N}\}_2\text{C}_{10}\text{H}_6$  and  $(\text{iPrN})_2\text{C}_{10}\text{H}_6$  (Figure 1.8). One of the interesting features of this reaction is that the metal possesses a reactive Ta-Me group and this resulted in some unexpected results. The Ta-Me group led to activation of the methyne CH proton to eliminate  $\text{CH}_4$  and to yield metallaaziridine. This

functional group remained intact during reactions to make organometallic species<sup>38</sup>. Deprotonated N,N'-disubstituted 1,8-diamidonaphthalenes H<sub>2</sub>R,R'-DAN<sup>2-</sup>; R = (CH<sub>3</sub>)<sub>2</sub>CH, C<sub>6</sub>H<sub>5</sub>, 3,5-Me<sub>2</sub>C<sub>6</sub>H<sub>3</sub>) were incorporated into Ta(V) complexes employing two methods. The direct proton transfer reaction of the parent amine, 1,8-(RNH)<sub>2</sub>C<sub>10</sub>H<sub>6</sub>, with TaMe<sub>3</sub>Cl<sub>2</sub> led to the elimination of methane and formation of TaCl<sub>3</sub>[1,8-(RN)<sub>2</sub>C<sub>10</sub>H<sub>6</sub>]. Clearly there were additional Me/Cl exchanges involved in this reaction. An alternative reaction of the dilithiated amido species, Li<sub>2</sub>R<sub>2</sub>DAN, with TaMe<sub>3</sub>Cl<sub>2</sub> or [Ta(NEt<sub>2</sub>)<sub>2</sub>Cl<sub>3</sub>] yielded TaMe<sub>3</sub>[1,8-(RN)<sub>2</sub>C<sub>10</sub>H<sub>6</sub>] and TaCl(NEt<sub>2</sub>)<sub>2</sub>[1,8-(RN)<sub>2</sub>C<sub>10</sub>H<sub>6</sub>], respectively as shown in Figure 1.10. X-ray structural studies of these complexes revealed the flexible coordination behavior of R,R'-DAN by demonstrating that the ligand bonded to Ta with a coordination array dependent on the identity of the other ligands bonded to tantalum. Computational analysis of these complexes confirmed that the energetic components for binding of R,R'-DAN to these TaX<sub>3</sub><sup>2+</sup> fragments were dominated by the electronic features of the metal fragment. Also, Figure 1.10 shows that the nitrogen donor ligand 2-methylpyrroline led to cleavage of the Ta-Cl bond in **1** and formation of **2**. The chloro ligands in these Ta species can be replaced by benzyl groups using a Grignard reagent giving **4**. Likewise, metathesis of Ta-Cl was also observed by adding two equivalents of LiCp\* and forming the pentamethylcyclopentadienyl compound **3**<sup>38,39</sup>.

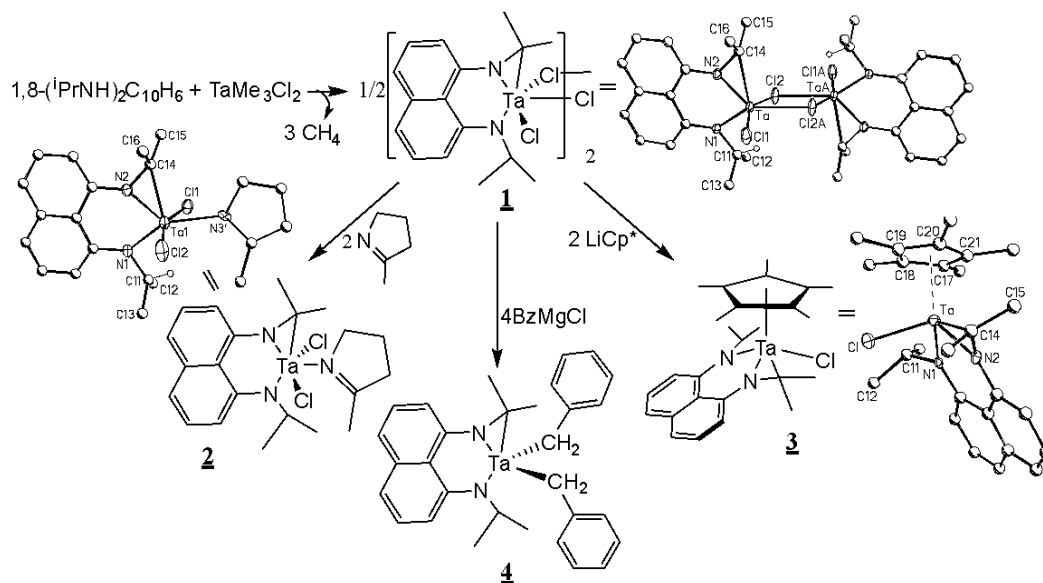


**Figure 1.10:** The isolation of metallaaziridine complex  $[\eta^3(\text{Me}_2\text{CN})(\text{Me}_2\text{CHN})\text{C}_{10}\text{H}_6]\text{TaCl}_2$  by  $\beta$ -H activation.

Bis(imido)W(VI) complexes of dianionic N, N'-disubstituted 1,8-diamidonaphthalene ( $\text{R}_2\text{DAN}^{2-}$ ) ( $\text{R} = i\text{Pr}, 3,5\text{-Me}_2\text{C}_6\text{H}_3$ ) were reported by a previous member in our lab. One of the main features of this reaction Figure 1.11 is that the X-ray structure and computational analysis of  $\text{W}(=\text{NtBu})_2[1,8-(i\text{PrN})_2\text{C}_{10}\text{H}_6]$  revealed that the nonplanar coordination of the  $(i\text{PrN})_2\text{C}_{10}\text{H}_6$  ligand to the W center is favored to allow for increased electron donation from the amido N centers to the  $\text{W}^{40}$ .

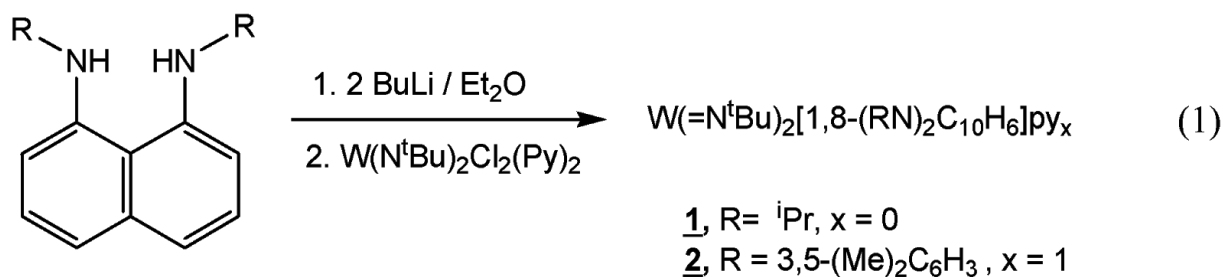


**Figure 1.11:** Synthesis of bis(imido)W(VI) complexes

Furthermore, experimental studies revealed that the R,R'-DAN<sup>2-</sup> amido linkage is the preferred reaction site with isocyanates to yield tridentate amido/N,N'-ureato ligands and that reactions with Al<sub>2</sub>Me<sub>6</sub> lead to methylation of W and formation<sup>32</sup> of heterobimetallic species via a μ<sub>2</sub>-bridging interaction of the R,R'-DAN<sup>2-</sup> ligand Figure 1.12.

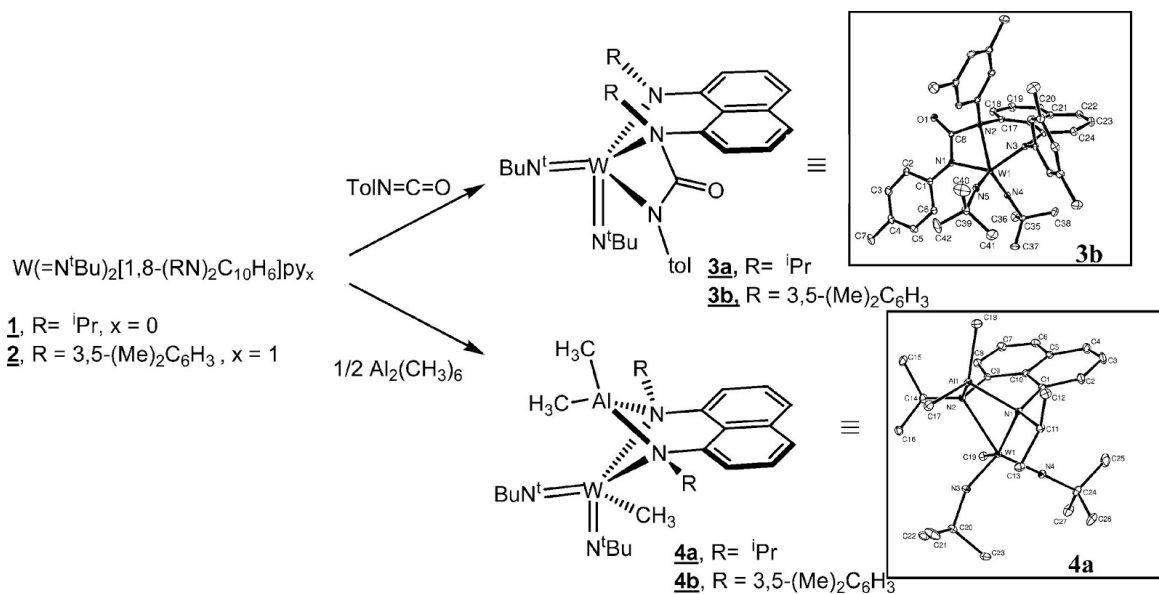


**Figure 1.12:** The reactivity of bis(imido)W(VI) complexes.

Group 15 chemistry of the R,R'DAN<sup>2-</sup> framework using P, As, Sb<sup>41,42,43</sup> was examined in our labs. This chemistry generated a new heterocyclic phosphonium cation captured in a six-membered, electron-rich framework. The cation reacts quantitatively with 1 equiv of Wilkinson's catalyst, Rh(PPh<sub>3</sub>)<sub>3</sub>Cl, to form a cationic rhodium-phosphonium complex, the first to be characterized in the solid state. We extended this chemistry to a family of diamidochloropnictines ClPn(NR)<sub>2</sub>C<sub>10</sub>H<sub>6</sub> (Pn = P, As, Sb) which were prepared via the dehydrohalide coupling reactions of N,N'-diisopropyl-1,8-diaminonaphthalene, (iPrNH)<sub>2</sub>C<sub>10</sub>H<sub>6</sub>, or N,N'-diphenyl-1,8-diaminonaphthalene, (PhNH)<sub>2</sub>C<sub>10</sub>H<sub>6</sub>, with the appropriate pnictogen trichloride. Using halogen abstraction reactions, cations of these compounds were formed and structurally characterized as shown in Figure 1.13.

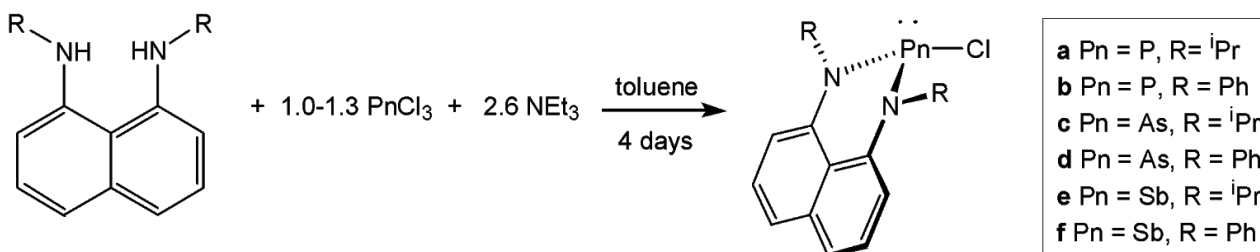


**Figure 1.13:** Synthetic approaches to group 15.

## 1.4 References

---

- (1) Atkins, P. W. Shriver & Atkins' Inorganic Chemistry. *Shriver Atkin's Inorg. Chem.* **2010**, 851.
- (2) McCleverty, J. a. Volume 1: Fundamentals: Ligands, Complexes, Synthesis, Purification, and Structure. *Transition* **2003**, 1.
- (3) Bowman-James, K. Alfred Werner Revisited: The Coordination Chemistry of Anions. *Acc. Chem. Res.* **2005**, 38 (8), 671–678.
- (4) Haas, K. L.; Franz, K. J. Application of Metal Coordination Chemistry To Explore and Manipulate Cell Biology. **2009**, 109, 4921–4960.
- (5) Jones, C.; Stasch, A. *Alkaline-Earth Metal Compounds*; **2013**; 45.
- (6) Miessler, G. L.; Fischer, P. J.; Tarr, D. A.; Macrae, C. F.; Bruno, I. J.; Chisholm, J. A.; Edgington, P. R.; McCabe, P.; Pidcock, E.; Rodriguez-Monge, L.; *Inorganic Chemistry*; **2008**; 41.
- (7) Karlin, K. D. *Progress in Inorganic Chemistry*; **2012**; 57.
- (8) Lucas, H. R.; Meyer, G. J.; Karlin, K. D. Carbon Monoxide, and Nitrogen Monoxide Ligand Dynamics in Synthetic Heme and Heme-Copper Complex Systems. *J. Am. Chem. Soc.* **2009**, 131, 13924–13925.
- (9) Holt, S. L. *Inorganic Syntheses*; 2006; 22.
- (10) Bourget-Merle, L.; Lappert, M. F.; Severn, J. R. The Chemistry of  $\beta$ -Diketiminatometal Complexes. *Chem. Rev.* **2002**, 102, 3031–3065.
- (11) Togni, A.; Venanzi, L. M. Nitrogen Donors in Organometallic Chemistry and Homogeneous Catalysis BT - Angewandte Chemie International Edition in English. **1994**, 33, 497–526.

- (12) Chen, C.; Bellows, S. M.; Holland, P. L. Tuning Steric and Electronic Effects in Transition-Metal  $\beta$ -Diketiminato Complexes. *Dalt. Trans.* **2015**, *44*, 16654–16670.
- (13) Lucht, B. L.; Bernstein, M. P.; Remenar, J. F.; Collum, D. B. Polydentate Amine and Ether Solvates of Lithium Hexamethyldisilazide (LiHMDS): Relationship of Ligand Structure, Relative Solvation Energy, and Aggregation State. *J. Am. Chem. Soc.* **1996**, *118*, 10707–10718.
- (14) Tsai, Y. C. The Chemistry of Univalent Metal  $\beta$ -Diketiminates. *Coord. Chem. Rev.* **2012**, *256*, 722–758.
- (15) Bai, G.; Wei, P.; Das, A.; Stephan, D. Mono- and Bimetallic (NacNac) Ni Cyclopentadienyl Complexes. *Organometallics* **2006**, *46*, 5870–5878.
- (16) McGeachin, S. G. Synthesis and Properties of Some  $\beta$ -Diketimines Derived from Acetylacetonone, and Their Metal Complexes. *Can. J. Chem.* **1968**, *46*, 1903–1912.
- (17) Roesky, P. W. Bulky Amido Ligands in Rare Earth Chemistry - Syntheses, Structures, and Catalysis. *Zeitschrift für Anorg. und Allg. Chemie* **2003**, *629*, 1881–1894.
- (18) Tomson, N. C.; Arnold, J.; Bergman, R. G. Halo, Alkyl, Aryl, and Bis(imido) Complexes of Niobium Supported by the  $\beta$ -Diketiminato Ligand. *Organometallics* **2010**, *29*, 2926–2942.
- (19) Basuli, F.; Kilgore, U. J.; Brown, D.; Huffman, J. C.; Mindiola, D. J. Terminal Zirconium Imides Prepared by Reductive C-N Bond Cleavage. *Organometallics* **2004**, *23*, 6166–6175.
- (20) Camp, C.; Arnold, J. On the Non-Innocence of “Nacnacs”: Ligand-Based Reactivity in  $\beta$ -Diketiminato Supported Coordination Compounds. *Dalt. Trans.*

- 2016**, *45*, 14462–14498.
- (21) Lyashenko, G.; Herbst-Irmer, R.; Jancik, V.; Pal, A.; Mösch-Zanetti, N. C. Molybdenum Oxo and Imido Complexes of Beta-Diketiminato Ligands: Synthesis and Structural Aspects. *Inorg. Chem.* **2008**, *47*, 113–120.
- (22) Jiménez, M. V.; Sola, E.; Egea, M. a; Huet, a; Francisco, a C.; Lahoz, F. J.; Oro, L. a. Key Factors Determining the Course of Methyl Iodide Oxidative Addition to Diamidonaphthalene-Bridged diiridium(I) and dirhodium(I) Complexes. *Inorg. Chem.* **2000**, *39*, 4868–4878.
- (23) Jiménez, M. V.; Sola, E.; Francisco, A. C.; Oro, L. A.; Lahoz, F. J.; Martínez, A. P. Methylene- and Diamidonaphthalene-Bridged diiridium(III) Complexes. *Inorganica Chim. Acta* **2003**, *350*, 266–276.
- (24) Clegg, W.; Horsburgh, L.; Mulvey, R. E.; Ross, M. J.; Rowlingsb, R. B.; Wilsonb, V. William Clegg,” Lynne Horsburgh,” Robert E. Mulvey,b\* Michael J. ROSS,~ Renk B. Rowlingsb and Victoria Wilsonb ‘. **1998**, 5387 (97).
- (25) Umaphy, P.; Harnesswala, R. A.; Dorai, C. S. Synthesis and Spectral Studies on Palladium and Platinum Complexes with Mono- and Bidentate N-Donor Organic Ligands and Their Interaction with Calf Thymus DNA in Solution. *Polyhedron* **1985**, *4* (9), 1595–1602.
- (26) Matsuzaka, H.; Kamura, T.; Ariga, K.; Watanabe, Y.; Okubo, T.; Ishii, T.; Yamashita, M.; Kondo, M. Preparation , Structure , and Reactivities of Amido-Bridged Dinuclear Rhodium ( III ) and Rhodium ( II ) Complexes. *Organometallics* **2000**, *19*, 216–218.
- (27) Cabeza, J. A.; Nöth, H.; Rosales-Hoz, M. D. J.; Sánchez-Cabrera, G. Reactivity of

- Triosmium Carbonyl Clusters with 1,8-Diaminonaphthalene - Synthesis and Structural Characterization of Amido, Diamido, and C-Metalated Trinuclear Derivatives. *Eur. J. Inorg. Chem.* **2000**, 11, 2327–2332.
- (28) Maruyama, S.; Kawanishi, Y. Syntheses and Emission Properties of Novel Violet-Blue Emissive Aromatic bis(diazaborole)s Electronic Supplementary Information (ESI) Available: Pictures DMF Using 366 Nm as Excitation Wavelength. *J. Mater. Chem.* **2002**, 12, 2245–2249.
- (29) Goetze, R.; Noth, H. Beitrage Zur Chemie Des Bors Xciii . Tricarbonylchromkomplexe von Benzodiazaborolen, Phenylboranen Und Verwandten Verbindungen. *J. Organomet. Chem.* **1978**, 145, 151–166.
- (30) Stokes, F. A.; Vincent, M. A.; Hillier, I. H.; Ronson, T. K.; Steiner, A.; Wheatley, A. E. H.; Wood, P. T.; Wright, D. S. Reactions of Cp<sub>2</sub>M (M = Ni, V) with Dilithium Diamido-Aryl Reagents; Retention and Oxidation of the Transition Metal Ions. *Dalton Trans.* **2013**, 42, 13923–13930.
- (31) Collman, J. P.; Zhong, M.; Zhang, C.; Costanzo, S. Catalytic Activities of Cu ( II ) Complexes with Nitrogen-Chelating Bidentate Ligands in the Coupling of Imidazoles with Arylboronic Acids N -Arylimidazoles Are Common Motifs in Pharmaceuti- Cal Research because of Their Biomedical Use as Throm- Boxane Sy. *J. Org. Chem.* **2001**, 66, 7892–7897.
- (32) Keller, P. C.; Rund, J. V. Reactions of Diborane with Some Chelating Bidentate Ligands. A One-Step Synthesis of [(LL)BH<sub>2</sub>]B<sub>2</sub>H<sub>7</sub> Salts. *Inorg. Chem.* **1979**, 18 , 3197–3199.
- (33) Onak, T.; Rosendo, H.; Siwapinyoyos, G.; Kubo, R.; Liauw, L. Reaction of 1,8-

- Bis(dimethylamino)naphthalene, a Highly Basic and Weakly Nucleophilic Amine, with Several Polyboranes and with Boron Trifluoride. *Inorg. Chem.* **1979**, *18*, 2943–2945.
- (34) Schaeffer, C. D.; Zuckerman, J. J. Tin(II) Organosilylamines. *J. Am. Chem. Soc.* **1974**, *96*, 7160–7162.
- (35) Bazinet, P.; Yap, G. P. A.; Richeson, D. S. Synthesis and Properties of a germanium(II) Metalloheterocycle Derived from 1,8-Di(isopropylamino)naphthalene. A Novel Ligand Leading to Formation of Ni{Ge[(iPrN)2C10H6]}4. *J. Am. Chem. Soc.* **2001**, *123*, 11162–11167.
- (36) Nowik, I.; Spinney, H. A.; Richeson, D. S.; Herber, R. H. Static and Dynamic Disorder in Organotin Compounds: A Bis(amido)stannylene Coordinated by N,N'-diisopropyl-1,8-Diamidonaphthalene. *J. Organomet. Chem.* **2007**, *692*, 5680–5682.
- (37) Bazinet, P.; Yap, G. P. A.; DiLabio, G. A.; Richeson, D. S. Synthesis and Molecular and Extended Structures for a Diaminonaphthalene-Derived Bis(amido)stannylene. *Inorg. Chem.* **2005**, *44*, 4616–4621.
- (38) Lavoie, N.; Gorelsky, S. I.; Liu, Z.; Burchell, T. J.; Yap, G. P. A.; Richeson, D. S. Disubstituted 1,8-Diamidonaphthalene Ligands as a Flexible, Responsive, and Reactive Framework for Tantalum Complexes. *Inorg. Chem.* **2010**, *49*, 5231–5240.
- (39) Bazinet, P.; Yap, G. P. A.; Richeson, D. S. Metallaaziridine Complexes of Tantalum Derived from 1,8-Bis(isopropylamino)naphthalene via B-H Activation. *Organometallics* **2001**, *20*, 4129–4131.

- (40) Lavoie, N.; Ong, T.; Gorelsky, S. I.; Korobkov, I.; Yap, G. P. A.; Richeson, D. S. Bis(imido)W(VI) Complexes Chelated by N,N'-Disubstituted 1,8-Diamidonaphthalene : An Analysis of Bonding , Isocyanate Insertion , and Al-Me Transfer. *Organometallics* **2007**, 6586–6590.
- (41) Spinney, H. A.; Korobkov, I.; DiLabio, G. A.; Yap, G. P. A.; Richeson, D. S. Diamidonaphthalene-Stabilized N-Heterocyclic Pnictogenium Cations and Their Cation-Cation Solid-State Interactions. *Organometallics* **2007**, 26 (20), 4972–4982.
- (42) Spinney, H. A.; Korobkov, I.; Richeson, D. S. Diamidonaphthalene-Supported Pnictogenium Cations: Synthesis of an N-Heterocyclic Stibenium Cation by a Novel Protonation Route. *Chem. Commun. (Camb)*. **2007**, No. 16, 1647–1649.
- (43) Spinney, H. A.; Yap, G. P. A.; Korobkov, I.; DiLabio, G.; Richeson, D. S. Construction of a Stable N-Heterocyclic Phosphenium Cation with an Electron-Rich Framework and Its Complexation to Rhodium. *Organometallics* **2006**, 25 (15), 3541–3543.

# Chapter II

## Ligand Synthesis

### 2.1 Introduction

It should be clear from the introduction that a key component of this thesis is to design and prepare 1,8-disubstituted diaminonaphthalene ( $H_2R,R'$ -DAN) as a proligand to dianionic  $R,R'$ -DAN<sup>2-</sup> (Figure 2.1). The current status of the literature on this topic was reviewed in Chapter I, which documented that most of the reports in the literature employed a silylated derivative (e.g.,  $R = SiR'_3$ )<sup>1</sup>. As this project was initiated, we suspected that the lack of broader application of this ligand was due to unwanted reactions involving the trialkylsilyl groups. Similar reactions had been observed with *N,N*-bis(trimethylsilyl)-*o*-phenylenediamine, which was shown to undergo *N*-SiMe<sub>3</sub> bond cleavage<sup>2</sup>. Based on this hypothesis, carbon-based substituents were targets as they would provide strong, stable C-N bonds to the diamine frame minimizing ligand rearrangements. Therefore, the focus of this thesis is on the preparation of ligands with alkyl and aryl substituents.

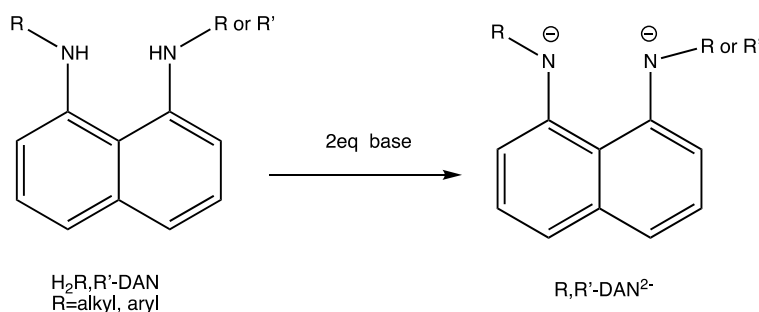


**Figure 2.1:** Deprotonating of 1,8-disubstituted diaminonaphthalene.

With these general goals in mind, we targeted the specific ligands,  $(\text{NpN})(^i\text{PrN})\text{C}_{10}\text{H}_6$ ,  $(\text{NpNH})_2\text{C}_{10}\text{H}_6$ ,  $(^i\text{PrNH})_2\text{C}_{10}\text{H}_6$  and  $(\text{PhN})_2\text{C}_{10}\text{H}_6$ . This provided an array of alkyl and aryl groups for exploring this chemistry. The synthetic methods for preparing proligands with primary, secondary and aryl groups are different. These reactions were based on the reductive amination<sup>3</sup>, which is common reaction in organic chemistry to prepare amines.

In order to prepare  $(\text{NpN})(^i\text{PrN})\text{C}_{10}\text{H}_6$  and  $(\text{NpNH})_2\text{C}_{10}\text{H}_6$  ligands, the introduction of a primary alkyl group was required. The approach employed for these targets was based on a nucleophilic acyl substitutions reaction. In this reaction amidation with acyl halide yields an amide. After that, a reduction of the carbonyl function of the amide yields the desired primary alkyl amine product (Figure 2.2).<sup>4</sup>

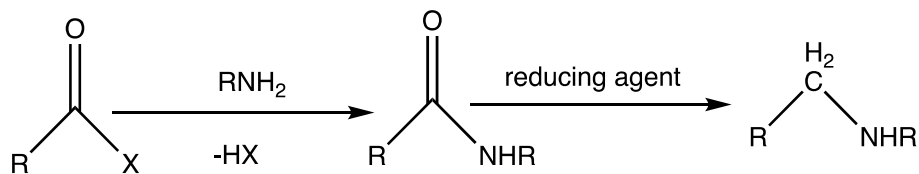


**Figure 2.2:** Generic scheme for the preparation of amine by using acyl halide.

The preparation of the  $(^i\text{PrNH})_2\text{C}_{10}\text{H}_6$  proligand, possessing secondary alkyl substituents, was designed around the well-known reductive amination reaction as shown Figure 2.3. This reaction provides for controlled alkylation of amine and involves the formation of an imine by condensation of a primary amine with a carbonyl compound.

The product of this reaction is then hydrogenated (reduced) to produce a final alkylated amine compound.

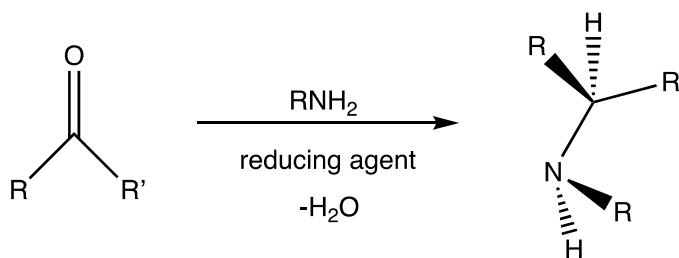


**Figure 2.3:** Generic scheme of the reductive amination reaction.

An alternative method was needed to introduce aryl groups. A copper catalyzed coupling reaction<sup>5</sup>, is one of the most efficient and convenient methods for the preparation of N-aryl 1,8-diaminonaphthalene. In this reaction, a mixture of diamine and CuI was used for coupling of aryl iodides with 1H,3H-perimidin-2-one under catalysis conditions. (Figure 2.4).<sup>6</sup>

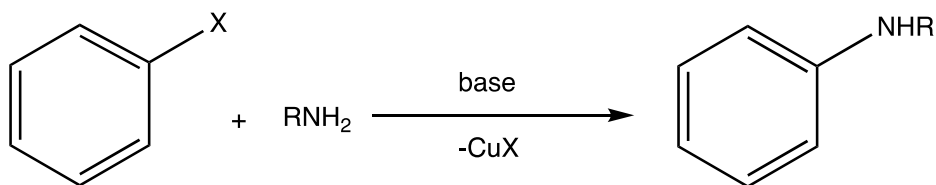


**Figure 2.4:** Generic scheme for the Cu-catalyzed cross-coupling of amine

## 2.2 Results and Discussion

### 2.2.1 N, N'- alkyl -1,8-diaminonaphthalene

Synthesis of  $(\text{NpCH}_2\text{NH})_2\text{C}_{10}\text{H}_6$  was based on the amidation with acyl halide as shown in Figure 2.5. Direct reaction of two equivalents of pivaloyl chloride with 1,8-diaminonaphthalene proceeded smoothly to yield the diamide intermediate<sup>7</sup> **2.3**. This compound was characterized by <sup>1</sup>H NMR. The <sup>1</sup>H NMR shows a unique singlet that integrates 18 protons from methyl groups for the neopentyl substituent. Reduction of both amide groups was affected by reaction of **2.3** with LiAlH<sub>4</sub> at low temperature. Intermediate **2.3** could be used without purification and followed by the addition of LiAlH<sub>4</sub> solution in dry ether at 0°C then the mixture was stirred overnight at room temperature, gave the final dineopentyl proligand **2.4**. Also, this reaction required anhydrous conditions, as well as an excess reducing agent. NaBH<sub>4</sub> can be used as well but is less reactive than LiAlH<sub>4</sub>. The mixture was quenched and then extracted with ether; the organic solution was separated from the aqueous portion, from which the product was further extracted with ether. The combined organic solution was dried over MgSO<sub>4</sub> and filtered. Pure **2.4** was obtained by silica gel column chromatography using a mixture of hexanes: ether. The purple solid isolated from this reaction was characterized by NMR spectroscopy and single crystal X-ray analysis. The <sup>1</sup>H NMR shows a single peak at δ 0.9 representing the methyl groups for the neopentyl substituent and one broad NH peak at δ 5.37 which indicate that the ligand **2.4** is a symmetric molecule. Furthermore, the <sup>13</sup>C

NMR displayed 6 carbons signals for the naphthyl ring. (Figure 2.5). Definitive evidence for this structure  $(\text{NpNH})_2\text{C}_{10}\text{H}_6$ , (**2.4**) was provided by characterization through single crystal X-ray diffraction analysis. This study revealed the molecular structure shown in Figure 2.12.

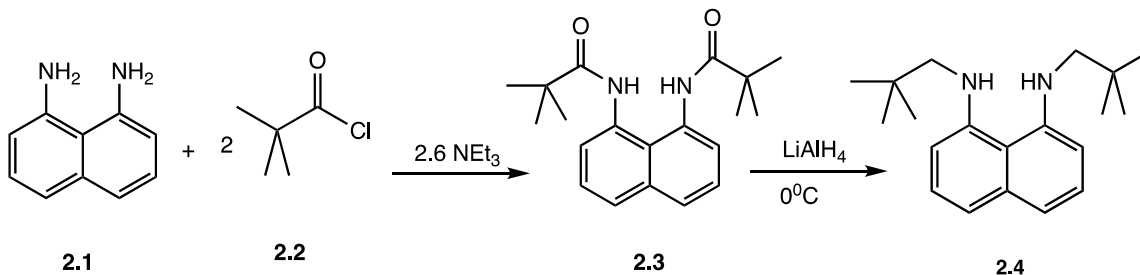


**Figure 2.5:** Preparation of  $(\text{NpNH})_2\text{C}_{10}\text{H}_6$  group

The amidation procedure does not provide a means to introduce a secondary alkyl substituent, and as a result, I attempted to use the reductive amination route described below in Figure 2.6. In order to incorporate an isopropyl substituent, the reaction would be carried out between acetone and 1,8-diaminonaphthalene. As described in more detail below, the condensation reaction of 1,8-diaminonaphthalene and acetone does not yield the simple imine that was targeted. Rather, the aminal species **2.6** was obtained. The most direct evidence of this reaction was the appearance of two equivalent singlets at  $\delta$  2.6 ppm for the methyl groups in the aminal **2.6**.

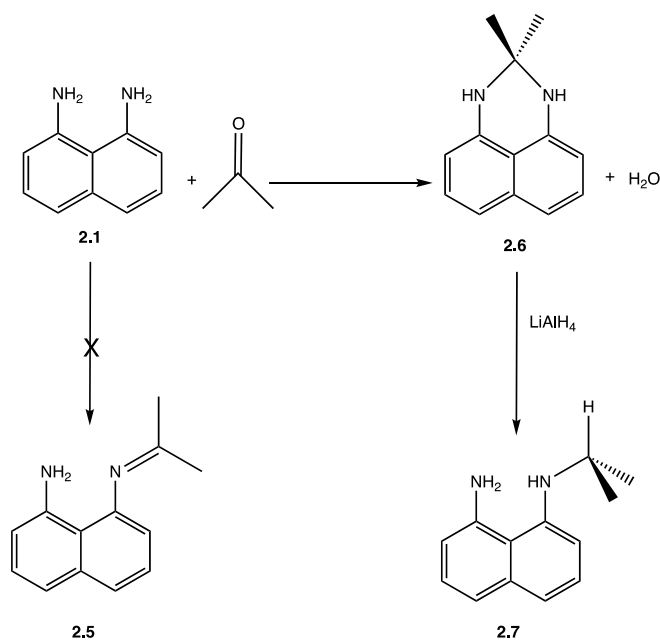


**Figure 2.6:** Initial attempts for the alkylation of 1,8-DAN

Fortunately, reduction of this compound afforded the N-isopropyl-1,8-diaminonaphthalene species (**2.7**) shown in Figure 2.6. The preparation of this compound provides an interesting possibility of preparing proligand with two different alkyl substituents. For example, N-(isopropyl)N'-(neopentyl)-1,8-diaminonaphthalene ( $(i\text{PrNH})(\text{NpNH})\text{C}_{10}\text{H}_6$ ) could be prepared from this compound as outlined in Figure 2.7. Addition of pivaloylchloride,  $(\text{CH}_3)_3\text{CCOCl}$  to **2.7** lead to the formation of trimethylacetamide intermediate **2.8**,  $(i\text{PrNH})(\text{NpCONH})\text{C}_{10}\text{H}_6$  (Figure 2.7). Following an analogous reduction procedure with  $\text{LiAlH}_4$  in anhydrous ether led to the formation of  $(\text{NpNH})(i\text{PrNH})\text{C}_{10}\text{H}_6$  **2.9**. The  $^1\text{H}$  NMR spectra show two different broad NH peaks at  $\delta$  6.0 and  $\delta$  5.1 ppm and unique signals for both isopropyl and neopentyl group at  $\delta$  3.6 ppm and  $\delta$  1.2 ppm respectively. These NMR resonances support an unsymmetrical molecular as well as  $^{13}\text{C}$  NMR that is consistent with an unsymmetrical environment in

the naphthyl ring this result in different N-substitutes. In the X-ray structure of (*i*PrNH)(NpNH)C<sub>10</sub>H<sub>6</sub> Table 2.1 the compound crystallizes in the monoclinic space group P21/n and has two different groups isopropyl ,neopentyl groups attached to nitrogen. In addition to the structural diagram of compound **2.9** provided in Figure 2.13, a summary of selected bond distances and angles is provided in Table 2.2.

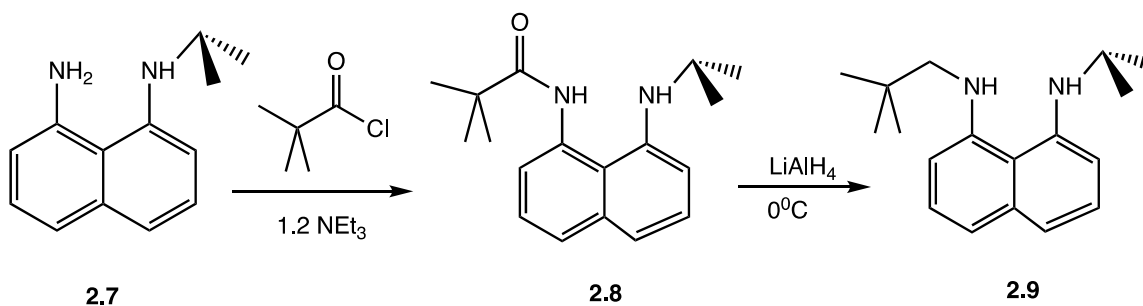


**Figure 2.7:** Preparation of (*i*PrNH)(NpNH)C<sub>10</sub>H<sub>6</sub> group

As was outlined above in Figure 2.6, the attempted imine formation from 1,8-diaminonaphthalene and acetone does not proceed. In fact, the product formed from this reaction is an amina **2.6**. (2,2-dimethyl-2,3- dihydroperimidine), which was identified by NMR spectroscopy with a <sup>13</sup>C NMR resonance for the quaternary carbon at 46.33 ppm.

As a result, the preparation of N,N'-diisopropyl-1,8-diaminonaphthalene (*i*PrNH)<sub>2</sub>C<sub>10</sub>H<sub>6</sub> as shown in Figure 2.8 was carried out in two sequential steps. The reduction steps were carried out under anhydrous conditions using a suspension of LiAlH<sub>4</sub> and cooling to 0°C with slow dropwise addition of the solution of amina **2.6** or **2.10**. These reactions generate hydrogen gas; therefore, they should be ventilated during the addition of amina solution. After the completion of the reaction, the excess hydride

reagent was quenched by adding isopropanol followed by water at low temperature. After the completion of the quenching, the resulting mixture was extracted with diethylether, the organic layer was dried ( $\text{Na}_2\text{SO}_4$ ) and the solvent was removed in vacuum. The residue was purified by silica gel column chromatography using a mixture of hexanes and ether. The first evidence for product formation was provided by the  $^1\text{H}$  NMR of this product shows a unique signal for the isopropyl peak at  $\delta$  3.6 ppm as a single septet.

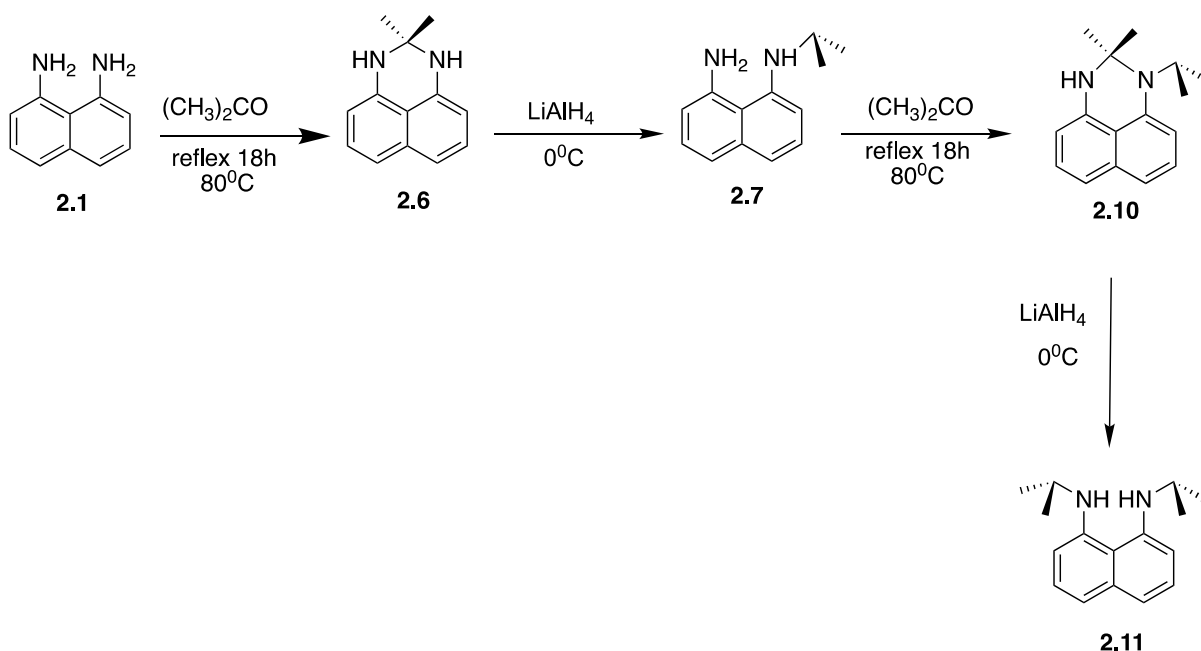


**Figure 2.8:** Preparation of  $(i\text{PrNH})_2\text{C}_{10}\text{H}_6$  ligand

It was observed that using a large excess of  $\text{LiAlH}_4$  transform the 2,2-dimethyl-2,3-dihydroperimidine **2.6** into the N-isopropyl-1,8-diaminonaphthalene derivative **2.7** (Figure 2.9). This reaction involves the breaking of C-N single bond and the opening of the amination ring. The exact mechanism for this reaction is not yet understood. However, a reasonable proposal is that the strongly basic  $\text{LiAlH}_4$  reagent deprotonates the amination **2.6** to form an anionic intermediate (Figure 2.9). Moreover, the localized negative charge on

the nitrogen could drive a rearrangement generating an imine derivative, which would be readily reduced by the excess of the  $\text{LiAlH}_4$ .

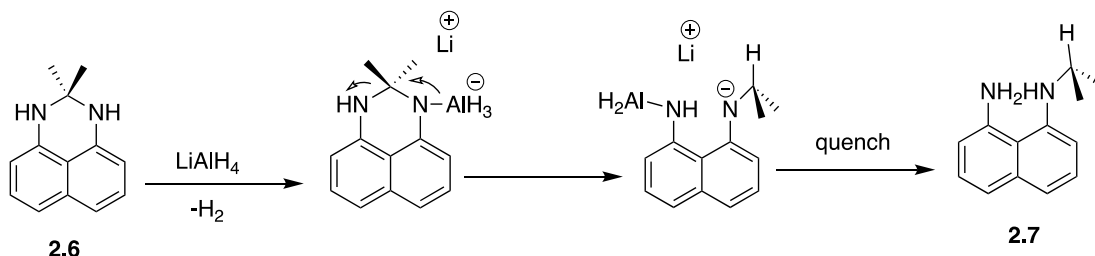


**Figure 2.9:** Proposed mechanism of reduction reactions.

### 2.2.2 N, N'-aryl-1,8-diaminonaphthalene

In addition to using alkyl groups to prepare disubstituted 1,8-diaminonaphthalene, it would be useful and interesting to explore the role of aryl groups. As outlined above, the amidation/reduction and reductive amination routes are not useful to this target. Our group has developed a method for the N,N'-diphenyl-1,8-diaminonaphthalene proligand that relies on a Cu catalyzed arylation of urea followed by conversion of the urea to an amine. To make this ligand we need to prepared 1H,3H-Perimidin-2-one<sup>8</sup> as starting material (Figure 2.10). The arylation of 1H,3H-perimidin-2-one **2.12** was carried out with iodobenzene and the catalyst mixture of  $\text{CuI}$ ,  $\text{K}_2\text{CO}_3$ , N,N'-dicyclohexylethane-1,2-diamine (0.50 g, 4.37mmol) with diphenyl ether as solvent. This solvent was chosen for its high boiling point since this reaction required heating to  $160^\circ\text{C}$  overnight under nitrogen atmosphere. The reaction follows a variant of the Goldberg reaction. The basic role of potassium carbonate is to neutralize the HI formed during the reaction. When the

reaction was cooled to room temperature, it was extracted with dichloromethane then purified by column chromatography to yield **2.13**. Finally, the free diamine **2.14** was formed through the reaction of this intermediate with 4 equivalents of  $\text{NaNH}_2$  at  $90^\circ\text{C}$  for 18 hours under nitrogen atmosphere. At the end, further purification is completed by extraction with dichloromethane as well as column chromatography with hexane and dichloromethane mixture. Although the preparation of *N,N'*-diphenyl-1,8-diaminonaphthalene required a quite complicated procedure including two applications of column chromatography, the anticipated compound was isolated successfully and characterized by  $^1\text{H}$  NMR,  $^{13}\text{C}$  NMR, and single crystal X-ray diffraction.

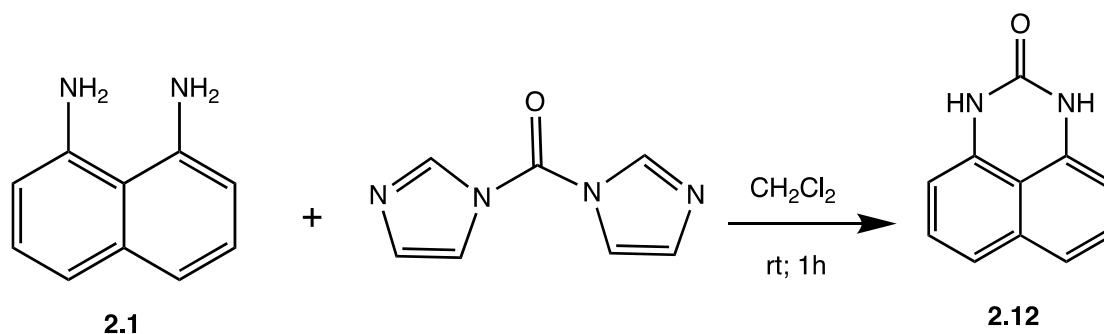


**Figure 2.10:** Preparation of 1H, 3H-perimidin-2-one

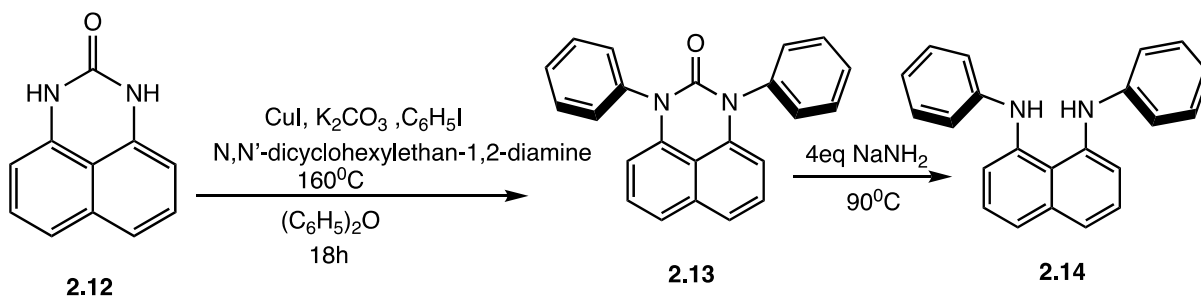


**Figure 2.11:** A copper catalyzed the reaction to prepare  $(\text{PhNH})_2\text{C}_{10}\text{H}_6$ .

More specifically,  $(\text{PhNH})_2\text{C}_{10}\text{H}_6$  gave NMR spectra for a symmetrical species with the observation of only three resonances for the phenyl groups in the  $^1\text{H}$  NMR and a single resonance attributed to the CH protons of the naphthyl protons ortho to the NHAr groups. The N-H peak in  $^1\text{H}$  NMR of **2.14** appeared as a single broad resonance at  $\delta$  7.15 ppm.

### **2.3 Conclusions**

Preparation of alkyl and aryl disubstituted 1,8-diaminonaphthalene pro-ligands ( $\text{H}_2\text{R}, \text{R}'\text{-DAN}$ ) have been successfully produced by amination and copper-catalyzed coupling reaction respectively. NMR, X-ray diffraction and element analysis provided a full characterization of these species, which allow help to study the structure of different complexes as seen in the following chapters

### **2.4 Experimental Section**

General Methods. All manipulations were carried out in either a nitrogen-filled dry box or under nitrogen using standard Schlenk line techniques. Unless otherwise noted, reaction solvents were sparged with nitrogen and then dried by passage through a column of activated alumina using an apparatus purchased from Anhydrous Engineering. Deuterated benzene was purchased from Aldrich Chemical Company and was dried by vacuum transfer from potassium. The following chemicals were purchased from Aldrich Chemical Company and used without purification: isopropanol, 1,8-diaminonaphthalene,

and LiAlH<sub>4</sub>. NMR spectra were run on either a Bruker Avance 400 MHz or a Bruker 600 MHz spectrometer, and <sup>13</sup>C{<sup>1</sup>H}NMR was on a Bruker 100 MHz or a Bruker 150 MHz with using deuterated chloroform or acetone as a solvent and internal standard.

The crystals of **2.4** and **2.7** were mounted on thin glass fibers using paratone oil. Prior to data collection, the crystals were cooled to 201(2) K. The data were collected on a Bruker AXS single-crystal diffractometer equipped with a sealed Mo tube (wavelength 0.71073 Å) and APEX II CCD detector. The raw data collection and processing were performed with Bruker APEX II software package<sup>10</sup>. Semi-empirical absorption corrections based on equivalent reflections were applied using SADABS<sup>44</sup>. The structures were solved by direct methods and refined with full-matrix least-squares procedures based on F<sup>2</sup>, using SHELXL<sup>11</sup> and WinGX<sup>12</sup>. All non-hydrogen atoms were refined anisotropically. All hydrogen atoms were placed in idealized positions. Displacement ellipsoid plots were produced using ORTEP.

#### **Preparation N,N'-dineopentyl-1,8-diaminonaphthalene, (NpCH<sub>2</sub>NH)<sub>2</sub>C<sub>10</sub>H<sub>6</sub> (**2.4**)**

Trimethylacetyl chloride (10.0g, 82.0mmol) **2.2** was slowly added to 1,8-diaminonaphthalene (5.0g, 31.6 mmol) **2.1** and excess amount of triethylamine base (10.0g, 99.0 mmol) in 50 THF ml at 0 °C. The reaction mixture was stirred overnight. The reaction mixture was filtered, and all volatiles were removed under vacuum to give 1,8-bis(pivaloylamino)naphthalene intermediate, (NpCONH)<sub>2</sub>C<sub>10</sub>H<sub>6</sub> **2.3** that was used

without further purification. In a Schlenk flask, lithium aluminum hydride (1.2g, 31.0 mmol) was dissolved in 50 ml of dry ether, cooled in ice bath. In a separate flask, the compound **2.3** (4.3g, 13.2 mmoles) was dissolved in ether and then added slowly to the solution to LiAlH<sub>4</sub> under nitrogen. The mixture was stirred for 18 h at room temperature and quenched with isopropanol followed by water. The organic layer was extracted with water, dried with sodium sulfate, and the solvent evaporated.<sup>3</sup> The product was purified by silica gel column chromatography using hexanes as the eluent to yield a purple solid. The product was recrystallized from ether cooled to -25<sup>0</sup>C, providing crystals **2.4** (3.71g, 94%)

<sup>1</sup>H NMR (CDCl<sub>3</sub>, 400MHz) [C<sub>10</sub>H<sub>6</sub>[NH{C(O)Np}]<sub>2</sub>]. (**2.3**): δ 1.33 (s, 18 H, <sup>t</sup>Bu), 7.38–7.70 (m, 6 H, C<sub>10</sub>H<sub>6</sub>), 8.31 (s, 2 H, NH).

<sup>1</sup>H NMR (CDCl<sub>3</sub>, 400MHz) (NPCH<sub>2</sub>NH)<sub>2</sub>C<sub>10</sub>H<sub>6</sub> (**2.4**). δ 0.91 (s, 18 H, <sup>t</sup>Bu), 2.74 (s, 4 H, CH<sub>2</sub>), 5.37 (s, 2 H, NH), 6.58–7.37 (m, 6 H, C<sub>10</sub>H<sub>6</sub>).

<sup>13</sup>C NMR: δ 28.1 [C(CH<sub>3</sub>)<sub>3</sub>], 31.8 [C(CH<sub>3</sub>)<sub>3</sub>], 58.5 (CH<sub>2</sub><sup>t</sup>Bu), 108.0, 119.7, 126.5, 137.7 and 147.7 (C<sub>10</sub>H<sub>6</sub>).

Analysis Calcd C<sub>20</sub>H<sub>30</sub>N<sub>2</sub> C, 80.48; H, 10.13; N, 9.39; Found C, 80.50; H, 10.13; N, 9.39%

### Preparation of 2,2-dimethyl-2,3-dihydroperimidine (2.6)

Dry acetone was first prepared by adding 5.0 g activated molecular sieves to (18.5g, 319 mmol) liquid acetone and the mixture was kept in a round flask for about 12 hours then the solvent was filtered. To the filtrate solvent (5.0 g, 31.6 mmol) of 1,8-diaminonaphthalene (**2.1**) was then added and the solution was refluxed at 80°C overnight. The reaction mixture was filtered, and all volatiles were removed under vacuum to give 6.12g (98%) of a red/purple solid that we have identified as the aminal, 2,2-dimethyl-2,3-dihydroperimidine (**2.6**).

<sup>1</sup>H NMR (CDCl<sub>3</sub>, 400MHz): δ 7.17-7.32 (m, 4H, CH), 6.45 (d, 2H, CH), 4.18 (br, 2H, NH), 1.40 (s, 6H, CH<sub>3</sub>).

<sup>13</sup>C NMR (CDCl<sub>3</sub>, 300MHz): δ 140.3, 134.4, 126.9, 116.6, 112.6, 105.6 (C<sub>arom</sub>), 64.3 (CHMe<sub>2</sub>), 28.4 (CH(CH<sub>3</sub>)<sub>2</sub>).

Analysis Calcd C<sub>13</sub>H<sub>14</sub>N<sub>2</sub> C, 78.75; H, 7.12; N, 14.13; Found C, 78.79; H, 7.23; N, 13.98

#### **Preparation of N-(isopropyl)-1,8-diaminonaphthalene, (*i*PrNH)(NH<sub>2</sub>)C<sub>10</sub>H<sub>6</sub> (**2.7**)**

A sample of compound **2.6** (5.0g, 25.2 mmol) was dissolved in diethylether and added dropwise to a suspension of LiAlH<sub>4</sub> (2.9g, 76 mmol) in 100 ml of diethylether at 0°C. The reaction was allowed to warm to room temperature and stirred for 12 hrs before quenching, at 0°C, with isopropanol followed by water. This organic layer of the mixture was extracted with diethylether and dried under vacuum to give **2.7** as a dark purple oil

(4.91g, 98%).  $^1\text{H}$  NMR ( $\text{CDCl}_3$ , 300MHz):  $\delta$  7.12-7.26 (m, 4H, CH), 6.55-6.59 (m, 2H, CH), 4.89 (br, 3H, NH), 3.60 (sept, 1H,  $\text{CHMe}_2$ ), 1.26 (d, 6H,  $\text{CH}_3$ ).

$^{13}\text{C}$  NMR ( $\text{CDCl}_3$ , 300MHz):  $\delta$  145.3, 144.1, 137.1, 126.2, 125.9, 119.9, 118.7, 117.3, 112.1, 108.5 ( $\text{C}_{\text{arom}}$ ), 45.8 ( $\text{CHMe}_2$ ), 22.7( $\text{CH}_3$ ).

Analysis Calcd  $\text{C}_{13}\text{H}_{16}\text{N}_2$  C, 77.96; H, 8.05; N, 13.99; Found C, 78.21; H, 8.35; N, 14.32.

### **The synthesis of N-(isopropyl)-N'-(neopentyl)-1,8-diaminonaphthalene**

#### **(NpN)( $^i\text{PrN}$ ) $\text{C}_{10}\text{H}_6$ (2.9)**

A sample of compound **2.7** (4.12g, 20.6 mmol) was dissolved in diethylether and then added dropwise to (2.48g, 20.6 mmol) pivaloylchloride in a round bottom flask. The mixture was then added to an excess amount of trimethylamine base and left overnight. The reaction mixture was dried under vacuum to give trimethylacetamide intermediate, ( $^i\text{PrNH}$ )( $^t\text{BuCONH}$ ) $\text{C}_{10}\text{H}_6$  **2.8** that was used without further purification. In a Schlenk flask, lithium aluminum hydride (1.46 g, 38.4 mmol) was dissolved in 50 mL of dry ether, cooled in an ice bath and stirred for 1 h. Then compound **2.7** (4.37 g, 15.3 mmol) was dissolved in ether and added slowly to the  $\text{LiAlH}_4$  solution under nitrogen. The mixture was stirred for 18 h at room temperature and quenched with isopropanol followed by water. The organic layer was extracted with water, dried with sodium sulfate, and the solvent evaporated. The product was purified by silica gel column

chromatography using hexanes as the eluent to yield a purple solid, and the product was recrystallized from pentene -25°C, providing colorless crystals (3.11g, 75%).

<sup>1</sup>H NMR (CDCl<sub>3</sub>, 400MHz): δ 7.19(m, 4H), 6.60 (dd, 2H), 5.23 (br, 2H), 3.65 (sept, 1H, J<sub>HH</sub>=6.4 Hz), 2.91 (s, 2H), 1.29 (d, 6H, J<sub>HH</sub>=6.4 Hz), 1.12 (s, 9H).

<sup>13</sup>C{<sup>1</sup>H} NMR (500MHz, CDCl<sub>3</sub>): δ 147.2, 144.8, 136.8, 126.1, 125.6, 118.7, 117.8, 117.3, 109.3, 105.4 (C<sub>arom</sub>), 57.2 (CH<sub>2</sub>Me<sub>3</sub>), 45.2 (CHMe<sub>2</sub>), 31.2(CMe<sub>3</sub>), 27.9 (CH<sub>3</sub>), 22.7 (CH<sub>3</sub>).

Analysis Calcd C<sub>18</sub>H<sub>26</sub>N<sub>2</sub>, 79.95; H, 9.69; N, 10.36; Found C, 79.63; H, 10.01; N, 10.39.

#### **Preparation of N, N'-diisopropyl-1, 8-diaminonaphthalene, (iPrNH)<sub>2</sub> C<sub>10</sub>H<sub>6</sub> (2.11)**

A sample of compound **2.7** (4.91g, 24.5 mmol) was dissolved in dried acetone (29.0g, 500 mmol) in an around the flask. The reaction was refluxed overnight. Then the product was isolated as a purple oil. A sample of the resulting aminal (14.0g, 58.33 mmol) **2.10** was allowed to react with LiAlH<sub>4</sub> (6.0g, 160 mmol) and stirred overnight. The reaction was then quenched, at 0°C, with isopropanol followed by water. The resulting mixture was extracted with diethylether, dried and the solvent evaporated to yield **2.11** as a purple oil (10.5g, 74%). This product can be further purified by silica gel column chromatography using a mixture of hexanes and diethylether (9:1 ratio) as the eluent.

<sup>1</sup>H NMR (CDCl<sub>3</sub>, 400MHz): δ 7.19-7.24 (m, 4H, CH), 6.58 (m, 2H, CH), 5.36 (br, 2H, NH), 3.58 (sept, 2H, CHMe<sub>2</sub>, J=6.28Hz), 1.24 (d, 12H, CH<sub>3</sub>, J=6.28Hz).

$^{13}\text{C}\{^1\text{H}\}$  NMR ( $\text{CDCl}_3$ , 100 MHz):  $\delta$  145.0, 137.3, 125.9, 119.3, 117.9, 110.3 (C arom), 46.4 ( $\text{CHMe}_2$ ), 22.6 ( $\text{CH}_3$ ).

Analysis Calcd  $\text{C}_{16}\text{H}_{22}\text{N}_2\text{C}$ , 79.29; H, 9.15; N, 11.56; Found C, 79.53; H, 9.35; N, 11.19

### **Preparation of 1H, 3H-perimidin-2-one (2.12)**

To solution of 1,8- diamionaphthalene (10.g, 63.2 mmoles) in 50ml dichloromethane was added dropwise a solution of (10.64 g, 6.61 mmoles) carbonyldiimidazole in 100ml dichloromethane at room temperature over a period of 30 minutes. After a short time, the product began to precipitate as a reddish powder. After one hour the reaction was complete, and the mixture was filtered, and the solid washed with dichloromethane to yield dark red powder<sup>8</sup> (9.52 g, 95%).

$^1\text{H}$ -NMR (400 MHz,  $\text{DMSO-d}_6$ );  $\delta$  / ppm = 10.06 (s, 2H, NH); 7.18 (dd, J = 8.3 Hz, J = 7.3 Hz, 2H, Ar-H); 7.10 (dd, J = 8.4 Hz, J = 0.9 Hz, 2H, Ar-H); 6.51 (dd, J = 7.3 Hz, J = 1.0 Hz, 2H, Ar-H).

$^{13}\text{C}$ -NMR (75.4 MHz,  $\text{DMSO-d}_6$ );  $\delta$  / ppm = 150.0, 137.6, 134.1, 127.9, 117.6, 113.6, 103.9.

Anal. Calcd. for  $\text{C}_{11}\text{H}_8\text{N}_2\text{O}$  (184.19): C 71.73; H 4.38; N 15.21; found: C 71.53; H 4.45; N 15.32.

### Preparation of [1,8-(NHC<sub>6</sub>H<sub>5</sub>)C<sub>10</sub>H<sub>6</sub>] (Ph)<sub>2</sub>-C<sub>10</sub>H<sub>6</sub>(**2.14**)

To a round bottom flask in a glovebox was added **2.12** 1H,3H-perimidin-2-one (3.91 g, 21.7 mmol), iodobenzene (9.30g, 45.6mmol), CuI (0.83g, 4.36mmol), K<sub>2</sub>CO<sub>3</sub> (8.99 g, 65.1n mmol), N,N'-dicyclohexylethane-1,2-diamine (0.50 g, 4.37mmol) and diphenyl ether (14.78 g, 86.8mmol). The reaction mixture was removed from the glovebox and heated to reflux to 160 °C overnight under a nitrogen atmosphere. After cooling, the reaction mixture was extracted with dichloromethane. The solvent was removed under reduced pressure to give a brown solid. This material was purified by column chromatography (silica gel, 1:1 hexane: dichloromethane) to afford an intermediate product **2.11**. This product was then dissolved in 40 mL pyridine allowed to react with 4 equiv of NaNH<sub>2</sub> at 90°C for 18 hours under a nitrogen atmosphere. The pyridine solvent was removed at 50°C to afford a black solid, which was cooled in an ice bath and a mixture of THF and water was added. This mixture was extracted with dichloromethane. The CH<sub>2</sub>Cl<sub>2</sub> was removed under vacuum to give a gray solid. Purification by column chromatography (silica gel, 70:30 hexane: dichloromethane) afforded a light green solid (**2.14**) (3.98 g, 50 %).

<sup>1</sup>H NMR (C<sub>6</sub>D<sub>6</sub>, 600MHz): δ 7.42 (dd, 2H, J=9.37, 1.30Hz), 7.15 (s, 2H, NH), 7.13 (m,2H), 7.08 (d, 1H, J=1.14Hz), 7.07 (d, 1H, J=1.02Hz), 16.99-7.02(m, 4H), 6.74-6.77(m, 6H)

<sup>13</sup>C{<sup>1</sup>H} NMR (C<sub>6</sub>D<sub>6</sub>, 150 MHz): δ 144.99, 140.61, 137.41, 129.28, 126.11, 123.39, 122.10, 121.09, 118.21, 117.01 (C<sub>arom</sub>).

## Structural Determination

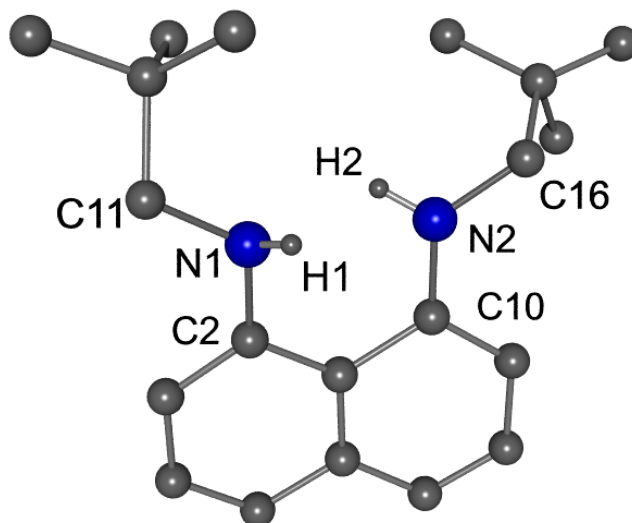


**Figure 2.12:** Structural representation of 2.4 (Hydrogen atoms bonded to carbon have been omitted for clarity)

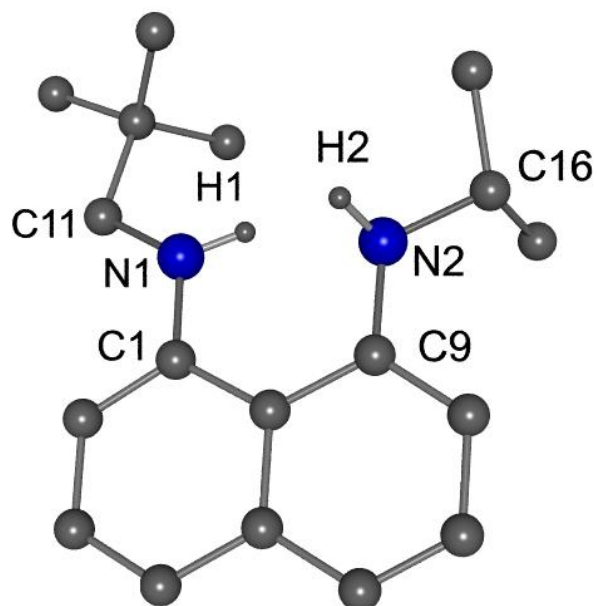


**Figure 2.13:** Structural representation of 2.7 (Hydrogen atoms bonded to carbon have been omitted for clarity)

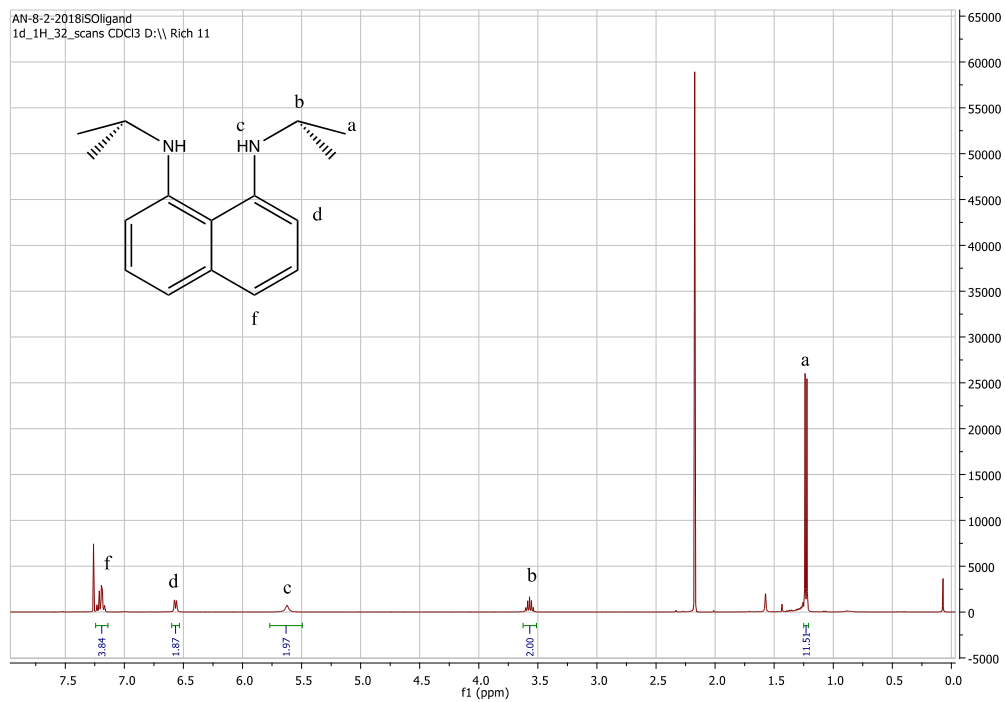


**Figure 2.14:** NMR Spectroscopy for N, N'-diisopropyl-1, 8-diaminonaphthalene,  
 $(i\text{PrNH})_2\text{C}_{10}\text{H}_6$

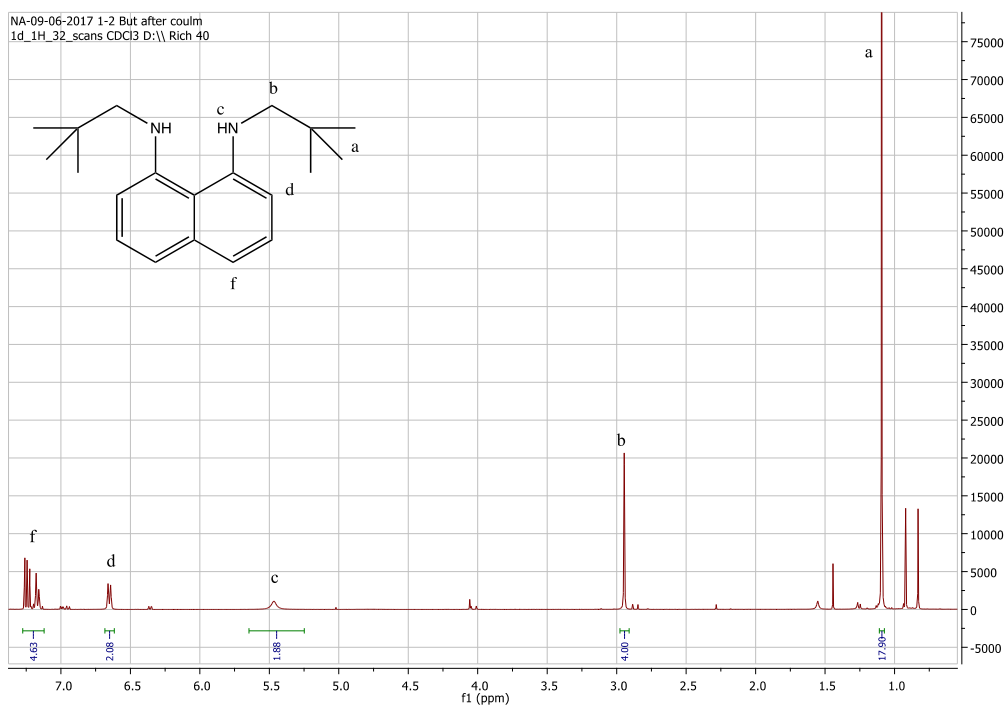


**Figure 2.15:** NMR Spectroscopy for N,N'-dineopentyl-1,8-diaminonaphthalene,  
 $(\text{NpCH}_2\text{NH})_2\text{C}_{10}\text{H}_6$

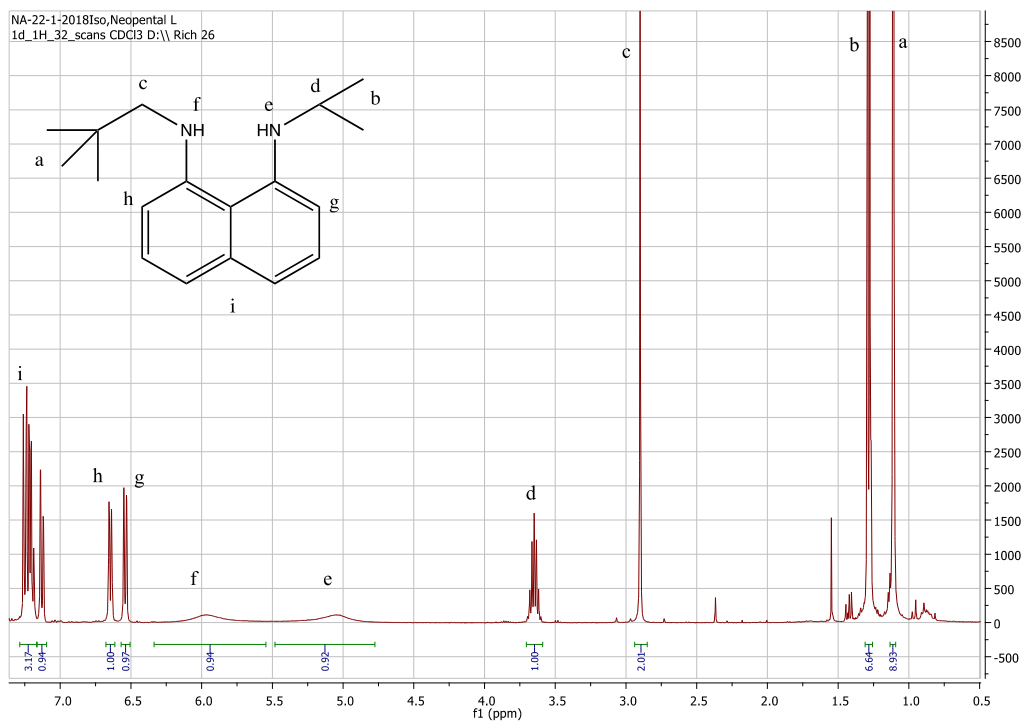


**Figure 2.16:** NMR Spectroscopy for N-(isopropyl)-N'-(neopentyl)-1,8-diaminonaphthalene ( $\text{NpN}(\text{iPrN})\text{C}_{10}\text{H}_6$ )

## 2.5 References

---

- (1) Schaeffer, C. D.; Zuckerman, J. J. Tin(II) Organosilylamines. *J. Am. Chem. Soc.* **1974**, *96*, 7160–7162.
- (2) Cameron, T. M.; Ortiz, C. G.; Ghiviriga, I.; Abboud, K. A.; Boncella, J. M. The Synthesis and Reactivity of a Molybdenum (IV) Stretched-Dihydrogen Complex. *J. Am. Chem. Soc.* **2002**, *124*, 922–923.
- (3) Abdel-Magid, A. F.; Carson, K. G.; Harris, B. D.; Maryanoff, C. A.; Shah, R. D. Reductive Amination of Aldehydes and Ketones with Sodium Triacetoxyborohydride. Studies on Direct and Indirect Reductive Amination Procedures. *J. Org. Chem.* **1996**, *61*, 3849–3862.
- (4) Furniss, B. S.; Hannaford, a J.; Smith, P. W. G.; Tatchell, an R. Vogel's S. Furniss. *Journal of Polymer Science Part A: Polymer Chemistry*. 1989, pp 1223–1223.
- (5) Zhang, S.; Ding, Y. Theoretical Study on Mechanism of copper(I)-Catalyzed Cross-Coupling between Aryl Halides and Alkylamines. *Organometallics* **2011**, *30*, 633–641.
- (6) Sheng, Q.; Ogata, T.; Hartwig, J. A Highly Efficient Catalyst for Pd-Catalyzed Amination of Aryl Halides. *Synfacts* **2008**, *2008*, 0859–0859.
- (7) DaniÃle, S.; Drost, C.; Gehrhus, B.; Hawkins, S. M.; Hitchcock, P. B.; Lappert, M. F.; Merle, P. G.; Bott, S. G. Synthesis, and Structures of Crystalline Dilithium Diamides and Aminolithium Amides Derived from N,N'-Disubstituted 1,2-Diaminobenzenes or 1,8-Diaminonaphthalene. *J. Chem. Soc. Dalton Trans.* **2001**, *2*, 3179–3188.

- (8) Zeiger, M.; Stark, S.; Kalden, E.; Ackermann, B.; Ferner, J.; Scheffer, U.; Shoja-Bazargani, F.; Erdel, V.; Schwalbe, H.; Göbel, M. W. Fragment Based Search for Small Molecule Inhibitors of HIV-1 Tat-TAR. *Bioorganic Med. Chem. Lett.* **2014**, *24*, 5576–5580.
- (9) APEX2 Software Suite v 2012. Bruker AXS Inc., Madison, Wisconsin, U. APEX2 Software Suite v 2012. Bruker AXS Inc.: Madison, Wisconsin 2012.
- (10) SADABS Bruker AXS Inc. Madison Wisconsin USA. SADABS. Bruker AXS Inc.: Madison, Wisconsin 2014.
- (11) Sheldrick, G. M. Crystal Structure Refinement with SHELXL. *Acta Crystallogr. Sect. C Struct. Chem.* **2015**, *71*, 3–8.
- (12) Farrugia, L. J. WinGX Suite for Small-Molecule Single-Crystal Crystallography. *J. Appl. Crystallogr.* **1999**, *32*, 837–838.

# Chapter III

## Synthesis of Transition Metal Complexes Supported by N,N' Diamidonaphthalene Framework Ligands

### 3.1 Introduction

Early transition metals are generally defined as the d-block metals in the groups that begin with scandium and continue across the periodic table to manganese. These are the groups 3-7 in the periodic table<sup>1</sup>. Although it is certainly true that the chemistry of the complexes of these metal centers is really quite varied, there are a few broad general features that are common and that contrast with the late transition metals in groups 8-11. The early transition metals are less electron rich than the late transition metals, and this results in some of the key differences. The compounds of the early transition metals often have the metal in a high oxidation state, and they often have high coordination numbers due to their electron deficient nature and high charge to radius ratio (i.e., stronger Lewis acidity). Redox chemistry is less common for much of the chemistry of the early metal complexes due to their strong preference for high oxidation states<sup>2</sup>. Not surprisingly, the characteristic chemistry of the early metal complexes arises from these defining features. Of course, it should be noted that these features are general guidelines and there are many examples of early metal complexes that are not limited to these features.

One of the most successful chemical transformations associated with early transition metal complexes is oligomerization of carbon-carbon double bonds. More specifically, olefin polymerization reactions by transition metal catalysts are of significant importance and have been examined extensively by both experimentalists and theoreticians over the last decades.<sup>3</sup> In fact, the 1963 Nobel Prize in chemistry was awarded to Ziegler and Natta for this class of reactions.<sup>4</sup> Early transition metals continue to play a central role in the synthesis of catalysts for olefin polymerization reactions. For example, complexes of zirconium in the +4 oxidation state such as metallocene derivatives of the type  $[\text{Cp}_2\text{ZrR}]^+$  exhibit high activity for  $\alpha$ -olefins and ethylene polymerization. For a number of years, the use of diamides has been considered by many researchers as alternatives to the ubiquitous metallocenes<sup>5</sup>.

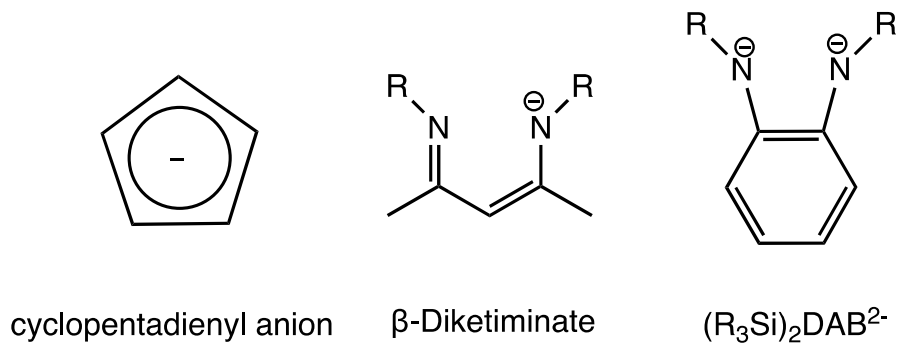


**Figure 3.1:** Examples of ligands that their complexes have been used as catalysts in polymerization reactions.

Interestingly,  $\beta$ -diketiminate and diamidobenzene ligands have been used for ethylene polymerization; this is due to the similarity between these ligands and cyclopentadienyl anion<sup>6</sup>. For instance,  $\beta$ -diketiminate, like cyclopentadienyl anion, can donate six electrons to a metal center. Four of these electrons would come in the form of

two  $\sigma$  bonds to the N centers while the other two electrons could come from a  $\pi$  interaction between the ligand and the metal. More specifically, these six electrons involve the ligand HOMO, HOMO-1 and HOMO-2 orbitals that are shown in Figure 1.5 in chapter I. For these reasons; amido ligands became one of the common replacement of the cyclopentadienyl ligand<sup>7,8</sup>.

Furthermore, the  $\beta$ -diketiminato and diamidobenzene ligands depicted in Figure 3.1 and 3.2 can be easily modified by varying the R groups in order to modulate the steric and electronic properties of the ligands, and this offers potential advantages relative to the cyclopentadienyl anion (Figure 3.1). For example, Collins' and Andres' groups<sup>9,10</sup> reported group 4 metal complexes bearing  $\beta$ -diketiminato ligands with electron-withdrawing groups, which displayed high catalytic activities for ethylene polymerization. Xie's group<sup>11</sup> prepared mono ( $\beta$ -diketiminato) titanium trichloride complexes **B** (Figure 3.2), which displayed high catalytic activities for the copolymerization of ethylene<sup>12</sup>.

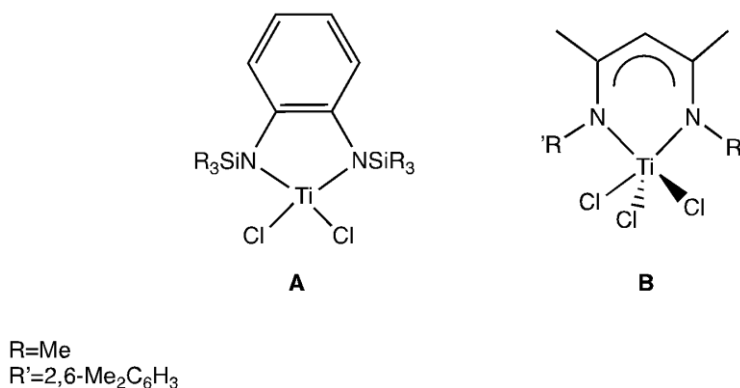


**Figure 3.2** Different amido ligand frameworks that have been used in group 4 complexes.

These reports attracted our attention and suggested that the disubstituted 1,8-diaminonaphthalene  $H_2R,R'$ -DAN proligand could be a useful source for supporting ligands due to their resemblance in structure to the NacNac ligand and their similarity in electronic properties to the diamidobenzene ligands. The size of the nitrogen substituent in these complexes influenced the catalytic activity indicating that the nitrogen substituents are an important factor in the catalytic cycle.

In this chapter, I will report the investigation into the use of the disubstituted 1,8-diaminonaphthalene ( $H_2R,R'$ -DAN) ligand as supporting ligands for the synthesis of Ti(IV) and Zr(IV) complexes. One of the routes to introduce this ligand was via the reaction of titanium halide compounds with the lithium complexes of disubstituted 1,8-diamidonaphthalene. Therefore, the preparation and characterization of the lithium compounds will begin these results. Furthermore, although it is not an early metal, I will also present efforts to prepare  $Zn^{2+}$  complexes of this ligand scaffold. These complexes were prepared as possible reagents for introducing the diamidonaphthalene ligand.

## 3.2 Results and Discussion

### A. $Li_2[(1,8-C_{10}H_6)R_2]$ [dilithium salt]

The dilithium compounds of  $H_2R,R'$ -DAN **3.1** and **3.2** are prepared in order to be used as precursors in salt metathesis reactions to yield transition metal complexes. The presence of NH groups in the proligands allows for these compound to be prepared by slowly adding two molar equivalent of BuLi or MeLi (in THF) to  $R,R'$ -DAN at low temperature

and under a nitrogen atmosphere as shown in Figure 3.3. The green/yellow solids isolated from these reactions were purified by crystallizations from THF. The single crystal X-ray analysis of the final crystalline products provided a formula indicating binding of two Li cations to the ligand in **3.3**. The coordination of the Li centers is completed by two coordinated THF molecules to give a tetrahedral geometry for each metal as shown in Figure 3.4. The structure of **3.4** is shown in Figure 3.5 and once again displayed the targeted diamido species with two Li centers. However, in this case, each Li is coordinated with only one THF molecule leading to three coordinate Li species. The reasons for this observed difference in coordination geometry is not immediately obvious and does not seem to be a result of the different steric load from the amido ligands. We attribute this difference to labile coordination of the THF groups and a result of slightly different crystallization conditions<sup>13</sup>. Selected bond lengths and angles for the two dilithium salts are listed in Table 3.1. Both compounds are nonplanar, and each Li is coordinated to the two amido nitrogen of the R,R'-DAN ligand, and the four Li-N distances are equal within experimental error (Table 3.2). Moreover, <sup>1</sup>H NMR spectrum for **3.3** showed that it is very symmetrical with the isopropyl group giving one doublet integrating for 12 protons at 0.99 ppm and one septet integrating for 2 protons at 3.4 ppm. In addition, two resonances, at 1.5 ppm and 3.4 ppm, corresponding to a single THF molecule and indicate the ease in losing THF during sample preparation for NMR. The most important feature of both dilithium salts is the loss of the N-H resonances of the starting materials.

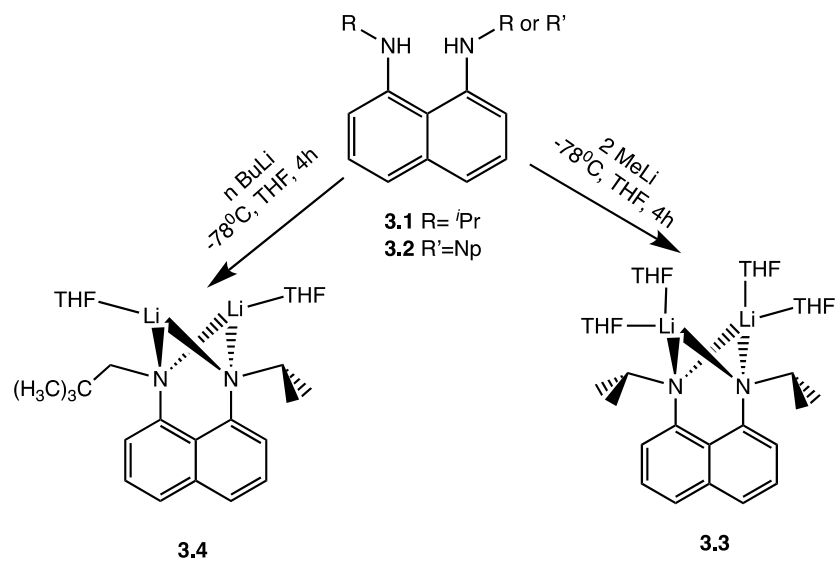


**Figure 3.3:** Synthesis of dilithium salts of different R, R'-DAN ligands

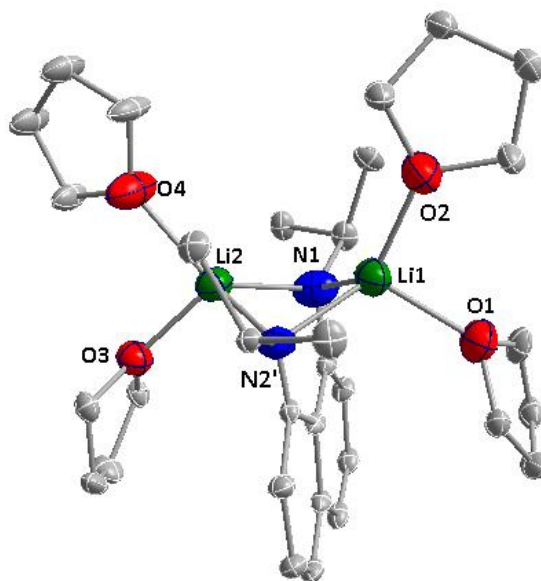


**Figure 3.4:** Molecular structure for **3.3** (hydrogen atoms have been omitted for clarity).

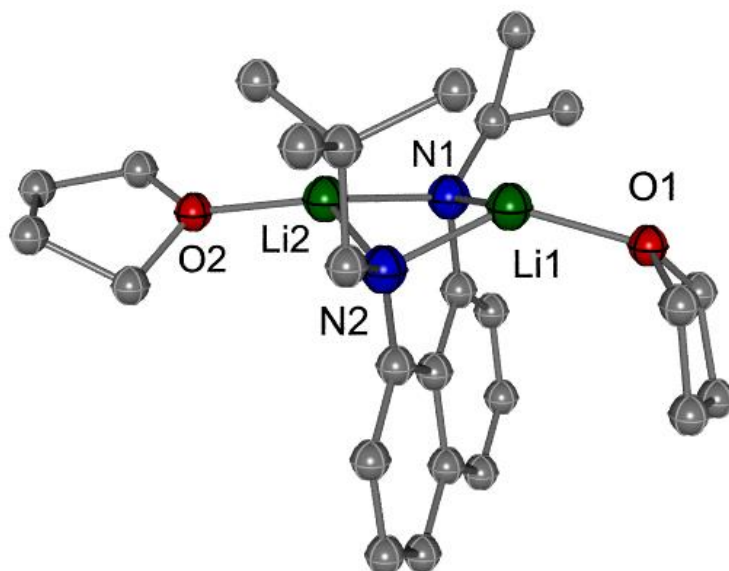


**Figure 3.5:** Molecular structure for **3.4** (hydrogen atoms have been omitted for clarity).

The primary purpose of preparing the dilithium salts was to use them for the synthesis of the titanium complexes through the reaction with titanium (IV) chloride as shown in Figure 3.6. The targeted preparation involved the reaction of one equivalent of  $\text{TiCl}_4$  with the dilithium salt in cold ether, and the mixture was stirred for 12 h. The resulting product was extracted with toluene, and the solvent was removed under vacuum to afford a purple solid. This purple solid is characterized by NMR spectroscopy and single crystal X-ray diffraction. The  $^1\text{H}$  NMR spectrum showed only one peak for the  $\text{CH}_3$  groups indicating a symmetric complex. The  $^{13}\text{C}$  NMR spectrum also supports this assignment with only 3 resonances for a naphthalene backbone. We obtained a crystal of the solid that was analyzed by single crystal X-ray diffraction. Unfortunately, this crystal did not provide adequate data for full analysis and structural details, but the results did

support the presence of one ligand and two Cl ions coordinating the metal to make compound **3.6** as depicted in Figure 3.7. Furthermore, the Ti(IV) complexes can also be prepared by reacting proligand  $H_2R,R'$ -DAN directly with  $TiCl_4$  in presence of an excess of triethylamine Figure 3.6. The first evidence for product formation was provided by the  $^1H$  NMR of this product shows a unique signal for the isopropyl peak at  $\delta$  5.11 ppm as a single septet.

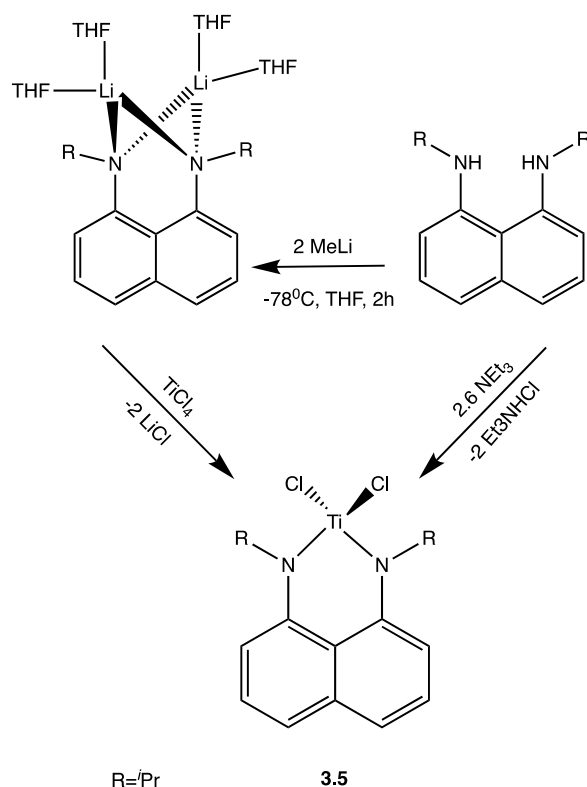


**Figure 3.6:** Synthetic approaches to group 4

Several similar attempts were made to isolate analogous Zr complexes following the same metathesis procedure as for Ti complex. However, we were unsuccessful and obtained only products from the protonation of the ligand and oxidation of Zr producing  $ZrO_2$  as shown in Figure 3.8. From this reaction, crystals were obtained, and single

crystal X-ray analysis confirmed that these were the HCl salt of the proligand **3.1** with the results shown in Figure 3.9.

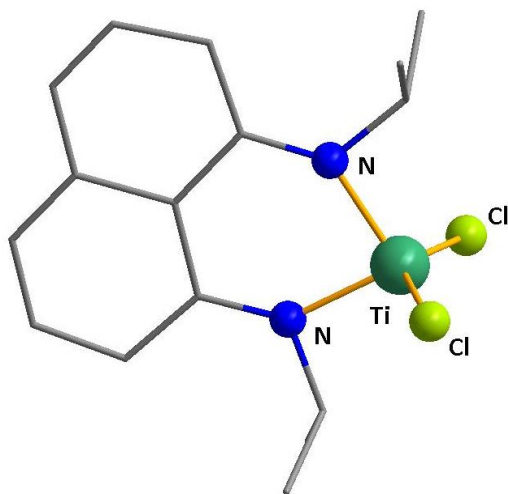


**Figure 3.7:** Molecular structure for **3.5** (hydrogen atoms have been omitted for clarity).

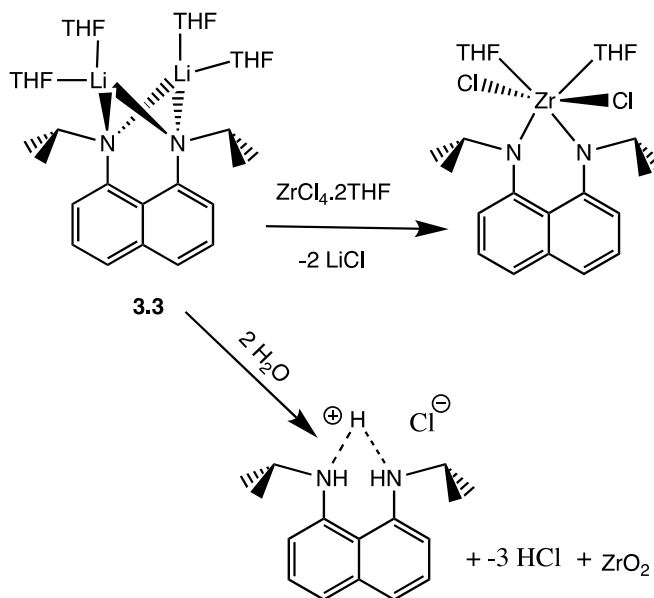


**Figure 3.8:** Reaction of  $\text{ZrCl}_4 \cdot \text{THF}$  with  $\text{H}_2\text{O}$ .

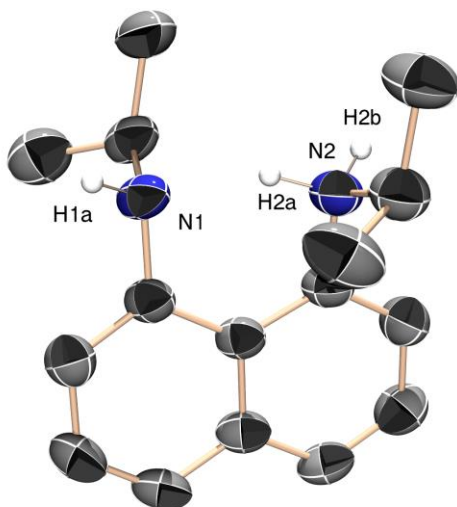


**Figure 3.9:** Molecular structure for (*i*PrNH)<sub>2</sub>C<sub>10</sub>H<sub>6</sub> salt.

## B. Alkane elimination

The successful preparation of the lithium complexes employed an alkane elimination route. Therefore, alkane elimination was considered as an alternative method to prepare group 4 complexes. Of course, this reaction relies on employing a Ti-alkyl starting material. The complex tetrabenzyltitanium meets this criterion and was therefore chosen as a potential target/starting material. The reaction of TiCl<sub>4</sub> with four equivalents of benzyl magnesium chloride was used to produce the corresponding organometallic Ti(IV) complex (Figure 3.10). This complex was successfully isolated, and its identity was confirmed by single crystal X-ray diffraction analysis (Figure 3.11) and <sup>1</sup>H NMR<sup>14</sup>. The key characteristic of this product is that the <sup>1</sup>H NMR has one resonance for the CH<sub>2</sub> group at δ 1.52 ppm. The crystals for the X-ray diffraction study were grown from a concentrated heptane solution at -25<sup>0</sup>C. As depicted in Figure 3.11, Ti(CH<sub>2</sub>Ph)<sub>4</sub> displays

four benzyl groups with the Ti-CH<sub>2</sub> distances being equal and the Ti-CH<sub>2</sub>-Ph bond angles ranging from 50.3° to 117° (Table 3.3, 3.4). Reacting the TiBn<sub>4</sub> complex with the diamino proligand **3.1** was expected to proceed according to Figure 3.9. Unfortunately, we were not able to isolate the final product **3.7**, which may be due to the low yield and highly moisture and air sensitive of compound **3.6**<sup>15</sup>.

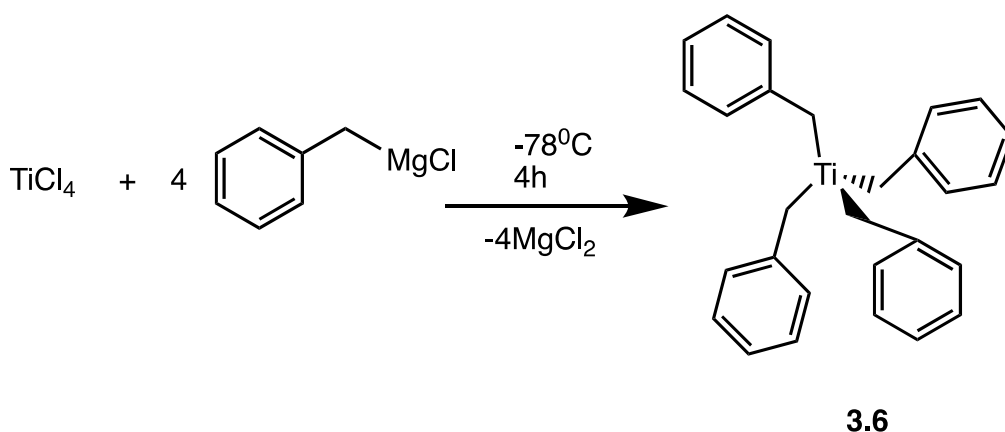


**Figure 3.10:** Synthesis route of Ti(CH<sub>2</sub>Ph)<sub>4</sub>

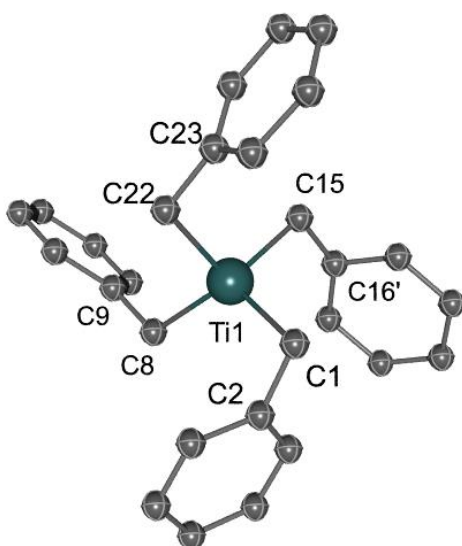


**Figure 3.11:** Molecular structure of compound **3.6** (hydrogen atoms have been omitted for clarity).

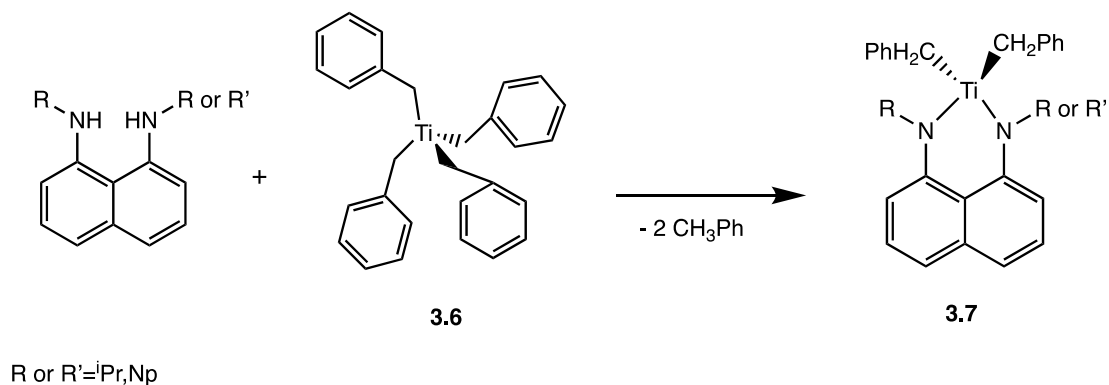


**Figure 3.12:** The Proposed reaction of the TiBn<sub>4</sub> complex by alkane elimination

Finally, lithium amido species are not the only complexes that could be used in the salt metathesis synthesis approach. Other species such as magnesium amido or zinc amido compounds may offer analogous approaches. With this in mind, the synthesis of a Zn complex shown in Figure 3.13 was explored. Similar to lithium alkyls, Zn alkyls can be used as a strong base to deprotonate the proligand **3.1**. Unfortunately, the reaction of H<sub>2</sub>R,R'-DAN with one equivalent of diethylzinc did not go to completion. <sup>1</sup>H NMR analysis shows these reaction products appeared to contain significant amounts of free ligand. Therefore, the reaction carried out with the use of excess diethylzinc. The <sup>1</sup>H NMR spectrum for final product showed that it has a very symmetric environment with one type of isopropyl CH<sub>3</sub> group (doublet, 12H), and one type CH<sub>2</sub> (q, 4H) and CH<sub>3</sub> (t, 6H) of the ethyl groups.

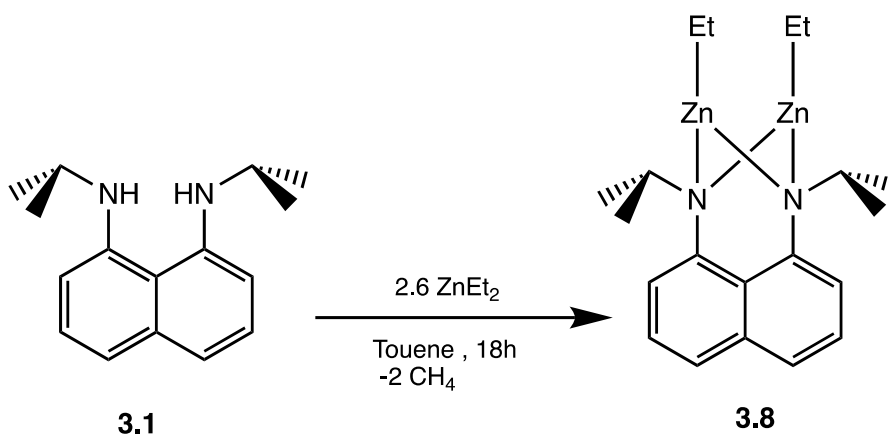


**Figure 3.13:** Preparation of Zn complex by alkane elimination route.

### C. Amine elimination

The amine elimination approach was used for preparation of the Zr(IV) complex as an alternative to a metathesis reaction of the lithiated ligand with a metal halide Figure 3.8 and this approach gave some unexpected results. Reaction of 1 equiv. of the ligand **2.9** and tetrakis(dimethylamido)zirconium in toluene produced the complex as yellow powder Figure 3.14. The  $^1\text{H}$  NMR shows an unique singlet peak at 2.55 ppm corresponding to 12 protons for dimethylamino groups that coordinating to the metal.

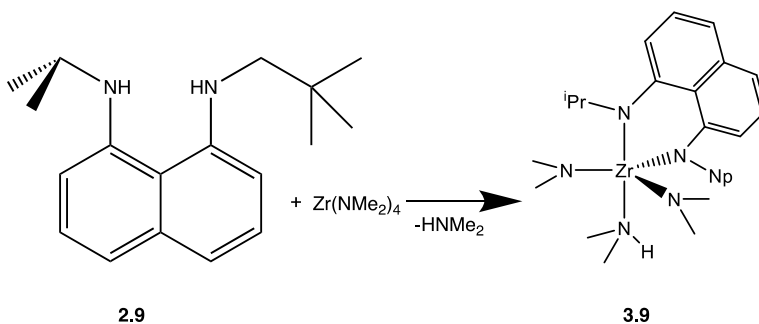


**Figure 3.14:** Preparation of Zr complex by amine elimination.

The structure of the complex was confirmed through single crystal X-ray crystallography which shows that the complex has a trigonal bipyramidal geometry (Figure 3.15). The most notable structural feature for the complex is the nonplanar arrangement of the metal with respect to the naphthyl moiety. In addition, the two dimethylamine that coordinate Zr are planar with  $sp^2$  hybridization. The five bond lengths associated with the Zr center, N(6)-Zr= 2.0914(16), N(7)-Zr= 2.1566(18), and N(8)-Zr= 2.0497(19) are shorter than N(10)-Zr= 2.479(2). This difference between the imido ligands is reflected in the observed bend angles of  $97.31(8)^\circ$  for N(8)-Zr-N(7) and N(6)-Zr-N(10) for  $84.69(7)$ . Table 3.6. These structural features of Zr complex closely resemble those previously reported for a W(IV) complex<sup>16</sup>.

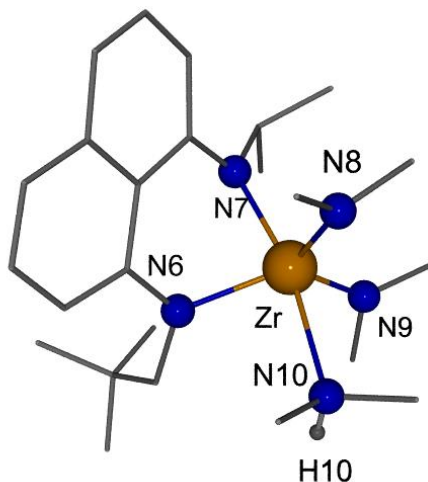


**Figure 3.15** X-ray crystal structure of the Zr complex.

DFT calculations were carried out using the B3LYP functional and the DGDZVP basis set and these provided for an analysis of the fragment orbital interaction for the  $R_2DAN^{-2}$  and  $Zr(NR)_2^{+2}$  fragment in the complex. The five highest occupied fragment

orbitals ( HOMO to HOMO-5) are depicted Figure 3.16. These computation show a clear metal ligand  $\sigma$  bond type interaction HOMO-1,HOMO-5 for the complex this looks like overlap with  $\pi$  type orbital of the ligand (HOMO-1,HOMO-2) and this interaction appears to be enhanced because of the bent of the ligand. In addition the occupied HOMO-2 and HOMO-3 orbitals for the complex show the contribution to  $\pi$  bonding interaction from two amido ligands ( $\text{NMe}_2$ ) to the Zr. The HOMO orbital for the complex is non-bonding, this looks like the ligand HOMO.

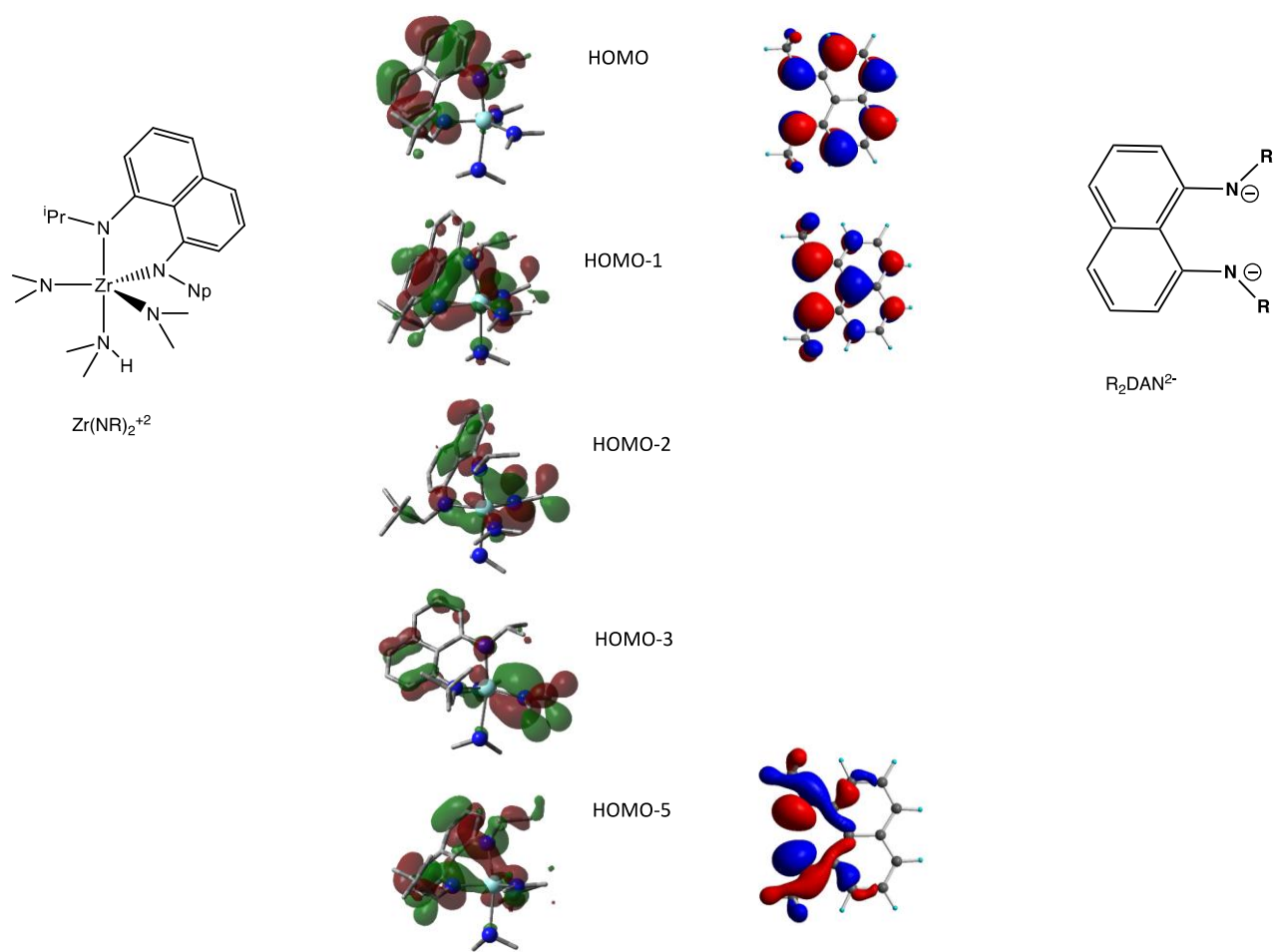


**Figure 3.16** Bonding Orbitals for the optimized Zr complex visualized with isovalue = 0.0

### 3.3 Conclusion

This work provides strong preliminary evidence that demonstrates the ability of dianionic ligand R,R'-DAN<sup>2-</sup> to stabilize Ti(IV) and Zn(II) metals and lead to mononuclear Ti complex **3.5** and dinuclear Zn complex **3.8**. Furthermore, preparation of these complex can be isolated by different routes such as dilithium salts of H<sub>2</sub>R,R'-DAN or alkane elimination.

### 3.4 Experimental Section

All manipulations were carried out in either a nitrogen filled dry box or under nitrogen using standard Schlenk techniques. Reaction solvent (anhydrous diethyl ether) was sparged with nitrogen then dried by passage through a column of activated alumina using an apparatus purchased from Anhydrous Engineering. Deuterated benzene was purchased from Aldrich. MeLi, nBuLi, ZnEt<sub>2</sub>, TiCl<sub>4</sub>, ZrCl<sub>4</sub>, benzyl magnesium chloride, anhydrous toluene, and anhydrous hexane were purchased from Aldrich and used without further purification. <sup>1</sup>H NMR, spectra were run on either a Bruker 300 MHz or Bruker 600 MHz spectrometer, <sup>13</sup>C{<sup>1</sup>H} NMR spectra were run on either a Bruker 300 MHz or Bruker 600 MHz, residual protons of the deuterated solvent for reference.

#### Preparation of Li<sub>2</sub>[1,8(<sup>i</sup>PrN)<sub>2</sub>C<sub>10</sub>H<sub>6</sub>] (**3.3**)

To a purple THF solution of (<sup>i</sup>PrNH)<sub>2</sub>C<sub>10</sub>H<sub>6</sub> (0.49 g, 2.0 mmol) was gradually added a hexane solution of nBuLi (1.8 ml, 2.5 M, 4.4 mmol) at -78 °C. The solution turned dark

brown, and the reaction medium was allowed to return to room temperature and stirred for 4h. The brown-red solution was evaporated to dryness, to give a green solid, which was washed with hexane to remove excess nBuLi. Drying this solid on a vacuum line yielded a green powder (0.46 g, 87%), and the solid purified by crystallization from THF at  $-25^{\circ}\text{C}$  to give colorless crystals.  $^1\text{H}$  NMR ( $\text{CD}_3\text{CN}$ , 300MHz):  $\delta$  6.97-6.89 (m, 4H, Ar-H), 6.40-6.38 (dd, 2H CH) 3.41(t, 4H,  $\text{CH}_2$ , THF) 3.34 (Sept, 2H,  $J_{\text{HH}}=6.06$  Hz), 1.55(t, 4H,  $\text{CH}_2$ , THF) 0.99(d, 12H,  $\text{CH}_3$   $J=6.30\text{Hz}$ ).

$^{13}\text{C}$  NMR ( $\text{C}_7\text{D}_8$ , 500 MHz):  $\delta$ 150 (C), 139.5 (C), 127.1 (CH), 110.9 (CH), 115.0 (C) 101.3 (CH), 68.0 ( $\text{CH}_2$ , THF), 47.3 ( $\text{CHMe}_2$ ), 25.6 ( $\text{CH}_2$ , THF), 25.1 ( $\text{CH}_3$ ).

Anal. Calcd for  $\text{C}_{32}\text{H}_{52}\text{N}_2\text{O}_4\text{Li}_2$ : C, 70.83; H, 9.66; N, 5.16. Found: C, 70.48; H, 9.29; N, 5.50.

#### **Preparation of $\text{Li}_2[1,8(\text{N}^i\text{Pr})(\text{NNp})\text{C}_{10}\text{H}_6]$ : (3.4)**

MeLi (2.4 ml, 1.6 M in diethyl ether, 3.9 mmol) was added dropwise to a solution of  $1,8(\text{N}^i\text{Pr})(\text{NNp})\text{C}_{10}\text{H}_6$  (0.521g, 1.9 mmol) in 5 ml in THF at  $-78^{\circ}\text{C}$  which led to an immediate color change of the solution to green then brown with the release of gases. The reaction mixture was warmed to room temperature and stirred for 4 h, and then all volatiles were removed under vacuum. The solid was washed with hexane and then purified by crystallization from THF at  $-25^{\circ}\text{C}$  to give colorless crystals (0.77g, 91%). Carbon and proton NMR both show coordination of one THF.

$^1\text{H}$  NMR ( $\text{CD}_3\text{CN}$ , 300MHz):  $\delta$  7.10-6.37 (m, 6H), 3.65 (t, 4H,  $\text{CH}_2$  THF) 3.57 (sept, 1H,  $J_{\text{HH}}=6.271\text{Hz}$ ), 2.85(s, 2H), 1.79  $\text{CH}_2$  THF, 1.21 (dd, 6H,  $J_{\text{H,H}}= 6.24, 240 \text{ Hz}$ ), 1.06 (s, 9H).

$^{13}\text{C}\{^1\text{H}\}$ NMR( $\text{CD}_3\text{CN}$ ,300MHz): 147.7, 145.1, 137.1, 126.4, 125.7, 120.1, 117.6, 116.9, 111.5, 105.2 (Caromatic), 67.3 ( $\text{CH}_2\text{THF}$ ), 56.9 ( $\text{CH}_2\text{Me}_3$ ), 46.2 ( $\text{CHMe}_2$ ), 31.3 ( $\text{CMe}_3$ ), 25.1 ( $\text{CH}_2\text{THF}$ ), 25.2 ( $\text{CH}_3$ ), 21.9 ( $\text{CH}_3$ )

### Preparation of $\text{TiCl}_2[1,8\text{-}(\text{N}^i\text{Pr})_2\text{C}_{10}\text{H}_6]$ (3.5)

$\text{TiCl}_4$  (0.14 ml, 1.24 mmol) was added dropwise to a solution of  $\text{Li}_2[1,8(\text{N}^i\text{Pr})_2\text{C}_{10}\text{H}_6]$  (0.3g, 1.24 mmole) in 5 ml of diethyl ether at  $-78^\circ\text{C}$  which lead to an immediate color change to dark purple. The reaction mixture was warmed to room temperature and stirred for 12 h, and then all volatiles were removed under vacuum. The solid was extract with toluene and then purified by crystallization from hexane at  $-25^\circ\text{C}$  to give colorless crystals

(0.102 g, 23%).

$^1\text{H}$  NMR (300 MHz,  $\text{C}_6\text{D}_6$ ):  $\delta$  7.34 (d, 2H, Ar-H), 7.12-7.18 (m, 2H, Ar-H), 5.53 (d, 2H, Ar-H), 5.11 (sept, 2H,  $\text{CH}(\text{Me})_2$ ), 1.42 (d, 12H,  $\text{C}(\text{CH}_3)_2$ )

$^{13}\text{C}\{^1\text{H}\}$  NMR (75 MHz,  $\text{C}_6\text{D}_6$ ):  $\delta$  19.5 ( $\text{CH}_3$ ), 37.0 ( $\text{CH}(\text{Me})_2$ ), 103.9 ( $\text{C}_{\text{ArH}}$ ), 123.5 ( $\text{C}_{\text{Ar}}$ ), 125.0 ( $\text{C}_{\text{ArH}}$ ), 125.6 ( $\text{C}_{\text{ArH}}$ ), 136.9 ( $\text{C}_{\text{Ar}}$ ), 142.6 ( $\text{C}_{\text{Ar}}$ ).

### Preparation of tetrabenzyltitanium $\text{Ti}(\text{CH}_2\text{Ph})_4$ (3.6)

A solution of  $\text{TiCl}_4$  (2 ml, 1M in toluene, 2 mmoles) was added dropwise to  $(\text{PhCH}_2)\text{MgCl}$  (8 ml, 1 M in ether, 8 mmol) in 50 ml of ether at  $-78^\circ\text{C}$ , which lead to an immediate color change of the solution to dark red. The reaction mixture was allowed to stir for 3h at  $-78^\circ\text{C}$ . The solution was filtered while cool and the residue extracted with ether (3 x 50 ml). The solvent was removed under vacuum and the red residue extracted with n-heptane at room temperature. Slow cooling of the heptane solution at  $-25^\circ\text{C}$  gave dark red crystals 0.11g 15 % of  $\text{Ti}(\text{CH}_2\text{Ph})_4$

$^1\text{H}$  NMR ( $\text{C}_6\text{H}_6$  300 MHz):  $\delta$  1.52 [s, 8H,  $\text{Ti}(\text{CH}_2)_4$ ], 6.37 [d, 8H,  $\text{Ti}(\text{CH}_2\text{Ph})$ ], 6.95 [t, 4H,  $\text{Ti}(\text{CH}_2\text{Ph})$ ], 7.05 [t, 8H,  $\text{Ti}(\text{Ph})$ ].

#### **Preparation of $\text{ZnEt}_2[\mathbf{1,8-(N^iPr)_2C_{10}H_6}](\mathbf{3.8})$**

The diamine  $(i\text{PrNH})_2\text{C}_{10}\text{H}_6$  (0.3g, 1.24 mmol) was dissolved in approximately of 15 ml toluene in 50 ml round bottom flask equipped with a stir bar. To this solution was added a 1.0 M hexanes solution of diethylzinc  $\text{ZnEt}_2$  (2.7 ml, 2.73 mmol) to give a dark purple solution. The solution was stirred overnight. The volatiles was removed under vacuum (0.21g, 39%).

$^1\text{H}$  NMR ( $\text{C}_6\text{H}_6$  300 MHz):  $\delta$  7.26 (m, 4H, Ar-H), 6.41 (m, 2H, Ar-H), 3.32 (sept, 2H,  $\text{C}(\text{CH}_3)_2$ ), 1.15 (m, 18H  $\text{C}(\text{CH}_3)_6$ ), 1.12 (t, 6H,  $\text{CH}_2\text{CH}_3$ ), 0.34 (q, 6H  $\text{C}(\text{CH}_2)_2$ ).

#### **Preparation of $\text{ZrNMe}_2(\text{NpN})(i\text{PrN})\text{C}_{10}\text{H}_6(\mathbf{3.9})$**

A solution of  $\text{Zr}(\text{NMe}_2)_4$  (1.00 g, 3.738 mmol) in toluene (20 mL) was added dropwise to a suspension of an equimolar amount of the  $(\text{NpN})(i\text{PrN})\text{C}_{10}\text{H}_6$  **2.9** ligand in toluene (20

mL).The resulting orange solution was stirred over night at room temperature. Afterwards, all volatiles were removed under vacuum, and the solid residues were recrystallized from toluene at  $-25^{\circ}\text{C}$  to give orange crystal (0.90g, 50 %).

$^1\text{H}$  NMR (300 MHz,  $\text{C}_6\text{D}_6$ , 298 K):  $\delta$ = 7.10-6.56 (m, 6H, Ar-CH), 4.23 [sept, 1 H, HN(CH<sub>3</sub>)], 3.78 [sept, 1 H CH(CH<sub>3</sub>)<sub>2</sub>],  $\delta$  3.73 [sept, 1 H, HN(CH<sub>3</sub>)], 3.51 [s, 2 H, CH(CH<sub>3</sub>)<sub>2</sub>], 2.55 [12 H, N(CH<sub>3</sub>)<sub>4</sub>], 1.72 [d, 6 H, HN(CH<sub>3</sub>)<sub>2</sub>], 1.35 [d, 6 H, CH<sub>2</sub>(CH<sub>3</sub>)<sub>2</sub>], 1.18 [s, 9 H, C(CH<sub>3</sub>)<sub>3</sub>]

## Structural Determinations

**Table 3.1:** Crystal data and structure refinement for **3.3** and **3.4**.

Compounds	<b>3.3</b>	<b>3.4</b>
Empirical formula	C <sub>32</sub> H <sub>52</sub> Li <sub>2</sub> N <sub>2</sub> O <sub>4</sub>	C <sub>26</sub> H <sub>40</sub> Li <sub>2</sub> N <sub>2</sub> O <sub>2</sub>
Formula weight	542.63	426.48
Temperature (K)	200(2)	200(2)
Wavelength (Å)	0.71073	0.71073
Crystal system	Monoclinic	Monoclinic
Space group	P 21/n	P 21/n
a (Å)	9.4226(12)	10.384(3)
b (Å)	18.059(2)	17.473(5)
c (Å)	19.331(2)	14.413(4)
α	90°	90°
β	99.290(2)°	98.728(3)°
γ	90°	90°
Volume (Å <sup>3</sup> )	3246.2(7)	2584.7(12)
Z	4	4
Density (calculated) (Mg/m <sup>3</sup> )	1.110	1.096
Absorption coefficient (mm <sup>-1</sup> )	0.071	0.067
F(000)	1184	928
Crystal size	0.600 x 0.386 x 0.356 mm <sup>3</sup>	0.700 x 0.600 x 0.400 mm <sup>3</sup>
Theta range for data collection	1.553 to 25.249°.	1.844 to 25.776°.
Index ranges	-11 ≤ h ≤ 11 -21 ≤ k ≤ 21 - 23 ≤ l ≤ 23	-12 ≤ h ≤ 12 -21 ≤ k ≤ 21 - 17 ≤ l ≤ 17
Reflections collected	29732	27659
Independent reflections	5875 [R(int) = 0.0240] = 25.242°	4917 [R(int) = 0.0362]
Completeness to theta	100.0 %	100.0 %
Refinement method	Full-matrix least-squares on F <sup>2</sup>	Full-matrix least-squares on F <sup>2</sup>
Data / restraints / parameters	5875 / 643 / 545	4917 / 80 / 344
Goodness-of-fit on F <sup>2</sup>	0.861	1.036
Final R indices [I > 2σ(I)]	R <sub>1</sub> = 0.0697 wR <sub>2</sub> = 0.1910	R <sub>1</sub> = 0.0631 wR <sub>2</sub> = 0.1782
R indices (all data)	R <sub>1</sub> = 0.1057 wR <sub>2</sub> = 0.2538	R <sub>1</sub> = 0.0981 wR <sub>2</sub> = 0.2104
Extinction coefficient	n/a	n/a
Largest diff. peak and hole (e.Å <sup>-3</sup> )	0.341 and -0.263	0.282 and -0.281

**Table 3.2:** Selected Bond Lengths [Å] and Angles [°] for **3.3** and **3.4**

3.3		3.4	
Bond Lengths (Å)		Bond Lengths (Å)	
N(1)-Li(1)	1.999(12)	N(1)-Li(2)	1.927(5)
N(1)-Li(2)	2.016(12)	N(1)-Li(1)	1.961(4)
N(2)-Li(1)	2.028(12)	Li(1)-N(2)	1.936(4)
N(2)-Li(2)	2.016(11)	Li(2)-N(2)	1.935(4)
Angles [°]			
Li(1)-N(1)-Li(2)	86.6(4)	N(1)-Li(2)-N(2)	90.80(19)
Li(2)-N(2')-Li(1)	85.9(3)	N(2)-Li(1)-N(1)	89.78(18)
N(1)-Li(1)-N(2)	87.4(5)	N(2)-Li(1)-Li(2)	47.63(13)
N(2')-Li(1)-N(1')	86.2(3)	N(1)-Li(1)-Li(2)	47.31(14)

**Table 3.3:** Crystal data and structure refinement for **3.6**

Empirical formula	C <sub>28</sub> H <sub>28</sub> Ti
Formula weight	412.40
Temperature (K)	200(2)
Wavelength (Å)	0.71073
Crystal system	Orthorhombic
Space group	P 21 21 21
a (Å)	9.206(3)
b (Å)	12.991(4)
c Å	19.138(5)
α	90°
β	90°
γ	90°
Volume (Å <sup>3</sup> )	2288.6(11)
Z	4
Density (calculated) (Mg/m <sup>3</sup> )	1.197
Absorption coefficient (mm <sup>-1</sup> )	0.384
F(000)	872
Crystal size (mm <sup>3</sup> )	0.590 x 0.400 x 0.140
Theta range for data collection	1.895 to 29.213°

Index ranges	-12<=h<=12 -17<=k<=17 -26<=l<=25
Reflections collected	41727
Independent reflections	5900 [R(int) = 0.0306]
Completeness to theta = 25.242°	100.0 %
Refinement method	Full-matrix least-squares on F2
Data / restraints / parameters	5900 / 135 / 326
Goodness-of-fit on F2	0.995
Final R indices [I>2sigma(I)]	R1 = 0.0380 wR2 = 0.0932
R indices (all data)	R1 = 0.0925 wR2 = 0.1239
Absolute structure parameter	0.017(8)
Extinction coefficient	n/a
Largest diff. peak and hole (e.Å <sup>-3</sup> )	0.169 and -0.215

**Table 3.4:** Selected Bond Lengths [Å] and Angles [°] for **3.6**.

<b>3.6</b>			
<b>Bond Lengths (Å)</b>		<b>Angles [°]</b>	
Ti-C1	2.119(4)	Ti-C15-C16	46.2
Ti-C8	2.103(4)	Ti-C22-C23	110.2(3)
Ti-C15	2.000(14)	Ti-C8-C9	117.9(2)
Ti-C22	2.064(6)	Ti-C1-C2	53.89(19)

**Table 3.5** Crystal data and structure refinement for **3.9**

Empirical formula	C <sub>24</sub> H <sub>43</sub> N <sub>5</sub> Zr
Formula weight	492.85
Temperature (K)	200(2)
Wavelength (Å)	0.71073
Crystal system	Monoclinic
Space group	P 21/n
a(Å)	22.286(5)
b(Å)	9.967(2)
c(Å)	23.643(5)

$\alpha$	90°
$\beta$	91.753(4)°
$\gamma$	90°
Volume Å <sup>3</sup>	5250(2)
Z	8
Density (calculated)	1.247 Mg/m <sup>3</sup>
Absorption coefficient	0.437 mm <sup>-1</sup>
F(000)	2096
Crystal size	0.730 x 0.370 x 0.120 mm <sup>3</sup>
Theta range for data collection	1.237 to 30.679°.
Index ranges	-31<=h<=31, -14<=k<=14, -33<=l<=33
Reflections collected	98449
Independent reflections	15417 [R(int) = 0.0588]
Completeness to theta = 25.242°	100.0 %
Refinement method	Full-matrix least-squares on F2
Data / restraints / parameters	15417 / 2 / 571
Goodness-of-fit on F2	1.036
Final R indices [I>2sigma(I)]	R1 = 0.0391 wR2 = 0.0878
R indices (all data)	R1 = 0.0670 wR2 = 0.1012
Extinction coefficient	n/a
Largest diff. peak and hole e.Å <sup>-3</sup>	0.972 and -0.926

**Table 3.6** Bond lengths [Å] and angles [°] **3.9**

<b>Bond lengths(Å)</b>	
N(6)-Zr	2.0914(16)
N(7)-Zr	2.1566(18)
N(8)-Zr	2.0497(19)
N(9)-Zr	2.0439(19)
N(10)-Zr	2.479(2)
<b>Angles [°]</b>	
N(8)-Zr-N(7)	97.31(8)
N(6)-Zr-N(7)	82.48(7)
N(9)-Zr-N(10)	85.62(7)
N(8)-Zr-N(10)	86.33(8)
N(6)-Zr-N(10)	84.69(7)

### 3.5 References

---

- (1) Atkins, P. W. Shriver & Atkins' Inorganic Chemistry. *Shriver Atkin's Inorg. Chem.* **2010**, 851.
- (2) Karlin, K. D. *Progress in Inorganic Chemistry*; 2012; 57.
- (3) Mecking, S. Olefin Polymerization by Late Transition Metal Complexes-A Root of Ziegler Catalysts Gains New Ground. *Angew. Chem. Int. Ed. Engl.* **2001**, *40*, 534–540.
- (4) Sinn, H.; Kaminsky, W.; Vollmer, H. -J; Woldt, R. "Living Polymers" on Polymerization with Extremely Productive Ziegler Catalysts. *Angew. Chemie Int. Ed. English* **1980**, *19*, 390–392.
- (5) Carone, C. L. P.; Fim, F. C.; Bisatto, R.; Jahno, V. D.; Lemos, C.; Basso, N. R. S.; Einloft, S.; Galland, G. B. Ethylene Polymerization Catalyzed by Diamide Complexes of Ti(IV) and Zr(IV). *J. Appl. Polym. Sci.* **2008**, *110*, 270–275.
- (6) Gong, S.; Ma, H.; Huang, J. Zirconium Complexes with Versatile  $\beta$ -Diketiminato Ligands: Synthesis, Structure, and Ethylene Polymerization. *J. Organomet. Chem.* **2008**, *693*, 3509–3518.
- (7) Vela, J.; Zhu, L.; Flaschenriem, C. J.; Brennessel, W. W.; Lachicotte, R. J.; Holland, P. L. Macrocyclic Binucleating  $\beta$ -Diketiminato Ligands and Their Lithium, Aluminum, and Zinc Complexes. *Organometallics* **2007**, *26*, 3416–3423.
- (8) Mindiola, D. J.; Holland, P. L.; Warren, T. H. Complexes of Bulky  $\beta$ -Diketiminato Ligands: Introduction. In *Inorganic Syntheses*; 2010, 1–4.
- (9) Rahim, M.; Taylor, N. J.; Xin, S.; Collins, S. Synthesis, and Structure of Acyclic Bis(ketenimine) Complexes of Zirconium. *Organometallics* **1998**, *17* (7), 1315–1323.

- (10) Andrés, R.; De Jesús, E.; De La Mata, F. J.; Flores, J. C.; Gómez, R. Dendritic  $\beta$ -Diketiminato Titanium, and Zirconium Complexes: Synthesis and Ethylene Polymerisation. *J. Organomet. Chem.* **2005**, *690*, 939–943.
- (11) Xie, G.; Qian, C. Dramatic Electronic Effect of Fluoro Substituents on the Olefin Polymerization Activity of Mono  $\beta$ -Diiminato Titanium Complexes. *Journal of Polymer Science, Part A: Polymer Chemistry*. 2008, pp 211–217.
- (12) Gibson, V. C.; Spitzmesser, S. K. Advances in Non-Metallocene Olefin Polymerization Catalysis. *Chem. Rev.* **2003**, *103* (1), 283–315.
- (13) El-Zoghbi, I.; Verguet, E.; Oguadinma, P.; Schaper, F. Coordination Modes in Zirconium  $\beta$ -Diketiminato Complexes. *Inorg. Chem. Commun.* **2010**, *13*, 529–533.
- (14) Boden, N.; Emsley, J. W.; Feeney, J.; Sutcliffe, L. H. Nuclear Magnetic Resonance (N. M. R.) Spectra of Mercaptophosphazenes. *Chem. Ind. (London, United Kingdom)* **1962**, 1909.
- (15) A, E. S. S.; Zucchini, U.; Albizzati, E.; Milano, C. R. Synthesis, and Properties of Some Titanium and Zirconium Nenzyl Derivatives. **1970**, *26*
- (16) Lavoie, N.; Ong, T.; Gorelsky, S. I.; Korobkov, I.; Yap, G. P. A.; Richeson, D. S. Bis(imido)W(VI) Complexes Chelated by N,N'-Disubstituted 1,8-Diamidonaphthalene : An Analysis of Bonding , Isocyanate Insertion , and Al-Me Transfer. *Organometallics* **2007**, 6586–6590.

# Chapter IV

## N,N' Diamidonaphthalene as a Versatile Ligand to Stabilize Complexes of Group 13

### 4.1 Introduction

Boron hydrides and alkylaluminum species are core functional groups in the chemistry of the group 13 elements. They can be exploited from both fundamental and applied perspectives and have been employed for their reactivity and as building blocks in synthesis. Modulation of the chemistry of these and other group 13 element functionalities can be achieved through changes to the ligand environment. For example, the application of  $\beta$ -diketiminato ligands has vitalized the synthetic chemistry of group 13 elements.<sup>1,2,3</sup> As supporting ligands,  $\beta$ -diketiminates exhibit strong and diverse binding modes combined with adjustable steric demands through variation of the NR substituents<sup>4</sup>. These features have promoted their application in group 13 and across the periodic table. These observations provided an impetus for our efforts to design and implement ligands that are reminiscent of the  $\beta$ -diketiminato scaffold in both geometry and frontier orbital topology as displayed in Figure 1.5 in **Chapter I**. This target has led us to investigate the application of the dianions, N,N'-disubstituted-1,8-diamidonaphthalene (R,R'-DAN<sup>2-</sup>) as ligands in group 13 chemistry. The R,R'-DAN<sup>2-</sup> scaffold presents a rigid dianionic ligand with delocalized  $\pi$ -electrons in a framework with similarities to the  $\beta$ -diketiminato scaffold. Diamidonaphthalene-based ligands have

seen some application with borohydride and alkylaluminum chemistry with particularly noteworthy examples being silyl-substituted tetraminoperylene and 1,8-bis(trialkylsilylamino)naphthalene group 13 compounds represented by **A-D**<sup>5,6,7,8</sup> Figure 4.1. Importantly, reports have been restricted to trialkylsilyl, R<sub>3</sub>Si, substituents and are therefore limited by the electronic, steric and potential N-silyl reactivity of these groups.

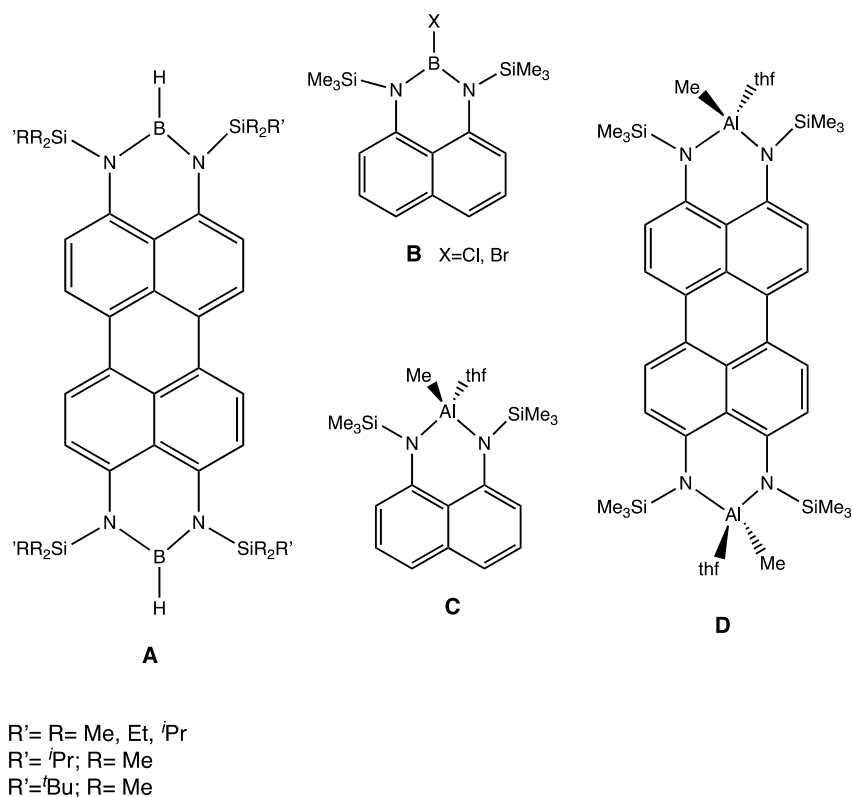


**Figure 4.1:** Some applications of diaminonaphthalene-based ligands in group 13 chemistry

Our desire is to explore the modification to the steric and electronic features of the R,R'-DAN<sup>2-</sup> framework by introduction and variation of the N-substituents to include both alkyl and aryl groups. We previously reported the syntheses of ligands **4.1-4.3** (Figure 4.2) through a multi-step reductive amination method<sup>9</sup> or using a Cu catalyzed

coupling reaction<sup>10,11,12</sup>, respectively. These ligands were characterized and discussed in more detail in **Chapter II**. Furthermore, among the main group elements, this framework has been successfully applied to group 14 divalent species and to low coordinate group 15 cations. We now wish to report the use three disubstituted 1,8-diaminonaphthalene species **4.1-4.3**<sup>13</sup> for the isolation and characterization of monomeric, borohydrides with unusual air stability as well as mono- and dinuclear A-Me complexes. These new compounds make a substantial and fundamental contribution to the limited number of compounds reported with the 1,8- diaminonaphthalene. Based scaffold and represent potential building blocks for the further synthetic chemistry of these elements.

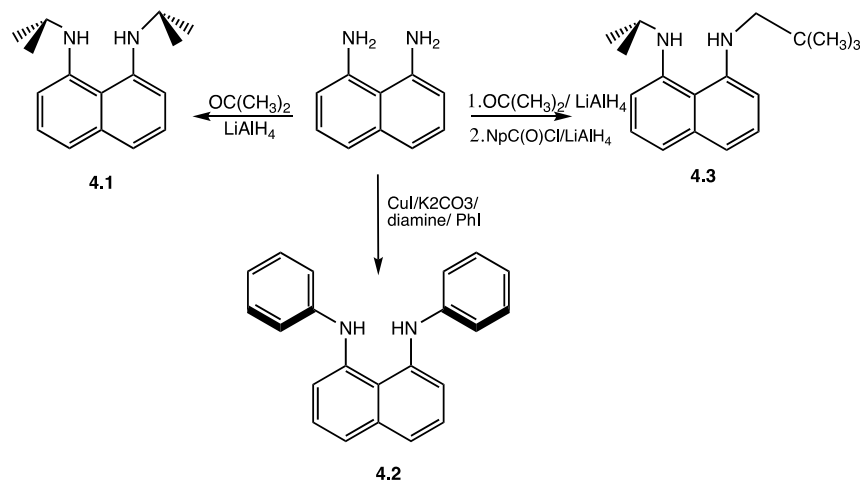


**Figure 4.2:** Preparation of different diaminonaphthalene proligands ( $\text{H}_2 \text{R}$ ,  $\text{R}'\text{-DAN}$ )

Most of the results presented in this chapter also appear in a recently accepted manuscript from the group. This manuscript is entitled “N,N’-Diamidonaphthalene as a Versatile Ligand to Stabilize Mono- and Bimetallic Complexes of Group 13” and the co-authors of the manuscript are Sojung Lee, Nawal Almalki, Bulat Gabidullin and Darrin Richeson. The experimental work reported was carried out by my co-worker Sojung Lee

or myself. The crystallography was done by Dr. Gabidullin. More specifically, my work on this paper includes the synthesis of complexes A1 and B that are supported by  $(i\text{PrNH})(\text{NpNH})\text{C}_{10}\text{H}_6$  ligand while complexes A1 and B with different ligands  $(i\text{PrNH})_2\text{C}_{10}\text{H}_6$  and  $\text{H}_2(\text{Ph})_2\text{-DAN}$  were prepared by the first author. We focused on one route that is based on elimination of hydrogen or methane from borane or trimethylaluminum when reacted with N,N'-disubstituted- 1,8-diaminoaphthalene.

## 4.2 Results and Discussion

The diamionaphthalene proligands **4.1-4.3** possess reactive NH protons allowing for their direct reaction with inorganic and organometallic compounds that possess basic groups. These compounds include boron hydrides, with reactive BH groups, and trimethylaluminum with strongly basic AlMe moieties. For example, both **4.1** and **4.2** react directly with  $\text{BH}_3(\text{SMe}_2)$  as summarized in Figure 4.3. From these reactions, compounds **4.4**, **4.5** and **4.6** were isolated as colorless and light orange crystals, respectively. The multi-nuclear NMR spectra of these two new 1,3,2-diazaborine species provide clear indications for the structures proposed for **4.4**, **4.5** and **4.6**. Specifically, both compounds exhibited  $^1\text{H}$  and  $^{13}\text{C}$  NMR resonances indicating a symmetrical ligation for the  $\text{R}_2\text{DAN}^{2-}$  group. A broad resonance for the BH group was observed in each of the  $^1\text{H}$  NMR spectra at  $\delta$  4.74 ppm (**4.4**) and 4.26 ppm (**4.5**) with these values being comparable to silylated N,N';N'',N''''-diborylene-3,4,9,10-tetraaminoperylenes (**A**), which gave corresponding B-H resonances observed at  $\delta = 4.71\text{--}4.75$  ppm.<sup>8</sup> The  $^{11}\text{B}$  NMR spectra further support the proposed formulations with compound **4.4** and **4.6** displaying a proton decoupled  $^{11}\text{B}$  resonance at  $\delta$  25.9 and 24.2 and ppm while compound

**4.5** showed such resonance at  $\delta$  28.4 ppm. For comparison, the perylene analogue **A** (R = Me) had an  $^{11}\text{B}$  resonance at  $\delta = 29.8$ .<sup>6</sup> Although they are not completely analogous, the monomeric species **B**,  $\text{BX}[(\text{NSiMe}_3)_2\text{C}_{10}\text{H}_6]$ , gave  $^{11}\text{B}$  NMR resonances at similar chemical shifts of 32.1 ppm (X = Cl) and 28.0 ppm (X = Br)<sup>7</sup>. Finally, the microanalysis data on **4.4** and **4.5** was consistent with the suggested formulations. Similarly, boron complexes can be isolated by different route alkane elimination which required preparation of the reaction of lithium complexes diamidonaphthalene. This compound already characterized and discussed more with details in Chapter III. Figure 4.4 showed the alternative synthesis of boron complex. Dilithium diamido 3.4 reacts with tetrafluoride to form  $\text{BF}[1,8(\text{}^i\text{PrNH})(\text{NpNH})\text{C}_{10}\text{H}_6]$ . The main feature of compound **4.7** is  $^{11}\text{B}$  NMR resonances 23.29 ppm.

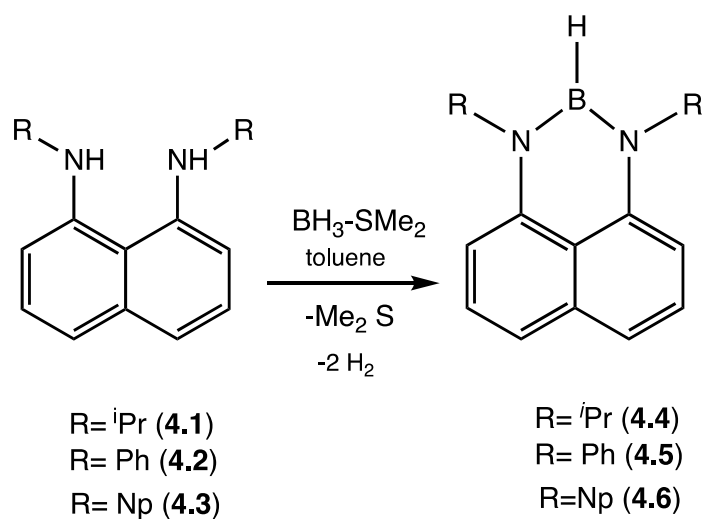


**Figure 4.3:** Synthesis of boron complexes by a hydrogen elimination route

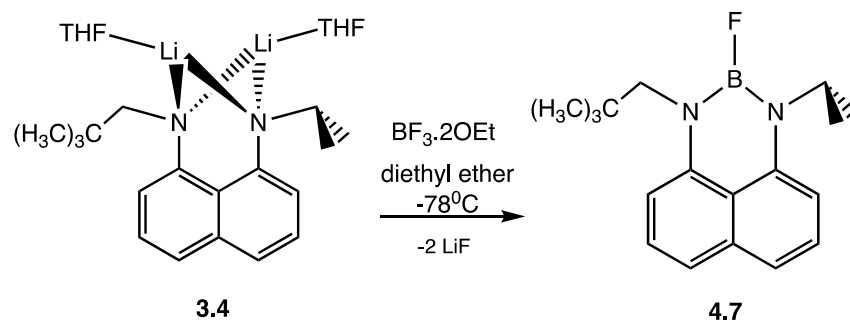


**Figure 4.4:** Synthesis of boron complex by an alkanle elimination.

Interestingly, both **4.4**, **4.5** and **4.6** are stable to air in both solid state and in solution, and NMR solutions of these compounds can be prepared in the air using deuterated solvents directly from the bottle as received from the supplier. These observations are in sharp contrast with the reactivity of the diazaborine species **A**, which are sensitive in both solid state and solution<sup>8</sup>. Similarly, five-membered 2-hydrido-1,3,2-diazaboroles are reported to be colorless air- and moisture-sensitive solids<sup>14</sup>. In contrast, it is interesting that  $\text{BF}[(^i\text{PrNH})(\text{NpNH})\text{C}_{10}\text{H}_6]$  changes color rapidly when exposed to air indicating that this is an air sensitive compound.

Definitive confirmation for the structural features of **4.4**, **4.5** and **4.7** was obtained from single crystal X-ray analyses, and results are summarized in Figures 4.4, 4.5 and 4.6, and selected bond lengths and angles are given in Table 1. Both structures display a diamidonaphthalene group chelating to a trigonal planar B center. The NBN unit and naphthalene backbone are nearly coplanar with the angle between these two planes being only  $4.5^\circ$  in **4.4**,  $8.2^\circ$  in **4.5**. For both **4.4** and **4.5**, the H atom bonded to B were refined freely and yielded average B-H bond distances of  $1.11 \text{ \AA}$ . While in **4.7** the B-F bond

distance is 1.34 Å. All three compounds exhibited similar N-B-N bite angles of 120.8(3)<sup>o</sup> in **4.4**, 119.2(1)<sup>o</sup> in **4.5** and 122.5(2)<sup>o</sup> in **4.7**, a feature that is consistent with sp<sup>2</sup> hybridized B centers. Finally, the B centers are bonded symmetrically to the ligand with **4.4**, and **4.7** displaying two equal B-N distances (1.405(5) and 1.409(5) Å) and **4.5** showing slightly longer but equivalent distances at 1.4163(16) Å and 1.4186(16) Å. These bond lengths are, in all three cases, slightly shorter than those reported for the tetraaminoperylene compounds **A**, which averaged 1.43 Å<sup>8</sup>. Reported six-membered compounds with saturated rings, HB(RR'C<sub>6</sub>H<sub>3</sub>NCHMe)<sub>2</sub>CMe<sub>2</sub> (R = R' = <sup>i</sup>Pr; R = <sup>i</sup>Pr, R'=H), displayed B-N distances that ranged from 1.396(4) Å to 1.414(5) Å and these distances were judged to optimize B-N pπ-pπ interactions<sup>15</sup>.

The air stability of **4.4**, **4.5** and **4.6**, as well as the observed B-N bond lengths, could be attributed to B-N π bonding and in order to further reveal the more detailed features of these interactions we carried out a computational study on compound **4.4**. Starting with the crystal structure data, compound **4.4** was optimized using DFT and the Gaussian 09 program employing the B3LYP functional and a 6-311+G(d,p) basis set<sup>16</sup>. The resulting structure was well aligned with the experimentally determined X-ray data.

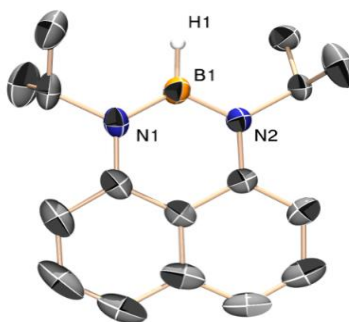


**Figure 4.5:** Structural representation of HB[1,8-(*i*PrN)<sub>2</sub>C<sub>10</sub>H<sub>6</sub>] (**4.4**). Carbon-bound hydrogen atoms have been omitted for clarity.

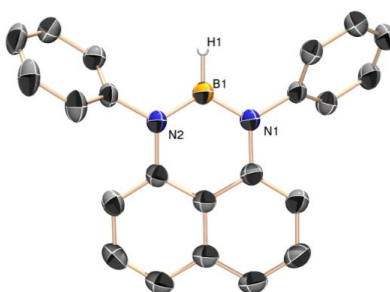


**Figure 4.6:** Structural representation of HB[1,8-(PhN)<sub>2</sub>C<sub>10</sub>H<sub>6</sub>] (**4.5**). Carbon-bound hydrogen atoms have been omitted for clarity.

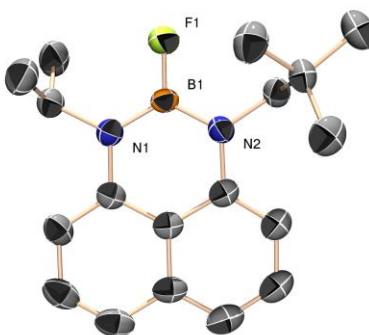


**Figure 4.7:** Structural representation of BF[*i*PrNH)(NpNH)C<sub>10</sub>H<sub>6</sub>] (**4.7**). Carbon-bound hydrogen atoms have been omitted for clarity.

The frontier orbitals obtained from these computations show a clear NBN  $\pi$  bonding interaction as presented in Figure 4.7. While the HOMO and LUMO for **4.4** are non-bonding with respect to the BN linkages, the occupied HOMO-2, and HOMO-1 orbitals show the contribution to NBN  $\pi$ -bonding. Taken together the experimental as well as the theoretical data agree with a significant delocalization of the nitrogen  $2p$ -centered lone electron pairs into the vacant  $2p_z$  orbital of the boron atom in **4.4**.

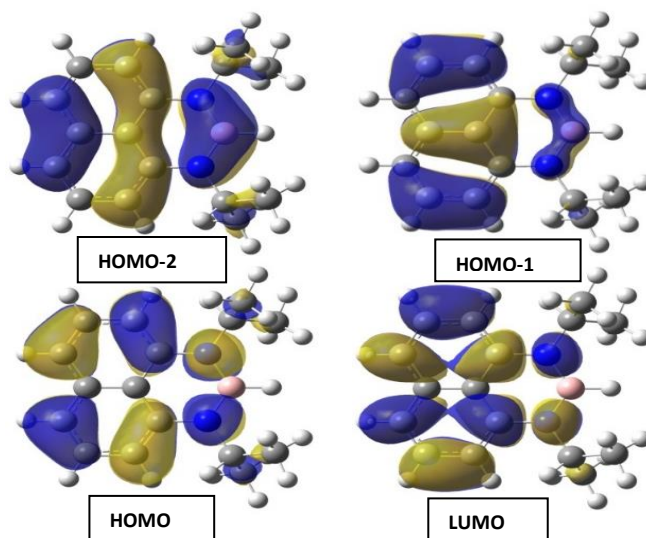


**Figure 4.8:** The frontier orbitals (HOMO-2 to LUMO) representing the  $\pi$ -bonding in **3** obtained from DFT (B3LYP, 6-311+G(d,p)) on compound **4.4**.

The protonation reaction of trimethylaluminum with ligands **4.1-4.3** offers an analogous method for introducing the  $1,8\text{-(RN)}_2\text{C}_{10}\text{H}_6^{2-}$  group in aluminum chemistry as shown in Figure 4.9. For example, the direct reaction of an equimolar ratio of **1.2** and  $\text{AlMe}_3$  proceeded smoothly to yield the unanticipated bimetallic product  $(\text{AlMe}_2)_2[1,8\text{-}(\text{iPrN})_2\text{C}_{10}\text{H}_6]$  (**4.8**) Figure 4.9. The first indication of a bimetallic species was the

appearance of two equal intensity (6H) proton NMR signals at  $\delta$  -0.10 ppm and -1.18 ppm consistent with four Al-CH<sub>3</sub> groups. Furthermore, the <sup>1</sup>H NMR spectrum of **4.8** displayed two equal integral doublet peaks at  $\delta$  1.38 ppm and 1.28 ppm assigned to the methyl groups of the *i*Pr substituents Table 4.2.

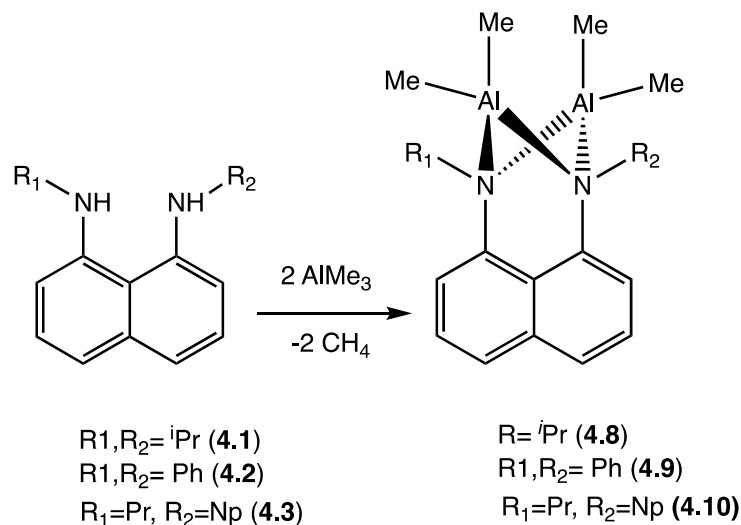


**Figure 4.9:** Synthesis Al complexes by methane elimination

Surprisingly, this product was the only isolated species regardless of the reaction stoichiometry between **4.1** and AlMe<sub>3</sub>, and an improved synthesis was achieved using 2 equiv of AlMe<sub>3</sub> to produce **4.8** which could be obtained as colorless crystals from cold (-25°C) ether. An X-ray diffraction study was performed and confirmation of the connectivity was obtained with the molecular structure shown in Figure 4.10. The corresponding values for selected bond distances and angles are provided in Table 4.2.

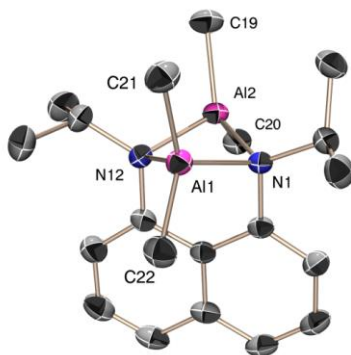


**Figure 4.10:** The molecular structure for  $(\text{AlMe}_2)_2[1,8-(i\text{PrN})_2\text{C}_{10}\text{H}_6]$  (**4.8**). Hydrogen atoms have been omitted for clarity

Compound **4.8** is a bimetallic Al species,  $[\mu-1,8-(i\text{PrN})_2\text{C}_{10}\text{H}_6](\text{AlMe}_2)_2$ , with each aluminum center possessing a four-coordinate distorted tetrahedral geometry consisting of two methyl groups and the two nitrogens of a 1,8-diamidonaphthalene ligand. Each of the anionic nitrogen centers formally possesses two electron pairs, and both of these are donated to the two different Al centers. The result is a puckered, butterfly shaped  $\text{Al}_2\text{N}_2$  metallacycle with approximate  $C_{2v}$  symmetry. A similar structure has been reported from the related trimethylsilyl ligand,  $[\mu-1,8-(\text{Me}_3\text{SiN})_2\text{C}_{10}\text{H}_6](\text{AlMe}_2)_2$  (**E**). The four Al-N bond lengths in **4.8** range from 1.9710(15) Å to 1.9873(15) Å and are slightly shorter than in compound **E** with Al-N of 1.998(4) and 1.995(4) Å. The bimetallic core positions the two methyls on each Al in inequivalent environments consistent with the NMR observations. Crystallographically there are four Al-C bond lengths ranging from 1.9554(19) Å to 1.9627(19) Å. In **4.8** the two N-Al-N bite angles were  $80.74(6)^\circ$  and  $80.73(6)^\circ$  which are only slightly smaller than the angle of  $83.0(2)^\circ$  observed for compound **E**.

Employing this same stoichiometric ratio but using ligand **4.2** or **4.3** generated the analogous bimetallic Al species **4.9** and **4.10** (Figure 4.9). The appearance of two inequivalent, equal intensity signals assigned to the Al-CH<sub>3</sub> groups in the <sup>1</sup>H NMR and the <sup>13</sup>C NMR spectra was a clear indication of analogous dimetallic structures. Furthermore, we were fortunate to obtain single crystals of both complexes, and their single crystal X-ray analyses confirmed that they displayed similar structures as represented in Figures 6 and 7. The selected bond distances and angles for **4.10** and **4.10** are provided in Tables 4 and 5, respectively. Complexes **4.9-4.0** displayed parallel structural features with small differences in bond lengths and bond angles Table 4.3 and 4.4 respectively.

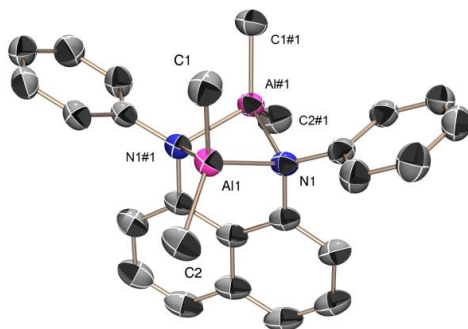


**Figure 4.11:** The molecular structure for (AlMe<sub>2</sub>)<sub>2</sub>[1,8-(PhN)<sub>2</sub>C<sub>10</sub>H<sub>6</sub>] (**4.9**). Hydrogen atoms have been omitted for clarity

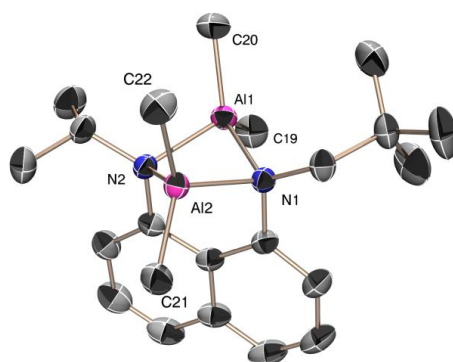


**Figure 4.12:** The molecular structure for  $(\text{AlMe}_2)_2[1,8\text{-(iPrN)(NpN)C}_{10}\text{H}_6]$  (**4.10**). Hydrogen atoms have been omitted for clarity

During the reaction of trimethylaluminum with proligand **2.4**, some crystals were inadvertently obtained. On the assumption that this was a complex related to compounds **4.8** - **4.10** the crystal structure was obtained for this species. The results of this analysis provided a structure for this compound **4.11** and are shown in Figure 4.13 with selected metrical parameters in Table 4.5. This species is what appears to be an interesting capture of the first step in a reaction between these two reagents. Simply put it is the adduct of an  $\text{AlMe}_3$  with the lone pair on the N center of proligand **2.4**.

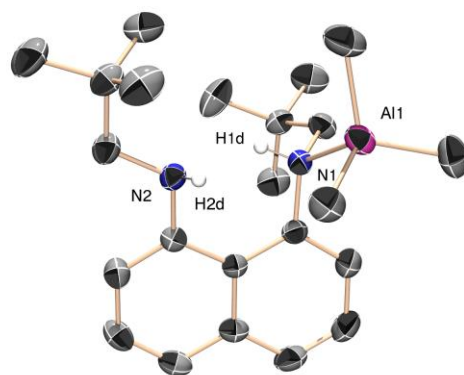


**Figure 4.13:** Captured intermediate in reaction of  $\text{AlMe}_3$  with proligand **4.11**

### 4.3 Conclusions

Elimination of hydrogen or methane from borane or trimethylaluminum when reacted with N,N'-disubstituted-1,8-diaminonaphthalene has been documented as a versatile route to dialkyl- and diaryl-1,8-diamidonaphthalene complexes for group 13. This ligand array supports unexpectedly air-stable, trigonal planar borane compounds HB[1,8-(NR)C<sub>10</sub>H<sub>6</sub>] (R = *i*Pr, **4.4**, R = Ph, **4.5** R<sub>1</sub> = *i*Pr R<sub>2</sub> = Np). The structural analysis combined with computations point to significant B-N p $\pi$ -p $\pi$  bonding, a feature which we attribute to the observed stability. In the case of the trimethylaluminum reactions, bimetallic systems supported by the 1,8-diamidonaphthalene dianion were obtained. The different coordination environments and ligand bonding features were documented by single crystal X-ray diffraction analyses, and the unanticipated bimetallic complexes feature four-membered M<sub>2</sub>N<sub>2</sub> rings with a puckered butterfly structures. The structural data suggested that the dialkyl and diaryl are stronger  $\sigma$ -bonding ligands compared to trimethylsilyl analogues. Compounds **4.4-4.10** represent interesting species as well as building blocks for further group 13 chemistry. Our continuing investigations are focused on expanding on the variation of the ligand as well as exploring changes to the bonding environment of the group 13 element.

### 4.4 Experimental Section

General: All manipulations were carried out in either nitrogen filled a dry box or under nitrogen using standard Schlenk techniques. Reaction solvent (anhydrous diethyl ether) was sparged with nitrogen then dried by passage through a column of activated alumina

using an apparatus purchased from Anhydrous Engineering. Deuterated benzene was purchased from Aldrich Chemical Company and was dried by vacuum transfer from potassium.  $\text{BH}_3\cdot\text{SMe}_2$ , and  $\text{AlMe}_3$ , anhydrous toluene, and anhydrous hexane were purchased from Aldrich Chemical Company and used without further purification.  $^1\text{H}$ ,  $^{13}\text{C}$ , and  $^{11}\text{B}$  NMR spectra were run on either a Bruker 300 MHz or Bruker 600 MHz spectrometer using the residual protons of the deuterated solvent for reference. Elemental analyses were performed by G.G. Hatch Stable Isotope Laboratory at the University of Ottawa or Midwest Micro Lab in Indianapolis, IN, USA

Structural determinations: The crystals were mounted on thin glass fibers using paraffin oil. Prior to data collection, crystals were cooled to  $200\pm 2$  K. Data were collected on a Bruker AXS single-crystal diffractometer equipped with a sealed Mo tube source (wavelength  $0.71073 \text{ \AA}$ ) and APEX II CCD detector. Raw data collection and processing were performed with Bruker APEX II software package<sup>17</sup>. Semi-empirical absorption corrections based on equivalent reflections were applied<sup>18</sup>. Systematic absences in the diffraction dataset and unit cell parameters were consistent with triclinic P-1 (#2) for **7** and **4.11**, monoclinic P21/n (#14) for **4.8** and **4.3**, and P21/c (#14) for **4.5**, monoclinic C2/c (#15) for **4.10**, orthorhombic P212121 (#19) for **4.4**. The structures were solved by direct methods and refined with full-matrix least-squares procedures based on  $F^2$ , using SHELXL<sup>19</sup> and WinGX<sup>20</sup>. All non-hydrogen atoms were refined anisotropically. The hydrogen atoms were placed in idealized positions, except for H(1) in **4.4**, H(1) in **4.5**, and H(1A), H(2A) in **4.3** that were located in the difference Fourier map and refined freely. In **4.4** one of the isopropyl groups is disordered over two positions with 0.61(3):0.39(3) occupancy ratio. It was refined using enhanced rigid-body restraints

(RIGU), and constraints (EADP) applied to the atomic displacement parameters. No additional restraints or constraints were used for refinement of **4.3**, and **4.5-4.9**.

#### **Preparation of HB[1,8-(<sup>i</sup>Pr)<sub>2</sub>C<sub>10</sub>H<sub>6</sub>] (4.4)**

The diamine (<sup>i</sup>PrNH)<sub>2</sub>C<sub>10</sub>H<sub>6</sub> **4.1** (0.40g, 1.65 mmol) was dissolved in approximately 30 ml of toluene and transferred to a Schlenk vessel equipped with a Teflon screw cap. To this solution was added BH<sub>3</sub>·SMe<sub>2</sub> (0.140g, 1.84 mmol) pre-dissolved in toluene. The solution was heated to 60°C overnight. The volatiles were removed under vacuum, and the crude product was crystallized by dissolving in hexane and cooling to -25°C. The product was isolated as colorless crystals and dried under vacuum (0.397g, 1.57 mmol, 95%). <sup>1</sup>H NMR (C<sub>6</sub>D<sub>6</sub>, 300 MHz): with 11B decoupling δ 7.20-7.22 (m, 4H, CH), 6.36-6.41 (m, 2H, CH), 4.74 (s br, 1H, BH), 3.67(sep, 2H, J= 6.03 Hz, CHMe<sub>2</sub>), 1.12 (d, 12H, J=6.54, CH<sub>3</sub>). <sup>13</sup>C NMR (C<sub>6</sub>D<sub>6</sub>, 300 MHz): δ 141.85, 137.28, 127.70, 127.10, 118.20, 102.97(C aromatic), 46.69 (CHMe<sub>2</sub>), 22.86 (CH<sub>3</sub>). <sup>11</sup>B NMR (C<sub>6</sub>D<sub>6</sub>, 300 MHz): with <sup>1</sup>H decoupling δ 25.9 (s BN<sub>2</sub>H).

#### **Preparation of HB[1,8-(NC<sub>6</sub>H<sub>5</sub>)<sub>2</sub>C<sub>10</sub>H<sub>6</sub>] (4.5)**

The diamine (C<sub>6</sub>H<sub>5</sub>NH)<sub>2</sub>C<sub>10</sub>H<sub>6</sub> **4.2** (0.320g, 1.03 mmol) was dissolved in approximately 30 ml of toluene and transferred to a Schlenk vessel equipped with a Teflon screw cap. To this solution was added BH<sub>3</sub>·SMe<sub>2</sub> (0.14ml, 1.115 mmol) pre-dissolved in toluene. The solution was heated to 60°C overnight. The volatiles were removed under vacuum, and the crude product was crystallized by dissolving in ether and cooling to -25°C. The product was isolated as light orange color crystals and dried under vacuum (0.303g, 0.95mmol, 92%).

$^1\text{H}$  NMR ( $\text{CDCl}_3$ , 300 MHz):  $\delta$  7.44-7.50 (m, 4H, CH), 7.30-7.37 (m, 6H, CH), 7.03-7.14 (m, 4H, CH), 6.15 (dd, 2H, CH), 4.26 (s br, 1H, BH).

$^{13}\text{C}$  NMR ( $\text{CDCl}_3$ , 300 MHz):  $\delta$  143.88, 142.97, 136.32, 129.90, 128.25, 127.06, 126.78, 120.32, 118.90, 106.15 (C aromatic).

$^{11}\text{B}$  NMR ( $\text{CDCl}_3$ , 300 MHz): with  $^1\text{H}$  decoupling  $\delta$  28.4 (s,  $\text{BN}_2\text{H}$ ).

### **Preparation of HB[1,8 (*i*PrNH)(NpNH) $\text{C}_{10}\text{H}_6$ (4.6)**

The diamine (*i*PrNH)(NpNH) $\text{C}_{10}\text{H}_6$  **4.3** (0.31g, 1.15 mmol) was dissolved in approximately 30 ml of toluene and transferred to a Schlenk vessel equipped with a Teflon screw cap. To this solution was added  $\text{BH}_3\cdot\text{SMe}_2$  (0.14ml, 1.115 mmol) pre-dissolved in toluene. The solution was heated to  $60^\circ\text{C}$  overnight. The volatiles were removed under vacuum, and the crude product was crystallized by dissolving in ether and cooling to  $-25^\circ\text{C}$ . The product was isolated as light orange color crystals and dried under vacuum (0.29g, 1.03mmol, 90%).

$^1\text{H}$  NMR ( $\text{C}_6\text{D}_6$ , 300MHz): with  $^{11}\text{B}$  decoupling  $\delta$  7.14-6.33 (m, 6H), 4.42(s br, 1H) 3.71 (sep,1H,  $J=6.57$ ), 3.2340 (s, 2H), 1.15 (d, 6H,  $J=6.54$ ), 0.83 (s, 9H).

$^{13}\text{C}\{^1\text{H}\}$  ( $\text{C}_6\text{D}_6$ , 300MHz):142.73, 142.07, 137.24, 127.073, 126.563, 121.98, 118.29, 117.99, 104.67, 103.01 (C aromatic), 58.45( $\text{CH}_2\text{Me}_3$ ), 46.12( $\text{CHMe}_2$ ), 33.79( $\text{CMe}_3$ ), 28.41( $\text{CH}_3$ ),25.13( $\text{CH}_3$ ).

$^{11}\text{B}\{^1\text{H}\}$  NMR ( $\text{C}_6\text{D}_6$ , 300 MHz): with  $^1\text{H}$  decoupling  $\delta$  24.9 (s  $\text{BN}_2\text{H}$ )

### Preparation of BF[1,8 (<sup>i</sup>PrNH)(N<sup>p</sup>NH)C<sub>10</sub>H<sub>6</sub>] (4.7)

Boron trifluoride diethyl etherate (0.11ml, 3.66mmole) was add drop wise to lithium complex **3.4** (0.52g, 3.66mmole) at -25<sup>0</sup>C. This reaction mixture changed from yellow to colorless with the precipitate formation. The reaction mixture was slowly warmed to room temperature, and stirring was continued for 18 h. After removal of the volatiles under vacuum, the residue was extracted with n-pentane (10 mL) to give a pale-yellow solution. Storage of the extract at -25 °C afforded colorless crystals.(0.44g, 40%)

<sup>1</sup>H NMR (CD<sub>3</sub>CN, 300MHz): δ 7.27-6.72 (m, 6H), 4.12 (sept, 1H, J<sub>HH</sub>=7.11Hz), 3.46(s, 2H), 1.46 (dd, 6H, J<sub>H,H</sub>= 6.81, 240 Hz), 0.95 (s, 9H).

<sup>13</sup>C {<sup>1</sup>H} NMR(CD<sub>3</sub>CN 300MHz) 143.05, 142.35, 127.18, 126.61, 117.86, 117.72, 105.55, 117.72, 105.55, 104.17, (Caromatic), 51.41(CH<sub>2</sub>Me<sub>3</sub>), 46.23(CHMe<sub>2</sub>), 33.86(CMe<sub>3</sub>), 27.86(CH<sub>3</sub>), 20.79(CH<sub>3</sub>).

<sup>11</sup>B {<sup>1</sup>H} NMR (C<sub>6</sub>D<sub>6</sub> 300MHz): 23.29 (s, br ).

### Preparation of [μ-1,8-C<sub>10</sub>H<sub>6</sub>(N<sup>i</sup>Pr)<sub>2</sub>](AlMe<sub>2</sub>)<sub>2</sub> (4.8)

The diamine (<sup>i</sup>PrNH)<sub>2</sub>C<sub>10</sub>H<sub>6</sub> **4.1** (0.242g, 1.0 mmol) was dissolved in approximately 15 ml of hexane in a round bottom flask equipped with a stir bar. To the solution was added a 2.0 M hexanes solution of AlMe<sub>3</sub> (1.0 ml, 2.0 mmol). The solution was stirred overnight as it turned black, then brown. The volatiles were removed to yield a beige solid. The product was recrystallized from ether at -25°C, affording colorless crystals (0.0174g, 49%). <sup>1</sup>H NMR (C<sub>7</sub>D<sub>8</sub>, 300MHz): δ 7.31-6.68 (m, 6H), 4.03 (sept, 2H,

J=7.14Hz), 3.58 (m, 1H), 1.38 (d, 6H, J= 7.05Hz), 1.28 (d, 6H, J=6.33Hz), -0.10 (s, 6H), -1.18 (s, 6H).

<sup>13</sup>C NMR (C<sub>6</sub>D<sub>6</sub>, 300 MHz): δ 125.31, 123.25, 122.16, 119.74, 113.44, 111.66(C aromatic), 47.41(CHMe<sub>2</sub>), 47.13(CHMe<sub>2</sub>), 22.49(CH<sub>3</sub>), 19.08(CH<sub>3</sub>), -5.23(AlMe<sub>2</sub>), -10.95(AlMe<sub>2</sub>).

#### **Preparation of [μ-1,8-C<sub>10</sub>H<sub>6</sub>(NC<sub>6</sub>H<sub>5</sub>)<sub>2</sub>](AlMe<sub>2</sub>)<sub>2</sub> (4.9)**

The diamine (C<sub>6</sub>H<sub>5</sub>NH)<sub>2</sub>C<sub>10</sub>H<sub>6</sub> **4.2** (0.105g, 0.5 mmol) was dissolved in approximately 15 ml of diethyl ether in a round bottom flask equipped with a stir bar. To this solution was added a 2.0 M hexanes solution of AlMe<sub>3</sub> (0.5 ml, 1.0 mmol). The solution was stirred overnight and turned green, then red color. The volatiles were removed and the product was recrystallized from ether at -25°C, providing red crystals (0.135g, 0.32mmol, 65%).

<sup>1</sup>H NMR (C<sub>6</sub>D<sub>6</sub>, 600 MHz): δ 7.18-7.28 (m, 9H), 7.11-7.13 (m, 2H), 6.93 (t, 3H, J=7.89Hz), 6.36(dd, 2H, J=7.72, 1.00Hz), -0.37 (s, 6H, AlMe<sub>2</sub>), -0.64 (s, 6H, AlMe<sub>2</sub>).

<sup>13</sup>C NMR (C<sub>6</sub>D<sub>6</sub>, 600 MHz): δ 152.14, 144.11, 135.85, 130.99, 130.03, 126.96, 126.76, 123.39, 121.82, 118.04, 113.85 (C aromatic), -8.15 (CH<sub>3</sub>Al), -10.04 (CH<sub>3</sub>Al).

#### **Preparation of [μ-1,8-C<sub>10</sub>H<sub>6</sub>(N<sup>i</sup>Pr)(NNp)](AlMe<sub>2</sub>)<sub>2</sub> (4.10)**

The diamine (iPrNH)(NpNH)C<sub>10</sub>H<sub>6</sub> **4.3** (0.300g, 1.15 mmol) was dissolved in approximately 15 ml of diethyl ether in a round bottom flask equipped with a stir bar. To this solution was added a 2.0 M hexanes solution of AlMe<sub>3</sub> (1.15 ml, 2.30

mmol).resulting in a green solution. The solution was stirred overnight and turned to a pinkish red color. The volatiles were removed and the product was recrystallized from ether at -25°C, providing red crystals (0.25g, 0.66mmol, 57%). <sup>1</sup>H NMR (C<sub>6</sub>D<sub>6</sub>, 300MHz): δ 7.22-6.89 (m, 6H), 4.02 (sept, 1H, J=7.11Hz), 3.29(s, 2H), 1.28 (d, 6H, J=7.20Hz), 0.95 (2, 9H), -0.18 (s, 6H), -1.09 (s, 6H).

<sup>13</sup>C{H} NMR (C<sub>6</sub>D<sub>6</sub>, 300 MHz): δ 147.79, 144.23, 136.02, 125.26, 125.16, 123.72, 123.19, 122.185, 113.63, 112.76 (C aromatic), 56.90(CH<sub>2</sub>Me<sub>3</sub>), 47.55(CHMe<sub>2</sub>), 30.75(CMe<sub>3</sub>), 18.99(CH<sub>3</sub>), 0.99(CH<sub>3</sub>), -7.70(AlMe<sub>2</sub>), -10.66(AlMe<sub>2</sub>)

### Structural Determinations

**Table 4.1.** Selected bond lengths [Å] and angles [°] for HB[(<sup>i</sup>PrN)<sub>2</sub>C<sub>10</sub>H<sub>6</sub>] (**4.4**), HB[(PhN)<sub>2</sub>C<sub>10</sub>H<sub>6</sub>] (**4.5**) and HB[1,8 (<sup>i</sup>PrNH)(NpNH)C<sub>10</sub>H<sub>6</sub>] (**4.7**)

Compound <b>4.4</b>		Compound <b>4.5</b>		Compound <b>4.7</b>	
N(1)-B(1)	1.405(5)	B(1)-N(1)	1.4163(16)	N(1)-B(1)	1.411(3)
N(2)-B(1)	1.409(5)	B(1)-N(2)	1.4186(16)	N(2)-B(1)	1.409(3)
B(1)-H(1)	1.11(4)	B(1)-H(1)	1.112(13)	F(1)-B(1)	1.342(3)
N(1)-B(1)-N(2)	120.8(3)	N(1)-B(1)-N(2)	119.21(11)	N(2)-B(1)-N(1)	122.5(2)
N(1)-B(1)-H(1)	123(2)	N(1)-B(1)-H(1)	119.5(7)	F(1)-B(1)-N(2)	118.3(2)
N(2)-B(1)-H(1)	115(2)	N(2)-B(1)-H(1)	121.3(7)	F(1)-B(1)-N(1)	119.2(2)
C(1)-N(1)-B(1)	120.6(3)	C(2)-N(1)-B(1)	120.84(10)	C(9)-N(2)-B(1)	119.67(19)
C(1)-N(1)-C(11)	118.5(3)	C(2)-N(1)-C(11)	118.89(9)	C(1)-N(1)-C(11)	118.36(18)
B(1)-N(1)-C(11)	120.6(3)	B(1)-N(1)-C(11)	120.27(10)	B(1)-N(1)-C(11)	123.11(19)
C(9)-N(2)-B(1)	120.2(3)	C(10)-N(2)-B(1)	121.07(10)	C(9)-N(2)-C(14)	121.31(18)

C(9)-N(2)-C(14)	119.2(7)		C(10)-N(2)-C(17)	119.49(9)	C(9)-N(2)-B(1)	119.67(19)
B(1)-N(2)-C(14)	120.7(7)		B(1)-N(2)-C(17)	119.41(10)	B(1)-N(2)-C(14)	121.31(18)

**Table 4.2.** Selected Bond lengths [ $\text{\AA}$ ] and angles [ $^\circ$ ] for  $[\text{Al}(\text{CH}_3)_2]_2[(^i\text{PrN})_2\text{C}_{10}\text{H}_6]$  (**4.8**)

Al(1)-C(21)	1.962(2)	Al(2)-C(19)	1.9554(19)
Al(1)-C(22)	1.9627(19)	Al(2)-C(20)	1.957(2)
Al(1)-N(12)	1.9744(17)	Al(2)-N(12)	1.9710(15)
Al(1)-N(1)	1.9836(15)	Al(2)-N(1)	1.9873(15)
C(21)-Al(1)-C(22)	116.15(10)	C(2)-N(1)-C(13)	114.34(14)
C(21)-Al(1)-N(12)	112.00(8)	C(2)-N(1)-Al(1)	103.76(10)
C(22)-Al(1)-N(12)	113.17(8)	C(13)-N(1)-Al(1)	117.48(12)
C(21)-Al(1)-N(1)	115.90(8)	C(2)-N(1)-Al(2)	103.09(11)
C(22)-Al(1)-N(1)	113.85(8)	C(13)-N(1)-Al(2)	122.91(11)
N(12)-Al(1)-N(1)	80.74(6)	Al(1)-N(1)-Al(2)	91.59(6)
C(21)-Al(1)-Al(2)	102.91(7)	C(10)-N(12)-C(16)	119.72(15)
C(19)-Al(2)-C(20)	114.93(9)	C(10)-N(12)-Al(2)	106.45(11)
C(19)-Al(2)-N(12)	109.74(8)	C(16)-N(12)-Al(2)	114.31(11)
C(20)-Al(2)-N(12)	114.90(8)	C(10)-N(12)-Al(1)	104.45(11)
C(19)-Al(2)-N(1)	119.14(8)	C(16)-N(12)-Al(1)	115.74(12)
C(20)-Al(2)-N(1)	112.81(8)	Al(2)-N(12)-Al(1)	92.35(7)
N(12)-Al(2)-N(1)	80.73(6)		

**Table 4.3** Selected Bond lengths [Å] and angles [°] for [Al(CH<sub>3</sub>)<sub>2</sub>]<sub>2</sub>[(PhN)<sub>2</sub>C<sub>10</sub>H<sub>6</sub>] (**4.9**).

C(1)-Al(1)	1.9544(16)	C(9)-N(1)	1.4633(16)
C(2)-Al(1)	1.9542(16)	N(1)-Al(1)	1.9868(12)
C(3)-N(1)	1.4491(17)	N(1)-Al(1)#1	1.9966(12)
C(2)-Al(1)-C(1)	118.16(8)	C(3)-N(1)-Al(1)	116.05(8)
C(2)-Al(1)-N(1)	115.05(7)	C(9)-N(1)-Al(1)	108.07(8)
C(1)-Al(1)-N(1)	111.38(6)	C(3)-N(1)-Al(1)#1	119.73(8)
C(2)-Al(1)-N(1)#1	112.44(6)	C(9)-N(1)-Al(1)#1	105.24(8)
C(1)-Al(1)-N(1)#1	114.29(6)		
N(1)-Al(1)-N(1)#1	79.43(6)		

**Table 4.4** Selected Bond lengths [Å] and angles [°] for [Al(CH<sub>3</sub>)<sub>2</sub>]<sub>2</sub>[(<sup>i</sup>PrN)(NpN)C<sub>10</sub>H<sub>6</sub>] (**4.10**).

C(19)-Al(1)	1.9544(17)	Al(1)-N(2)	1.9832(13)
C(20)-Al(1)	1.9680(17)	Al(1)-N(1)	1.9909(12)
C(21)-Al(2)	1.9570(16)	Al(2)-N(2)	1.9734(12)
C(22)-Al(2)	1.9603(16)	Al(2)-N(1)	1.9961(12)
C(19)-Al(1)-C(20)	115.04(8)	C(21)-Al(2)-C(22)	115.81(8)
C(19)-Al(1)-N(2)	114.15(7)	C(21)-Al(2)-N(2)	116.84(7)
C(20)-Al(1)-N(2)	109.85(7)	C(22)-Al(2)-N(2)	111.79(6)

C(19)-Al(1)-N(1)	113.16(7)	C(21)-Al(2)-N(1)	113.04(6)
C(20)-Al(1)-N(1)	118.84(7)	C(22)-Al(2)-N(1)	113.41(7)
N(2)-Al(1)-N(1)	81.17(5)	N(2)-Al(2)-N(1)	81.29(5)
C(1)-N(1)-C(11)	116.27(11)	C(9)-N(2)-C(16)	119.99(11)
C(1)-N(1)-Al(1)	106.65(8)	C(9)-N(2)-Al(2)	107.05(9)
C(11)-N(1)-Al(1)	125.22(9)	C(16)-N(2)-Al(2)	113.44(9)
C(1)-N(1)-Al(2)	102.11(8)	C(9)-N(2)-Al(1)	105.28(9)
C(11)-N(1)-Al(2)	111.32(8)	C(16)-N(2)-Al(1)	116.08(9)
Al(1)-N(1)-Al(2)	89.97(5)	Al(2)-N(2)-Al(1)	90.86(5)

**Table 4.5** Crystal data and structure refinement for **4.11**

Empirical formula	C <sub>23</sub> H <sub>39</sub> Al N <sub>2</sub>
Formula weight	370.54
Temperature (K)	200(2)
Wavelength (Å)	0.71073
Crystal system	Monoclinic
Space group	P 21/c
a (Å)	18.646(5)
b (Å)	11.715(3)
c (Å)	23.127(7)
$\alpha$	90°
$\beta$	110.145(4)°.
$\gamma$	90°
Volume Å <sup>3</sup>	4743(2)
Z	8

Density (calculated) Mg/m <sup>3</sup>	1.038
Absorption coefficient mm <sup>-1</sup>	0.094
F(000)	1632
Crystal size mm <sup>3</sup>	0.430 x 0.370 x 0.290
Theta range for data collection	1.163 to 30.494°.
Index ranges	-25<=h<=24-15<=k<=15-15<=l<=15
Reflections collected	52338
Independent reflections	13066 [R(int) = 0.0484]
Completeness to theta = 25.242°	99.1 %
Refinement method	Full-matrix least-squares on F <sup>2</sup>
Data / restraints / parameters	13066 / 0 / 503
Goodness-of-fit on F <sup>2</sup>	1.026
Final R indices [I>2sigma(I)]	R1 = 0.0525, wR2 = 0.1212
R indices (all data)	R1 = 0.1047 wR2 = 0.1440
Extinction coefficient	n/a
Largest diff. peak and hole e.Å <sup>-3</sup>	0.240 and -0.230

## 4.5 References

- (1) Camp, C.; Arnold, J. On the Non-Innocence of “Nacnacs”: Ligand-Based Reactivity in  $\beta$ -Diketiminato Supported Coordination Compounds. *Dalt. Trans.* **2016**, *45* 14462–14498.
- (2) Tsai, Y. C. The Chemistry of Univalent Metal  $\beta$ -Diketiminates. *Coord. Chem. Rev.* **2012**, *256*, 722–758.
- (3) Bourget-Merle, L.; Lappert, M. F.; Severn, J. R. The Chemistry of  $\beta$ -Diketiminato-metal Complexes. *Chem. Rev.* **2002**, *102*, 3031–3065.
- (4) Chen, C.; Bellows, S. M.; Holland, P. L. Tuning Steric and Electronic Effects in Transition-Metal  $\beta$ -Diketiminato Complexes. *Dalt. Trans.* **2015**, *44*, 16654–16670.
- (5) Yang, Z.; Ma, X.; Roesky, H. W.; Yang, Y.; Jiménez-Pérez, V. M.; Magull, J.; Ringe, A.; Jones, P. G. Syntheses, Characterizations, and X-Ray Single-Crystal Structures of 1,8-Bis(trimethylsilylamino)naphthalene Aluminum Hydride and the Methyl Derivative. *Eur. J. Inorg. Chem.* **2007**, 4919–4922.
- (6) Riehm, T.; Wadepohl, H.; Gade, L. H. Putting Group 13 Elements onto Perylenes: Highly Fluorescent N - B - N- and N - Al - N-Substituted Polycyclic Aromatics Complex Fragments Has given Rise to a New Class of Highly. *Inorg. Chem.* **2008**, *47* (24), 11467–11469.
- (7) Jiménez-Pérez, V. M.; Muñoz-Flores, B. M.; Roesky, H. W.; Schulz, T.; Pal, A.; Beck, T.; Yang, Z.; Stalke, D.; Santillan, R.; Witt, M. Monomeric Boron and tin(II) Heterocyclic Derivatives of 1,8-Diaminonaphthalenes: Synthesis, Characterization and X-Ray Structures. *Eur. J. Inorg. Chem.* **2008**, No. 13, 2238–2243.

- (8) Martens, S. C.; Riehm, T.; Wadepohl, H.; Gade, L. H. Tetra-N -Silylated Bis(borylene) Tetraaminoperylenes (“DIBOTAPs ”): Synthesis , Structures and Photophysics. *Eur. J. Inorg. Chem.* **2012**, 3039–3046.
- (9) Bazinet, P.; Yap, G. P. A; Richeson, D. S. Synthesis and Properties of a germanium(II) Metalloheterocycle Derived from 1,8-Di(isopropylamino)naphthalene. A Novel Ligand Leading to Formation of Ni{Ge[(iPrN)2C10H6]}4. *J. Am. Chem. Soc.* **2001**, *123*, 11162–11167.
- (10) Rimmler, G.; Krieger, C.; Neugebauer, F. A. 1,8-Bis(diphenylamino)- and 1,8-Bis(methylphenylamino)naphthalene: Molecular Structure and Dynamic Behavior. *Chem. Ber.* **1992**, *125*, 723–728.
- (11) Lavoie, N.; Gorelsky, S. I.; Liu, Z.; Burchell, T. J.; Yap, G. P. A; Richeson, D. S. Disubstituted 1,8-Diamidonaphthalene Ligands as a Flexible, Responsive, and Reactive Framework for Tantalum Complexes. *Inorg. Chem.* **2010**, *49*, 5231–5240.
- (12) Spinney, H. A.; Korobkov, I.; DiLabio, G. A.; Yap, G. P. A.; Richeson, D. S. Diamidonaphthalene-Stabilized N-Heterocyclic Pnictogenium Cations and Their Cation-Cation Solid-State Interactions. *Organometallics* **2007**, *26* (20), 4972–4982.
- (13) Bazinet, P.; Ong, T. G.; O Brien, J. S.; Lavoie, N.; Bell, E.; Yap, G. P. A.; Korobkov, I.; Richeson, D. S. Design of Sterically Demanding, Electron-Rich Carbene Ligands with the Perimidine Scaffold. *Organometallics* **2007**, *26*, 2885–2895.
- (14) Weber, L.; Dobbert, E.; Stammler, H.; Neumann, B.; Boese, R.; Bläser, D. **2007**, *1*, 433–437.

- (15) Carey, D. T.; Mair, F. S.; Pritchard, R. G.; Warren, J. E.; Woods, R. J. Borane and Alane Reductions of Bulky N , N J -Diaryl-1 , 3-Diimines : Structural Characterization of Products and Intermediates in the Diastereoselective Synthesis of 1 , 3-Diamines †. **2003**.
- (16) M. J. Frisch, G. W. Trucks, H. B. Schlegel, G. E. Scuseria, M. A. Robb, J. R. Cheeseman, G. Scalmani, et al. **2016**. “Gaussian 09, Revision A.02.” Gaussian, Inc
- (17) APEX2 Software Suite v 2012. Bruker AXS Inc., Madison, Wisconsin, **2012**.
- (18) SADABS Bruker AXS Inc. Madison Wisconsin USA, **2014**.
- (19) G. M. Sheldrick, *Acta Crystallogr. Sect. C Struct. Chem.* **2015**, *71*, 3–8.
- (20) L. J. Farrugia, *J. Appl. Crystallogr.* **1999**, *32*, 837–838.